UNIVERSITÀ DEGLI STUDI DI MILANO

PhD course in Environmental Sciences
XXXVI cycle

Department of Clinical Sciences and Community Health

The effect of Indoor Total Suspended Particles (TSP) on the human upper respiratory system: from the microbiome to HERV methylation

Scientific disciplinary sector:
MED44 – Occupational Medicine

PhD candidate: Giulia Solazzo

Tutor:
Prof. Valentina Bollati

Head of the doctoral course:
Prof. Marcella Guarino

Academic year 2022/2023

ABSTRACT

Air pollution is well known for its adverse effects on human health. Among all air contaminants, particulate matter is one of the most studied because of its effect on the cardiovascular and respiratory system. Almost the entire global population is exposed daily to an unhealthy level of these contaminants and most of the exposure comes from the indoor setting where we spend a large portion of our daily time. The link between particulate matter exposure and human disease is still not fully understood, although inflammation is commonly observed after exposure to particulate matter. For that reason, investigating how the upper respiratory microbiome responds to particulate matter exposure is critical. These microorganisms that inhabit our upper airways play a crucial role in the homeostasis of the immune system and defend against external environmental stimuli. Furthermore, inflammation is also correlated with the activation of human endogenous retroviral elements integrated in our genome, the HERV genes. These genes regulate essential processes, and their dysregulation is associated with various inflammatory and immune-related diseases.

The aim of this project is to investigate the effects of indoor Total Suspended Particles (TSP) on the upper respiratory microbiome and the methylation levels of HERV genes. Additionally, this study aims to examine whether the microbiome can influence the effect that indoor TSP has on HERV methylation. To achieve this aim, we recruited 34 healthy office workers from the University of Milan and the University of Como. We monitored them and their workplaces for six weeks total, three weeks during the winter and three weeks during the summer. At the end of every week, we collected both environmental and biological samples. The TSP samples were collected using an active filter-based technique. The biological samples included anterior nares and nasopharynx swabs to evaluate the upper respiratory microbiome, and buccal brushes to measure the HERV methylation.

The first part of the project analyzed the environmental samples collected in the two seasons. The indoor and outdoor TSP concentrations were calculated gravimetrically. Then, we used the DNA extracted from the TSP collected on cellulose ester filters to characterize the TSP microbiome through whole genome shotgun (WGS) sequencing. We observed differences between the outdoor and the indoor TSP in both concentration and microbiome composition. The differences in microbiome composition we observed were probably influenced by the presence of plants, animals, and human activity in the environment.

The second part of the project characterized the anterior nares microbiome in healthy subjects and described the seasonal variation in this microbiome using both 16S rRNA and whole genome shotgun (WGS) sequencing. Specifically, we compared the anterior nares microbiome with the nasopharynx microbiome, and we analyzed how the indoor TSP exposure affected them. We observed significant differences between the two seasons in both microbiome diversity and composition in the anterior nares samples. The winter samples were enriched in *Moraxella* species (*Moraxella catarrhalis* and *Moraxella nonliquefaciens*) and the diversity was lower. The microbiome of the anterior nares was similar in taxa composition to the nasopharynx microbiome. They were both mostly dominated by gram-positive bacteria. However, the nasopharynx microbiome reported a higher diversity, and enrichment in *Staphylococcus aureus*, while the anterior nares microbiome had a high abundance of *Corynebacterium*, *Cutibacterium acnes*, and *Staphylococcus epidermidis*. In both microbiomes, we observed that the indoor TSP exposure affects commensal gram-positive bacteria such as *Corynebacterium accolens* and *Streptococcus pneumoniae*. Consistent with in vitro studies, an increase in *Staphylococcus aureus* relative abundance was identified in response to TSP exposure. Finally, we observed positive correlations in the abundance of some respiratory bacteria found in both TSP and human samples.

The third part of the project examined the impact of indoor TSP exposure and the microbiome on HERV methylation, investigating whether the upper respiratory microbiome can modulate the effect of this pollutant on HERV genes. Indoor TSP exposure alone did not affect the DNA methylation of the HERV genes studied. However, the upper respiratory microbiome was associated with changes in methylation of HERV-K. Furthermore, in our analysis of the interaction between indoor TSP exposure and the microbiome on HERV methylation, we identified that at low abundance of *Cutibacterium acnes* and *Actinomyces naeslundii*, indoor TSP exposure is associated with increased methylation of HERV-W. This HERV sequence was previously found to be hypermethylated in response to air pollution exposure.

In conclusion, this evidence indicates that indoor TSP exposure directly affects the respiratory microbiome, and consequentially the methylation of HERV-K and HERV-W.

INTRODUCTION

1. AIR POLLUTION

The World Health Organization (WHO) describes air pollution as the contamination of the environment by any chemical, physical or biological agent that modifies the natural characteristics of the atmosphere. The WHO sets the guidelines for each air pollutant as a tool for the management of air quality (**Table 1**). However, almost the entire global population is exposed to unhealthy concentrations of air pollutants (www.who.int/health-topics/air-pollution#tab=tab_1). Most air pollution is generated through large-scale human activities, and can be classified into six main types of pollutants: particle pollution (also known as particulate matter), ground-level ozone (O_3), carbon monoxide (CO), sulfur oxides (SOx), nitrogen oxides (NOx), and lead (Pb) (Manisalidis et al., 2020), **Figure 1**.

Table 1. The WHO air quality guidelines for air contaminants

Air pollutant	Threshold
NO_2	25 µg/m^3 (1-day mean) 10 µg/m^3 (annual mean)
PM_{10}	45 µg/ m^3 (1-day mean) 15 µg/m^3 (annual mean)
$PM_{2.5}$	15 µg/m3 (1-day mean) 5 µg/m3 (annual mean)
SO_2	40 µg/ m^3 (1-day mean)
O_3	100 µg/ m^3 (daily 8h mean)
CO	4 mg/ m^3 (1-day mean)
Pb	0.5 µg/ m^3 (annual mean)

Particulate matter (PM) is composed of inhalable particles composed of sulfate, nitrates, ammonia, sodium chloride, black carbon, dust, or water. PM comes from human activities as well as natural sources, and its particles are classified based on the size of their aerodynamic diameter. The PM with the smallest diameter (of less than 0.10 µm) are called ultrafine particles, while the biggest with a diameter (less than 100 µm) are called Total Suspended Particles (TSP). Ground-level ozone (O_3) is the main component of smog. It is produced by photochemical reactions between other air

pollutants such as carbon monoxide and nitrogen oxides that are released into the environment by vehicles and industrial activity. Carbon monoxide (CO) is an odorless gas produced by partial combustion of carbon compounds (i.e., wood, coal, kerosene). One of the main sources of CO is motor vehicles. Among the sulfur oxides, the most studied is sulfur dioxide (SO_2) which is a gas derived from the combustion of fossil fuels from industrial activities and domestic heating. Nitrogen dioxide (NO_2), is a strong oxidant gas produced by high temperature combustion of fuels. NO_2 is an important O_3 precursor. Finally, lead (Pb) and lead particulate compounds are mostly found in dust and come from several home products such as ceramics, pipes, and cosmetics (www.who.int/teams/environment-climate-change-and-health/air-quality-and-health/health-impacts/types-of-pollutants).

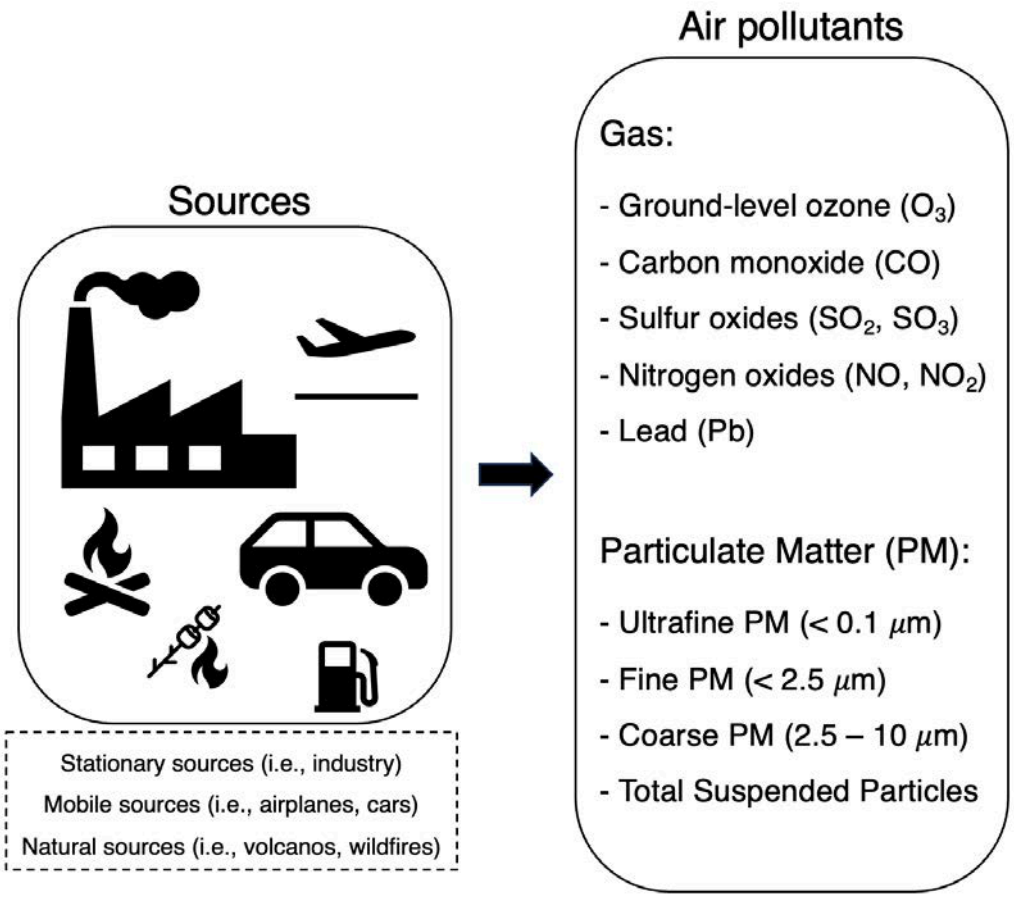

Figure 1. List of the main air pollutants: ground-level ozone, carbon monoxide, sulfur oxides, nitrogen oxides, lead, and particulate matter.

All these pollutants affect humans in different ways and exposure to them is associated with about 7 million premature deaths annually. Most of these pollutants are associated with cardiovascular and respiratory diseases, but they can also impact pregnancy and child development. Their effects on human health can be both indirect and direct (Bezirtzoglou et al., 2011; Palacio et al., 2023). Indirectly, air pollution is strictly correlated with climate change, which is associated with a higher incidence of several infectious diseases across the world (Bezirtzoglou et al., 2011; Peden, 2024). On the other hand, exposure to air pollutants also directly affects human health because pollution compounds cause inflammation. Numerous studies have shown that both short and long-term exposure to air pollution is associated with different symptoms including headache, asthma exacerbation, and hospitalization for cardiac dysfunction (Palacio et al., 2023).

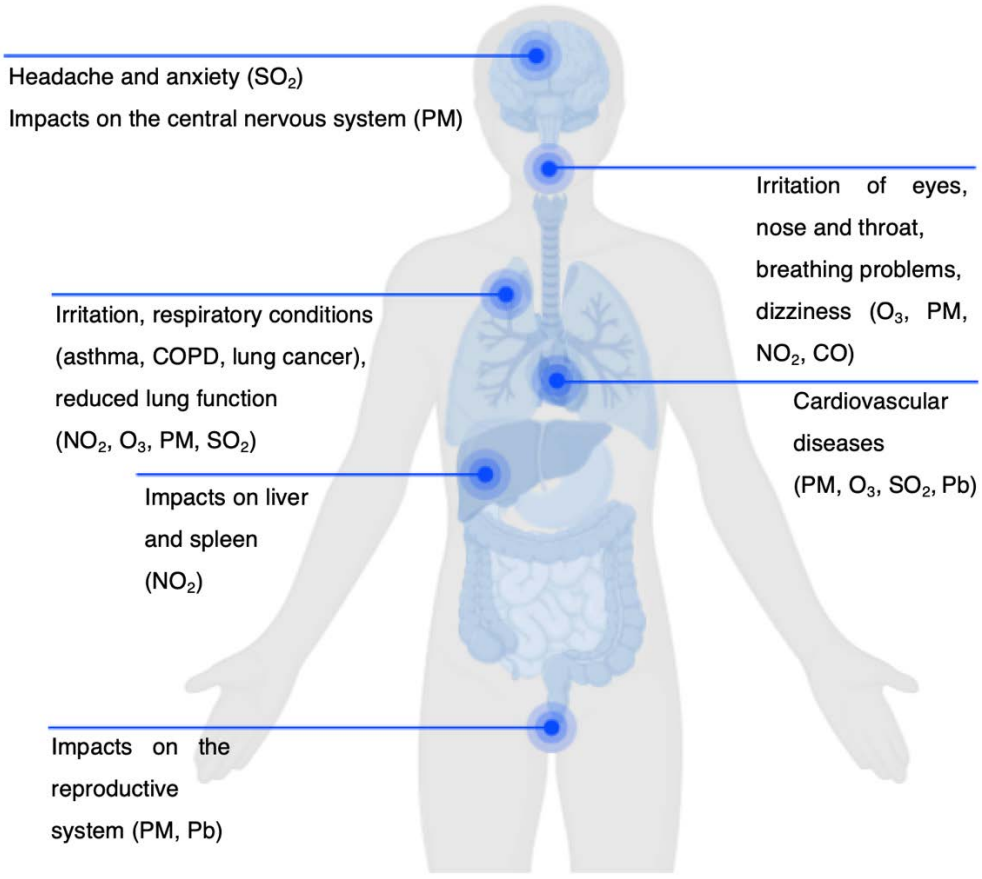

Figure 2. Summary of the health impact of the primary air pollutants on human health retrieved from the European Environment Agency (EEA) at www.eea.europa.eu and the World Health Organization (WHO) at www.who.int. The image was created on BioRender.com.

2. PARTICULATE MATTER IN INDOOR SPACE

We are constantly exposed to air pollutants in both *outdoor* and *indoor* settings. Because people usually spend most of their time, about 80% - 90% of the day, in indoor spaces (i.e., home, school, office, gyms), indoor exposure is recognized as an important risk factor that involves populations from low-income to high-income countries (Bennitt et al., 2021; Li et al., 2023; Peixoto et al., 2023; Jinze Wang et al., 2023). Outdoor exposure can influence the indoor air quality (outdoor infiltrations). This is usually estimated using the ratio of pollutant concentrations in indoor and outdoor air (I/O ratio). However, the correlation is not so strong because other factors influence the concentrations of indoor pollutants, like internal emissions (Jinze Wang et al., 2023; Zhang et al., 2005). Among air pollutants, PM is one of the most studied for its effects on human health, especially in small sizes ($PM_{2.5}$ and PM_{10}). However, there are few epidemiological studies on the effects of indoor PM on human health compared to the large number of studies on the outdoor exposure (Jinze Wang et al., 2023). The Environmental Protection Agency (EPA) summarizes the main sources of indoor PM in cooking and cleaning activities; combustion (i.e., candles, use of fireplaces, smoking); biological contaminants (i.e., pets, plants, mold, human skin flakes); printers and copiers (i.e., laser-jet printers, 3D printers); and chemical reactions. In addition, other activities that involve using wood, metal or glues can generate indoor particulate matter such as hobby and craft activities (https://www.epa.gov/indoor-air-quality-iaq/sources-indoor-particulate-matter-pm). Besides these factors, the levels of indoor PM can be affected by other factors like the outdoor infiltrations and the types of ventilation systems used, **Figure 3**. Currently, studies on PM indoor exposure are mostly focused on schools and households (Baumgartner et al., 2011; Clark et al., 2013; Kalisa et al., 2023; Young et al., 2019), and as described in the previous paragraph, these pollutants seem mostly associated with cardiovascular and respiratory disease (Manisalidis et al., 2020).

Figure 3. Summarizes all the main sources of indoor particulate matter (PM): cooking, cleaning, combustion, biological contaminants (i.e., mold and bacteria), printers, chemical reactions, and outdoor infiltrations. The image can be found at www.epa.gov/iaq.

3. UPPER RESPIRATORY MICROBIOME

The human upper respiratory tract (URT) includes an anterior nares, nasal cavity, sinuses, nasopharynx, and a larynx (**Figure 4**). The URT is an important interface between the internal and external environment, and performs the vital functions of conditioning inspired air, providing local defense, and filtering inhaled particulate matter and gasses (Sahin-Yilmaz and Naclerio, 2011). The differences in oxygen levels, temperature, humidity, pH, nutrients, and chemical factors in the URT create several ecological niches where communities of microorganisms live in a symbiotic relationship with humans. These communities vary in taxa abundance and composition, due to specific characteristics of each niche (Kumpitsch et al., 2019). High-throughput sequencing methods have made it possible to study these microbial communities using the information collected in their genomes. Studies focusing on the analysis of microbial communities through sequencing data are known as microbiome studies, and the microorganisms that live together in a specific environment are known as microbiome (de Steenhuijsen Piters et al., 2015; Lloyd-Price et al., 2017). The human microbiome, in addition to performing the specific function based on its location (i.e., gut, nasopharynx, oral, skin), also contributes to the homeostasis of the host immune system (Hou et al., 2022).

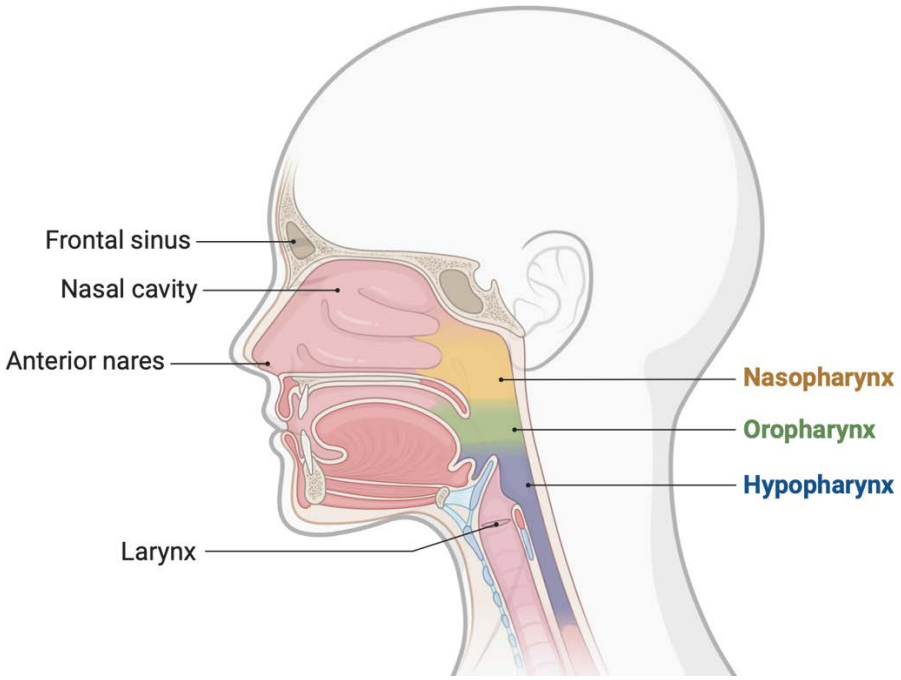

Figure 4. Description of the main components of the upper respiratory tract, from the most external part: anterior nares, nasal cavity, frontal sinus, nasopharynx, and larynx. The image was created on BioRender.com.

For many years, healthy human lungs were considered sterile, and the respiratory microbiome was not a subject of study. However, today we know the lungs have a microbiome and this microbiome is influenced by the upper respiratory microbiome (Dickson and Huffnagle, 2015). In newborns the upper respiratory microbiome has a low complexity and is very similar to the skin or the maternal vaginal microbiome (Biesbroek et al., 2014). The main genera that are found in the nares and nasopharyngeal microbiome of infants are *Moraxella*, *Staphylococcus*, *Haemophilus*, *Dolosigranulum*, and *Corynebacterium*. Even if the genera found in the respiratory tract are the same in all infants, their abundance can be affected by several factors such as birth mode, vaccination, feeding type, antibiotics and infections (Man et al., 2017). In adults, the microbiome gets more complex with age, and we observe that the upper respiratory microbiome is more diverse compared to the children microbiome. Additionally, a child's microbiome is more dense (higher bacterial load), (Kumpitsch et al., 2019). Lastly, the microbiome composition in each respiratory site is deeply influenced by the physiological characteristic of that site (**Figure 5**).

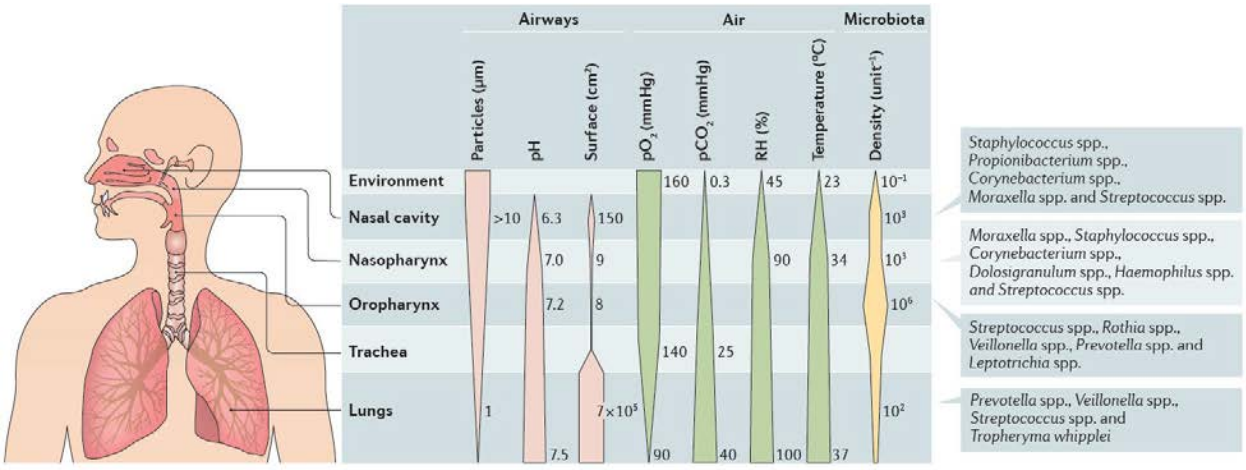

Figure 5. The physiological differences along the respiratory tract influence the respiratory microbiome composition. Image from Man et al., 2017.

The adult anterior nares microbiome is usually enriched in *Actinobacteria* and can be generally classified in one of four "microbial types" which are characterized by the predominance of either *Corynebacterium*, *Cutibacterium*, *Moraxella* or *Staphylococcus*. Among these microbial types, the *Cutibacterium* and the *Corynebacterium* seem to be more 'tolerant' to other genera, while the *Moraxella* type seems the least tolerant to other genera (de Steenhuijsen Piters et al., 2015). In

addition, it seems that the microbial types dominated by *Moraxella* are less common than the others (De Boeck et al., 2017). The nasopharynx microbiome of healthy adults shows a high similarity with the microbiome of the anterior nares in bacteria composition. Most of the bacteria identified in the nasopharynx microbiome are Gram-positive aerobes, such as *Staphylococcus*, *Dolosigranulum*, *Corynebacterium*, and *Cutibacterium* (de Steenhuijsen Piters et al., 2015). However, a smaller percentage of healthy people can have a *Moraxella*-dominated microbiome, a gram-negative bacterium, and the most abundant *Moraxella* species described in the respiratory microbiome are *Moraxella nonliquefaciens* and *Moraxella catarrhalis* (De Boeck et al., 2017). In both sites, anterior nares and nasopharynx, a disruption of the microbiome is associated with several disease like chronic obstructive pulmonary disease (COPD), asthma, chronic rhinosinusitis, and respiratory infections (Elgamal et al., 2021; Hou et al., 2022), **Figure 6**.

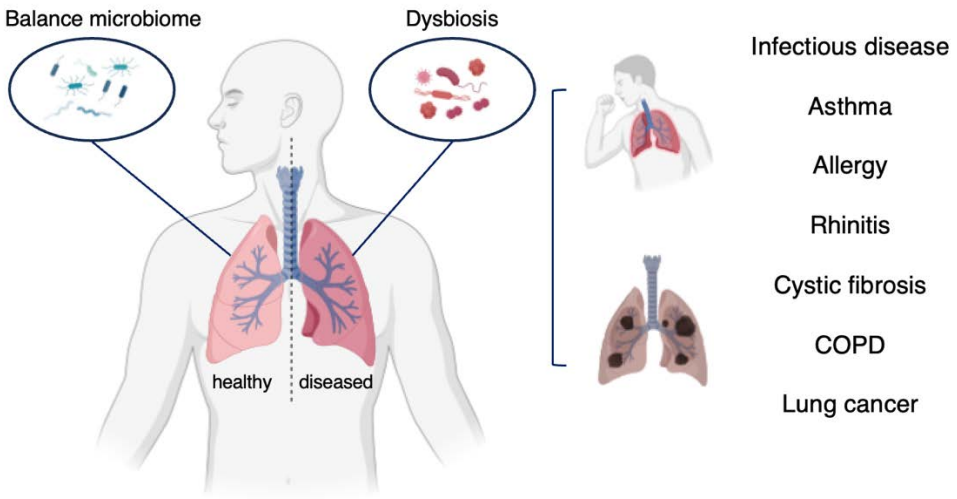

Figure 6. The respiratory microbiome plays an important role in human health and disease. Disruption in these microbial communities, also known as dysbiosis, is associated with several diseases, including respiratory infections (such as coronaviruses and influenza virus), asthma, allergy, rhinitis, cystic fibrosis, chronic obstructive pulmonary disease (COPD), and lung cancer. The image was created on BioRender.com.

4. PARTICULATE MATTER AND RESPIRATORY MICROBIOME

The human upper respiratory microbiome has an important role in the host's health, but it is constantly challenged by the external environment. Several environmental factors have been associated with alterations in microbiome like smoke exposure, and air pollution (Charlson et al., 2010; Elgamal et al., 2021; Hassoun et al., 2015; Mariani et al., 2021, 2018; Phipps et al., 2010). As a consequence of air pollution exposure, an increase of oxidative stress, inflammation, epithelium damage, and immune dysregulation have all been observed in the respiratory tract; These alterations lead to microbiome dysbiosis and pathogen colonization (Xue et al., 2020). These relationships between the respiratory microbiome and air pollution seem bidirectional because air pollutants affect the microbiome, and the microbiome affects air pollutants. For example, the microbiome can enable air pollutant biotransformation; however, the mechanisms underneath these interactions are still unclear (Hamidou Soumana and Carlsten, 2021). Among environmental factors, the association between particulate matter exposure and the upper respiratory microbiome is one of the least studied. The few studies identified are summarized in **Table 2**. Although the number of studies is modest, all of them suggest that this type of exposure can affect the microbiome (Vieceli et al., 2023). Specifically, they suggest that particulate matter exposure is associated with a decrease in microbial diversity. Common commensal bacteria, that are primarily gram-positive aerobic, such as *Corynebacterium* seem to be negatively correlated with the particulate matter exposure. On the other hand, some gram-negative bacteria species, such as *Moraxella* and *Haemophilus*, seem positively correlated with this pollutant (Mariani et al., 2021; Padhye et al., 2021; Qin et al., 2019; Zhao et al., 2022, 2020).

Table 2. Summary of papers focused on particulate matter exposure and the upper respiratory microbiome of adults*

Author, year	Country	Sample	N subjects	Population details	Results
(Padhye et al., 2021)	US	Nasal swab	122	Patients with chronic rhinosinusitis and healthy controls	$PM_{2.5}$ associated with decreased abundance of *Corynebacterium*
(Qin et al., 2019)	China	Pharyngeal swab	83	Workers from a farmer's market	Increased abundance of *Moraxella catarrhalis*, *Haemophilus influenzae* and *Staphylococcus*
(Mariani et al., 2018)	Italy	Nasal swab	40	Healthy adults	PM_{10} and $PM_{2.5}$ increased abundance of *Moraxella*, decreased abundance of *Corynebacterium*, *Actinomyces*, *Dermabacter*, *Micrococcus*, *Pasteurella* and *Streptococcus*
(Zhao et al., 2020)	China	Oropharyngeal	22	Asthmatic adults	$PM_{2.5}$ correlation with *Cupriavidus* and *Acinetobacter*
(Zhao et al., 2022)	China	Nasal swab	8	College students	$PM_{2.5}$ positive correlation with *Acidobactereia*, *Gemmatimonadetes, Symbiobacterium*

*reference (Vieceli et al., 2023)

5. HUMAN ENDOGENOUS RETROVIRUSES (HERVs)

Human endogenous retroviruses (HERVs) are viral elements that persist within the human genome and are derived from ancient retroviral infections in germline cells (Dopkins and Nixon, 2023). The integration of HERVs into the human genome probably took place more than 100 million years ago and it is estimated that they represent about 8% of the human genome (Mazúrová and Kabát, 2023). In healthy individuals, HERVs are involved in immune responses and developmental processes, such as the formation of syncytiotrophoblasts and tissue differentiations (Dopkins and Nixon, 2023; Jichang Wang et al., 2023). It seems that no HERVs are able to replicate and that they are dormant in our genome. However, a recent study suggested that HERV becomes active in the aging process (Liu et al., 2023). HERVs can either be classified into three main classes based on their homologies to retroviruses (Class I or gamma/epsilon-like; Class II or beta-like; Class III or spuma-like), or into 31 families based on structural characteristics (Belshaw et al., 2005; Vargiu et al., 2016). Even if HERVs can be classified in different ways, they share some characteristics. For example, they have two long terminal repeats (LTR) that act as promoters. These regions are usually methylated which means that these DNA regions have a methyl group in their cytosines that repress gene activation. However, HERVs gene can be demethylated by external stimuli and then activated (Reddam et al., 2023), **Figure 7**.

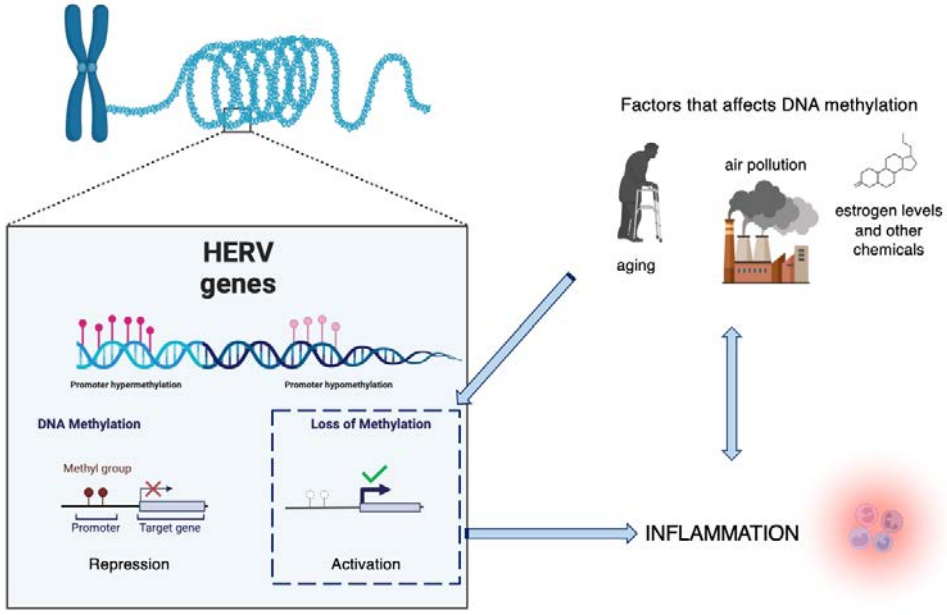

Figure 7. The methylation of HERV genes regulates their activation. External stimuli, such as aging, air pollution and hormonal changing, can demethylate their promoters and activate them. Their activation is usually associated with inflammation (Reddam et al., 2023). The image was created on BioRender.com.

HERV genes are closely related with immune response and for this reason these genes are associated with several human diseases (i.e., cancer, multiple sclerosis, rheumatoid arthritis, COVID-19), (Rangel et al., 2022). It seems that inflammation can activate HERV genes, and HERV genes are involved in innate and adaptative immune response. In addition, because air pollutions is often associated with global DNA hypomethylation, some studies have suggested that there might be a link between air pollution, HERVs activation, and inflammation (Byun et al., 2013; Reddam et al., 2023).

AIM OF THE PROJECT

This project aims to describe the effects of indoor Total Suspended Particles (TSP) on bacteria and viruses in the human respiratory tract using sequencing and methylation data. To achieve this goal, we recruited healthy volunteers in their workplace, and we divided the study into the following parts: **Section 1 -** Analysis of TSP exposure through an active sampling method and characterization of the microbiome associated with TSP by metagenomics analysis; **Section 2** - Association between the respiratory microbiota, using both 16S rRNA and shotgun sequencing data, and the TSP data obtained in Section 1; **Section 3** - Analysis of how the microbiome and TSP exposure influence DNA methylation of endogenous retrovirus genes (HERVs).

SECTION 1

Evaluation of TSP exposure and characterization of its microbiome

- *Quantification of TSP exposure among different seasons and workplaces*

- *Characterization of TSP indoor microbiome*

- *Comparison of indoor and outdoor TSP microbiome*

SECTION 2

The upper respiratory tract microbiome and the effects of the indoor TSP exposure

- *Anterior nares microbiome of healthy subjects and its seasonal variations*

- *Comparison of anterior nares and nasopharynx microbiome in healthy subjects*

- *Upper respiratory microbiome and its association with indoor TSP*

SECTION 3

Analysis of indoor TSP exposure and respiratory microbiome on HERV methylation

- *Quantification of HERV sequences methylation and its association with the TSP exposure*

- *Interaction analysis: TSP exposure, microbiome, and DNA methylation*

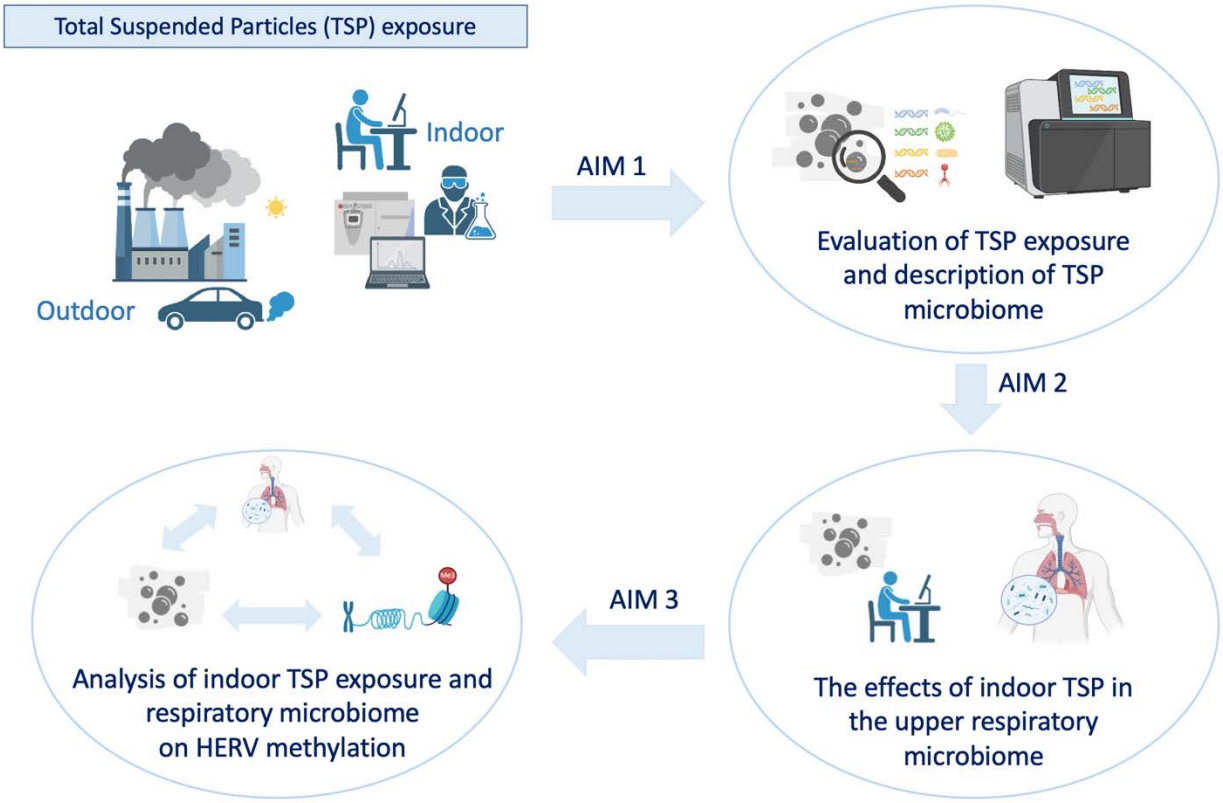

Figure 8. Overview of the study aims. Each circle describes a distinct section of the project, each section is defined by a specific aim. The first section analyzes the biological composition (microbiome) of indoor and outdoor TSP samples. The second section explores the association between indoor TSP exposure and the human upper respiratory microbiome. The last section investigates the relationship among indoor TSP exposure, respiratory microbiome and HERV methylation.

NOTE:

Some of the results presented in this thesis, specifically in Section 1 and Section 2, will be submitted in peer-reviewed journals as articles.

SECTION 1

Evaluation of TSP exposure and characterization of its microbiome

1.1 SUMMARY

The particulate matter (PM) is well known for its potential adverse effects on human health. Among the effects on health is the alteration of the human respiratory system through inflammation. In this scenario, the respiratory microbiome has an important role because it is closely associated with the respiratory system immunity and homeostasis (Panumasvivat et al., 2023). Two recent studies suggest that exposure to particulate matter can cause changes in the respiratory microbiota of healthy subjects with consequential activation of inflammation (Mariani et al., 2018; Rylance et al., 2016). However, the studies on particulate matter and respiratory microbiome are limited to the smaller fractions ($PM_{2.5}$ and PM_{10}) and none of them considered the Total Suspended Particles (TSP) that tend to deposit on the upper respiratory tract. In addition, the physical and chemical composition of particulate matter has been widely studied, but only a few studies have focused on the microbiota associated with these particles (Qin et al., 2020; Zhou et al., 2021). Consequently, the biological composition of these particles is mostly unknown and limited to $PM_{2.5}$ and PM_{10}. This section aims to describe the microbiome of indoor and outdoor TSP. We first evaluated the indoor and outdoor TSP levels in participant workplaces using a filter-based technique. Then, the DNA samples collected in these filters were characterized by whole genome shotgun (WGS) sequencing.

1.2 MATERIAL AND METHODS

Volunteer healthy subjects employed at the University of Milan and the University of Insubria Como were enrolled in the study in their workplace over 6 weeks. Specifically, recruited subjects were split into 3 population sub-groups (G1, G2, G3) and the TSP exposure of each sub-group was monitored in winter (November – March) and summer (May – July) for 3 consecutive weeks per season. Eligibility criteria included: age between 20-65 years old with no known chronic disease (e.g., cancer or asthma), no infectious disease at the time of enrollment and during the 3 weeks before the enrollment, working no less than 10 hours per week, and with more than 2 days per week spent in the office. Each participant was requested to fill out two different questionnaires. The first questionnaire contained all the general information about the subjects (i.e., gender, weight, height, age, type of job, smoking habits), the second was a weekly questionnaire to obtain relevant information about each monitoring week (i.e., number of cigarettes smoked, type of mask worn at work, number of hours spent using the mask, number of days in the office). After filling

out the weekly questionnaire, both biological and environmental samples were collected. Specifically, we collected from each participant an anterior nares swab (both winter and summer seasons) and a nasopharynx swab (only summer season). In addition, a buccal brush sample was collected from a random group of subjects (only winter season). Finally, each week Total Suspended Particle (TSP) samples were collected on cellulose ester filters in each office and outside the buildings where the participants worked (**Figure 9**).

This study was approved by the Ethics Committee of the University of Milan (approval number 24/22), in agreement with the principles of the Helsinki Declaration. All participants signed a written informed consent.

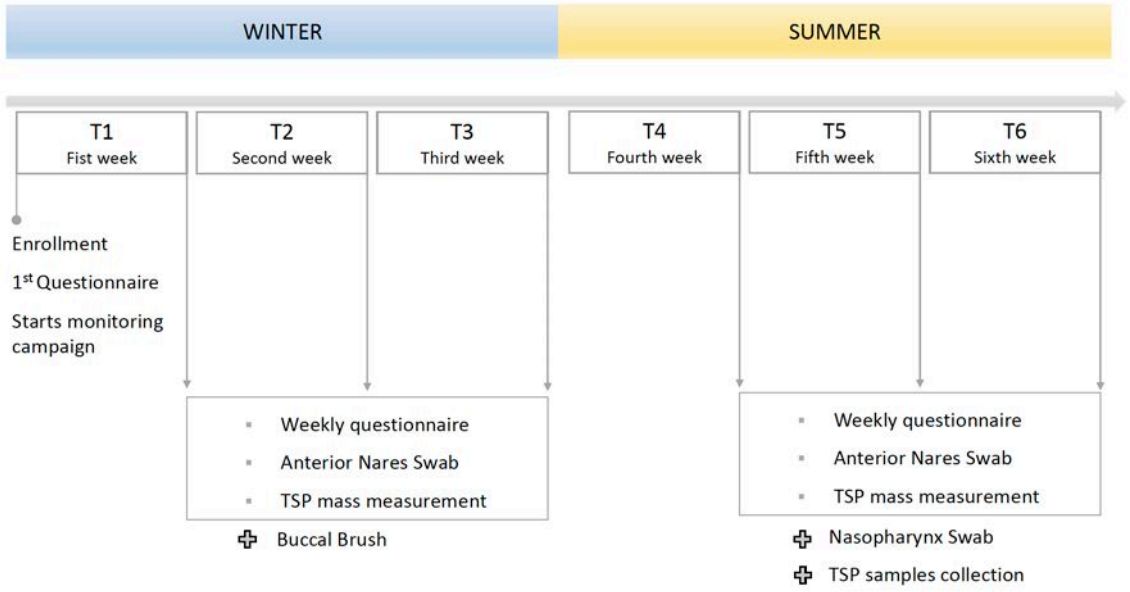

Figure 9. Sampling timeline of the study. Healthy subjects were enrolled in their offices for six weeks. Throughout each week, biological samples were collected. Total suspended particles (TSP) samples were collected each week in the summer season.

1.2.1 Total Suspended Particles (TSP): collection and mass measurements

The TSP exposure was monitored inside the offices of each participant (indoor TSP) and outside the buildings where they work (outdoor TSP). A total of 17 offices located in 4 different workplace buildings were included in the study. All the buildings are in Lombardy (Northern Italy), two in the city of Milan and two in the city of Como. The two buildings at the University of Insubria (Como) are modern buildings of recent construction (10-20 years old), located in the urban area of the city, at a distance of about 3 km from the city center. A busy main road and a secondary street

surround the university. Moreover, in one building the selected offices (67% of the total monitoring rooms in Como) are located at the basement level, with only a forced mechanical HVAC system (no operable windows), whereas in the other university building, the office rooms (33% of the total, on the first and second floors) are characterized by the presence of a hybrid ventilation system (natural ventilation and mechanical HVAC system). In Milan, the offices tested are located within a large university hospital in the city center, within a limited traffic zone that prohibits or limits the circulation of vehicles based on their Euro Standards. Most of the Milanese offices (84%) are on the first, second and third floors of an old hospital pavilion (about 60 years old); the remaining two offices (16%) are in a historical building of more than 100 years old. All the offices in Milan have natural ventilation, with windows that are not well maintained. A heating and/or cooling manual system was available in most of the offices. The monitoring campaign was split into three independent monitoring groups, two in Milan (R1 and R2) and one in Como (R3), (**Figure 10**). The labels R1, R2, and R3 indicate the TSP exposure of group G1, G2, and G3, respectively.

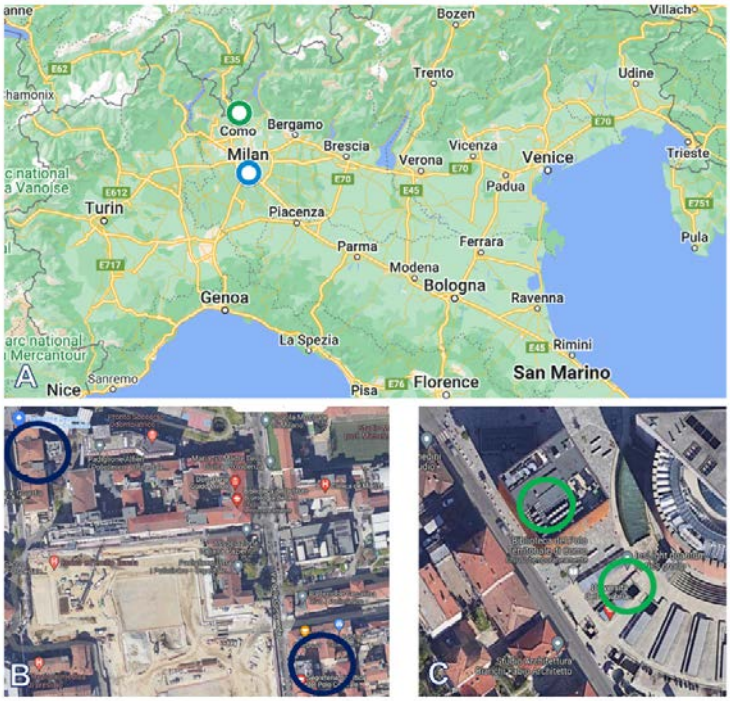

Figure 10. Location of sampling sites: A. the geographic locations of the two cities involved in the study are indicated with a blue circle (Milan) and a green circle (Como); B. Monitoring sites in Milan are highlighted with blue circles; C. Monitoring sites in Como are highlighted with green circles. The maps are retrieved from Google Maps (www. google.com/maps).

The TSP was collected weekly through an active sampling method using a filter-based technique from Monday morning to Friday afternoon (8 hours per day). Specifically, we used a low-flow air SKC sampling pump attached to a filter cassette (SKC inc.) and a 37-mm, 0.8 µm mixed cellulose esters (MCE) membrane filter (Omega, SKC Inc.). For the indoor sampling, the filter cassette was placed in the center of each room, not closer than 1 m to the wall and away from ventilation channels and heating sources, at the height of the breathing zone of seated occupants, i.e., approximately 110 cm from the floor (**Figure 11**). Each office building had two outdoor sites sampled, chosen to be as close as possible to the offices (i.e. < 300 m away) to obtain the best possible estimates of TSP outdoor concentration and composition. For both indoor and outdoor monitoring, the sampling pumps were set at a flow ranging from 2 to 4 L/min. The TSP mass of each filter was determined gravimetrically, weighing the filter at specified constant conditions before and after sampling. Before the weighing, each filter was conditioned at constant temperature (20°C ± 1°C) and relative humidity (50% ±5%) values, in a controlled environment (SCC 400L Climatic Cabinet, Sartorius, Varedo (MB), Italy) and an electrical C-shaped ionizer (HAUG GmbH & CO. KG, Germany) was used to eliminate electrostatic charges present on the filter surface. After this step, each filter was weighed three times using a micro-balance (GIBERTINI 1000, Novate, Milan, Italy). The same procedure was repeated after each sampling to determine the TSP mass. Two laboratory blanks were always weighed under the same conditions to verify possible anomalies in the weighing room conditioning. The average blank filter masses were then used to correct the filter mass results for each test. After the mass measurements, the filters were stored at -80ºC. The outdoor exposure was estimated using the mean of the two measurements performed in each building every week. A Wilcoxon rank-sum test was used to analyze the difference in TSP concentration between the two seasons (winter and summer) and between the two different locations (Milan and Como), while a Kendall correlation analysis was performed to check if the two types of exposures (indoor and outdoor) were correlated. These analyses were performed using R software v 4.2.1.

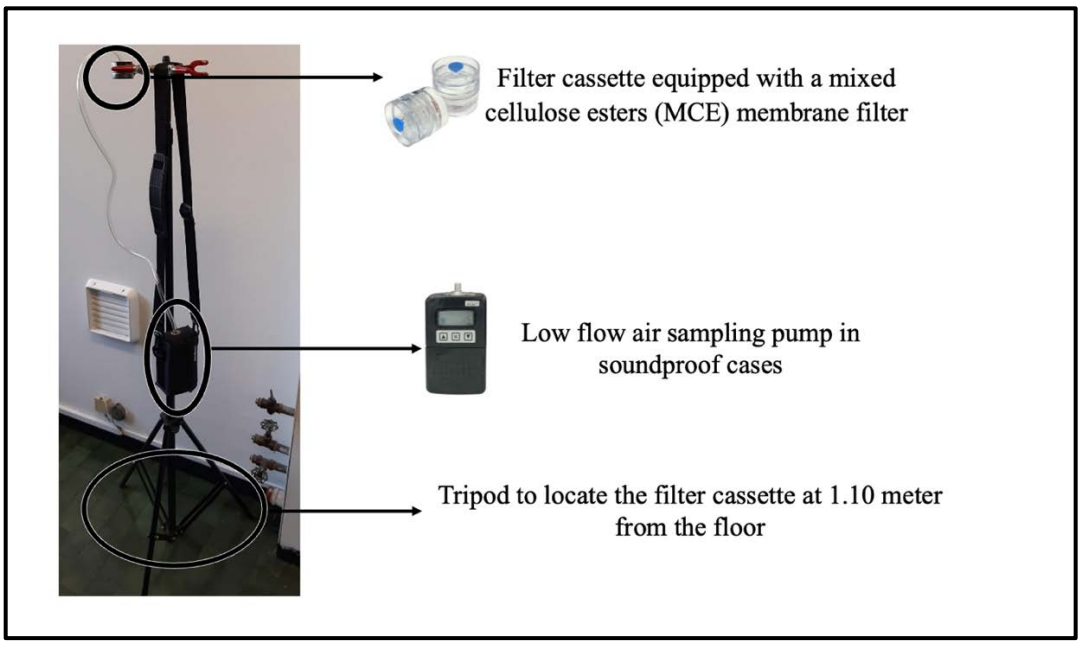

Figure 11. Active sampling method for total suspended particles (TSP) using a low-flow air sampling pump connected to a filter cassette.

1.2.2 Total Suspended Particles (TSP): DNA extraction and sequencing

In the summer, at the end of the monitoring campaign, we extracted the DNA from the filters collected using the NucleoSpin cfDNA XS kit (Macherey-Nagel). Each filter was put in Petri dishes and shaken for 2 hours with 1 mL of PBS to facilitate the release of the collected particulate material from the filter substrate. In addition, clean filters were put in Petri dishes at the same condition as negative controls for the DNA extraction step. After 2 hours, 240 µl of PBS was used for DNA extraction following manufacturer guidelines, then the samples were quantified using the Qubit dsDNA High Sensitivity Assay kit (Invitrogen). DNA extracted from the filters was sequenced by whole genome shotgun (WGS) sequencing. The sequencing pair-end library was prepared using the NexteraXT DNA library preparation kit (Illumina) following the manufacturer's protocol. To purify the library, we used the Agencourt AMPure XP beads (Beckman Coulter, Inc.). Therefore, we quantified the library using the Qubit dsDNA High Sensitivity Assay kit (Invitrogen), while the average fragment length was determined using a High Sensitivity D1000 ScreenTape Assay (Agilent). During the library preparation, we included one negative control for library reagents and one negative control from the DNA extraction step. Finally, samples were added to create one equimolar pool for the sequencing. At this point, the

sequencing pool was quantified and sequenced on the Illumina Novaseq 6000 S2 in one single run (sequence length 150 bp, paired-end).

1.2.3 Bioinformatics and Statistical analysis

The reads obtained from the WGS sequencing were demultiplexed using Bcl2fastq (v 2.20) and then trimmed using fastp (v 0.20.1) (Chen et al., 2018). Taxonomy was assigned using Kraken (v 2.1.2) and Bracken (v 2.5) (Lu et al., 2017; Wood and Salzberg, 2014). Host reads are filtered from the FASTQs by removing any reads mapping to a reference host genome using Bowtie (v 2.4.2) (Langmead et al., 2009). The processed reads were given a taxonomic assignment using a database consisting of human, bacteria, fungi, archaea, and viral RefSeq databases along with the EuPathDB46 database. Reads identified as human were removed using KrakenTools (v 1.2) for downstream analyses. The *Decontam* R package (v 1.18) was used to identify contaminants from all samples in the dataset using as reference two types of negative controls (DNA extraction and library preparation) (Davis et al., 2018). The alpha (α) diversity was calculated using the Shannon Index, Chao1 and Observe species metrics; the beta (ß) diversity using the Bray-curtis matrix. To calculate and analyze both the alpha and beta diversities we used the following R packages: *phyloseq* (v 1.42), and *MicrobiotaProcess* (v 1.10) using the default settings (McMurdie and Holmes, 2013; Xu et al., 2023). The non-parametric paired t-test was used to analyze the difference in alpha diversity among groups, and the Spearman correlation test was performed to test the correlation between the alpha diversity and the TSP concentration. The difference in beta diversity was analyzed with the Analysis of Similarities (ANOSIM) and the permutational multivariate analysis of variance (PERMANOVA) with 999 permutations using adonis2. The taxonomy composition was described using *microViz* (v 0.10) and *phylosmith* (v. 1.0.6). Finally, we used the Analysis of Compositions of Microbiomes with Bias Correction (ANCOM-BC) package (v. 1.6.4) to analyze observed taxa relative abundance, resistome (MEGARes), and KEGG pathways corrected for the three independent monitoring groups (R1, R2, and R3) (Lin and Peddada, 2020). The ANCOM-BC was performed using the default settings, and the mean difference (W) was considered significant when a p-value < 0.05 and FDR < 0.10 were reached. The bioinformatic pipeline is summarized in **Figure 12**. All statistical analyses were performed with R software, v 4.2.1.

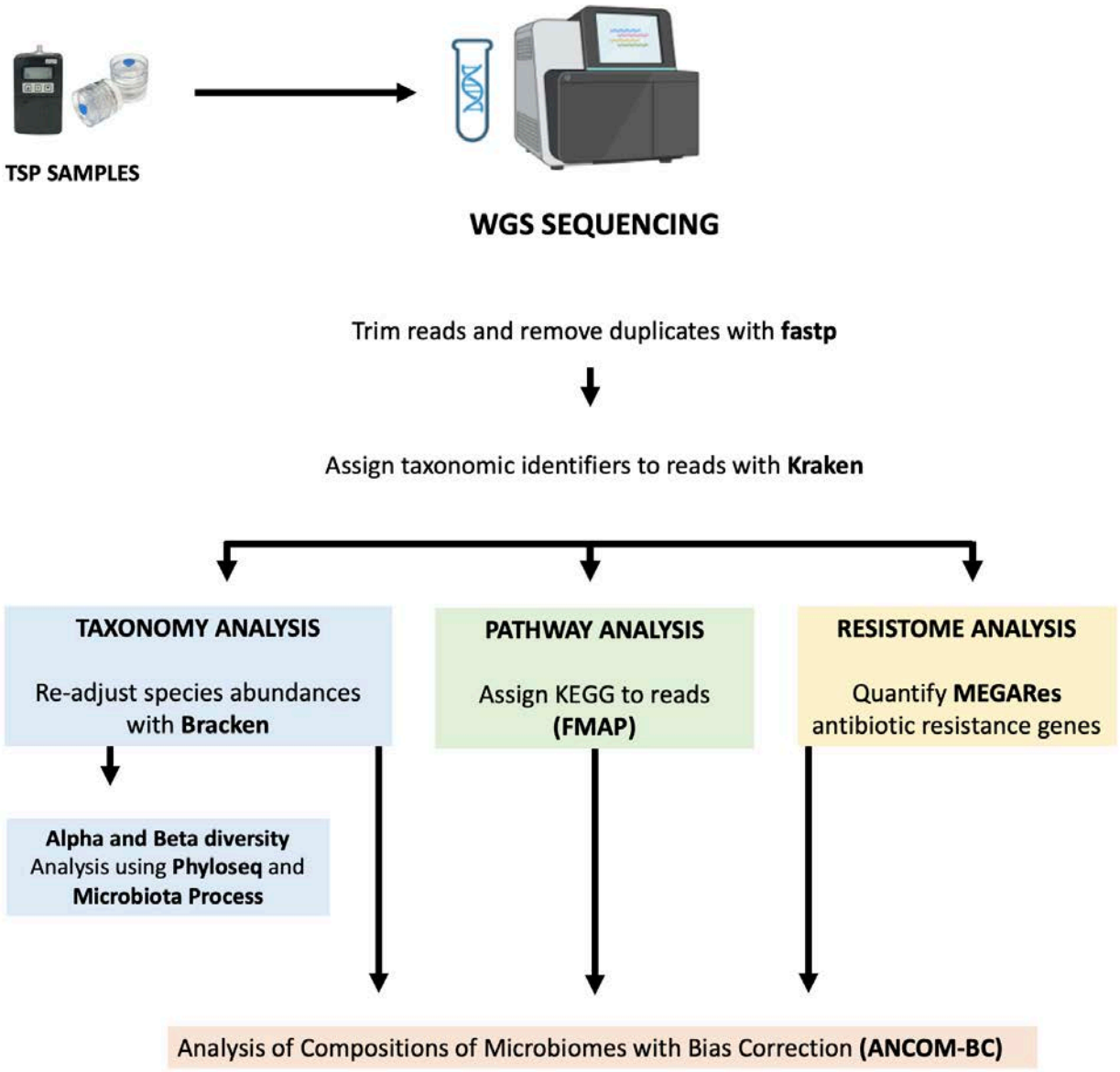

Figure 12. The bioinformatic pipeline used to analyze the TSP metagenomic data consisted of several steps. First, the sequencing data were cleaned and trimmed using fastq. Then, taxonomic assignment was carried out using Kraken. The operational taxonomic unit (OTU) table obtained from kraken was adjusted using Bracken, then the diversity analysis was performed using Phyloseq and Microbiota Process (blue boxes). For pathway analysis (green box) we used KEGG orthology genes, and for the resistome analysis (yellow box) the MEGARes database was used to identify antimicrobial resistance genes. All counts tables obtained in the previous steps were analyzed using ANCOM-BC.

1.3 RESULTS

1.3.1 Quantification of TSP exposure among different seasons and cities

By the end of the monitoring campaign, we had sampled 17 offices in the winter and 13 in the summer. Overall, the indoor TSP concentrations were lower than the corresponding outdoor ones, as described by the Indoor/outdoor (I/O) ratio that was mostly < 1, **Supplemental Table 1**. The indoor concentration of TSP did not a show significant difference between winter (Median = 29.2; Q1 - Q3 = 23.37 – 38.85) and summer (Median = 29.9; Q1 - Q3 = 17.08 – 38.13). However, the Wilcoxon test reported a slightly significant seasonal difference in indoor TSP concentration in the offices of the second group (R2, the second subgroup of Milan), where the average indoor concentration was higher in the winter (median = 35.8 $\mu g/m^3$ [Q1-Q3 = 32.3 - 45.3 $\mu g/m^3$]) compared to the summer (median = 33.4 $\mu g/m^3$ [Q1-Q3 = 27.5 - 34.9 $\mu g/m^3$]). In addition, we observed that the offices in the most recent buildings and with forced mechanical HVAC systems (R3, the subgroup of Como) have the lowest indoor TSP concentrations, **Figure 13-14**. Indeed, when we compared the indoor TSP exposure between Milan and Como, the TSP concentration was significantly higher in Milan for both seasons (winter, p-value < 0.001; summer, p-value < 0.001) as described in **Table 3**.

Conversely, the outdoor TSP concentration seems affected by the season. The concentration was estimated for 4 buildings, and the winter had higher concentrations (Median = 54.6; Q1 - Q3 = 41.75 – 69.14) compared to the summer (Median = 43.3; Q1 - Q3 = 36.52 – 50.41, **Figure 13**). In both seasons Milan reported higher levels of outdoor TSP compared with Como as described in **Table 3**. Finally, no correlation was found between the concentration of indoor and outdoor TSP. However, we observed some positive correlations in winter at the second recruitment (R2, tau = 0.5, p-value = 0.002) and in summer at the second and third recruitments (R2, tau = 0.6, p-value = 0.001; R3, tau = 0.5, p-value < 0.001, **Supplemental Figure 1**). As expected, we found differences in outdoor TSP exposure between the two seasons, with indoor TSP exposure only partially explained by these outdoor variations.

Table 3. TSP levels during the winter and the summer recruitments			
TSP	**Winter Median (Q1 – Q3)**	**Summer Median (Q1 – Q3)**	**P-value (Wilcoxon test)**
Indoor exposure			
All	29.2 (23.4 – 38.9)	29.9 (17.1 – 38.1)	0.6
City			
Milan	37.9 (28.3 – 47.5)	37.8 (33.4 – 41.8)	0.8
Como	18.8 (10.3 - 27.9)	16.4 (13.8 – 22.2)	0.8
Monitoring campaign			
R1 (Milan)	37.9 (28.1 - 44.1)	41.1 (39.7 - 46.9)	0.2
R2 (Milan)	35.8 (32.3 - 45.3)	33.4 (27.5 - 34.9)	0.04*
R3 (Como)	18.8 (10.3 - 27.9)	15.7 (13.8 - 22.3)	0.7
Outdoor exposure			
All	54.6 (41.8 – 69.1)	43.3 (36.5 – 50.4)	0.001*
City			
Milan	54.6 (36.4 – 89.9)	50.4 (49.7 – 56.3)	0.01*
Como	43.2 (41.7 – 59.4)	36.5 (29.3 – 43.3)	> 0.001*
Monitoring campaign			
R1 (Milan)	36.4 (36.1 - 69.1)	50.3 (49.7 - 50.4)	0.7
R2 (Milan)	89.9 (54.6 - 91.0)	56.3 (30.2 - 63.5)	0.001*
R3 (Como)	43.2 (41.7 – 59.4)	36.5 (29.3 – 43.3)	> 0.001*

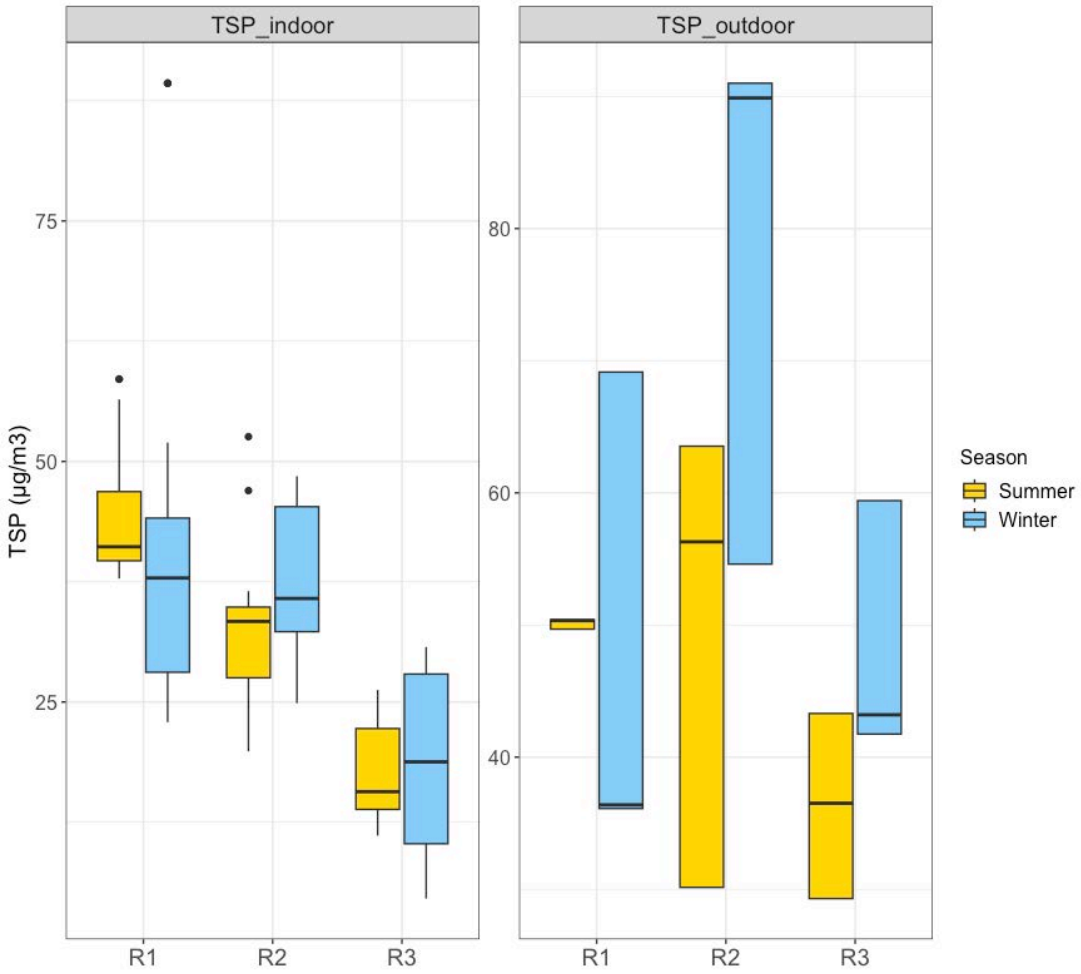

Figure 13. Comparison of the *indoor* and *outdoor* TSP concentration (µg/m^3) between winter (blue boxplots) and summer (yellow boxplots) seasons in the three groups: two in Milan (R1 and R2) and one in Como (R3).

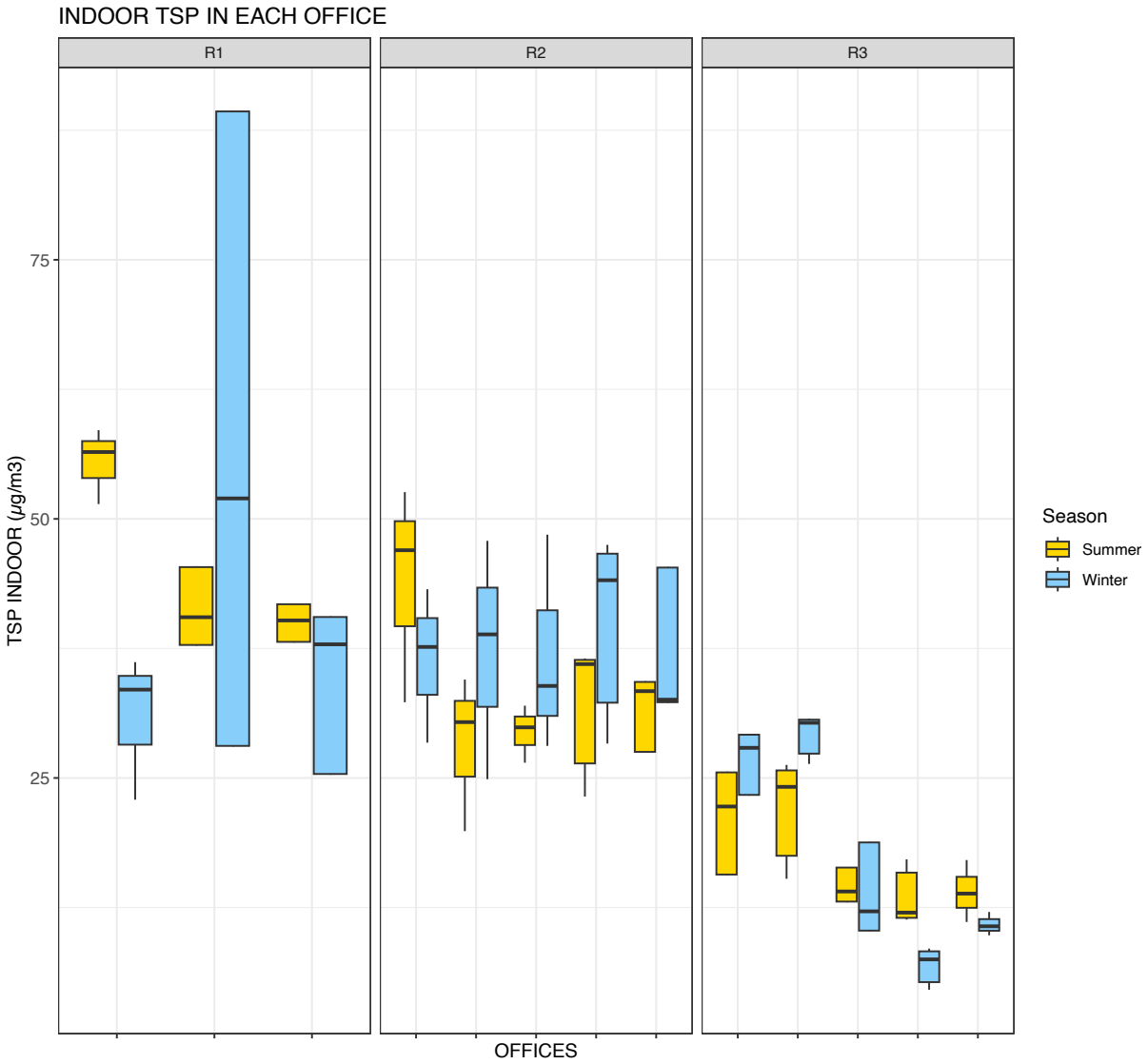

Figure 14. The *indoor* TSP concentration (µg/m^3) in each office among two seasons: winter (blue boxplots) and summer (yellow boxplots). The R1 and R2 are the offices located in Milan, the R3 are the offices located in Como.

1.3.2 Description of TSP indoor microbiome

The mean concentration of DNA extracted from indoor filters was 32.35 ng/µL (sd = 15.9). After sequencing, we excluded from the analysis samples with sequencing depth less than 100,000 reads. We obtained 37 samples of indoor TSP collected from the 13 offices monitored during the summer season (median sequencing depth = 385,900, range = 103,408 – 1,566,178); 22 samples from Milan and 15 samples from Como. The number of samples analyzed for each office is reported in **Supplemental Table 2**. The alpha diversity was higher in the indoor TSP samples from Milan (Shannon Index, Median = 6.5; Q1 - Q3 = 5.3 - 6.7) compared to the alpha diversity in the indoor TSP samples from Como (Shannon Index, Median = 5.6; Q1- Q3 = 5.5 – 6.0, **Figure 15A**). Specifically, the R1 showed higher alpha diversity compared to the others (R2, R3; **Figure 15B**). These differences in alpha diversity were also observed with Chao1 and Observed species metrics (**Supplemental Figure 2**). We also found that the office alpha diversity was positively correlated with the indoor TSP concentrations (Spearman correlation test, rho = 0.7, p-value < 0.001). There was a difference in beta diversity between the two cities (ANOSIM, R = 0.1, p-value = 0.05) and this difference explained about 6% of the total (PERMANOVA, Bray-curtis p-value = 0.005). The difference in beta diversity explained by the three groups was about 11% (PERMANOVA, p-value < 0.001), **Figure 16**. In the OTU table, 79% of the species identified were *Bacteria*. The top 15 most abundant bacteria across all the samples from the two cities (Como and Milan) are reported in **Figure 17A.** Most of them are bacteria found in soil, dust or in plants (i.e., *Xanthomonas campestris* and *Clavibacter michiganensis*), but some of them are also found in human skin and can be pathogens for immunocompromised people (i.e., *Micrococcus luteus, Paracoccus yeei*, *Staphylococcus aureus* and *Kocuria rosea*). Some of these bacteria were already described in airborne samples, such as *Micrococcus lutes*, *Kocuria* sp., and *Paracoccus* yeei (Kooken et al., 2012; Madsen et al., 2023). The second major taxon in our OTU table was *Virus* (16%); the top 10 viruses (genus level) across the two cities are described in **Figure 17B.** Most of the viruses identified are from the *Caudoviricetes* class (*Pahexavirus*, *Saikungvirus*, *Agricanvirus*, *Delepquintavirus*, *Derbicusvirus*, *Anayavirus*) which are the most ubiquitous bacteriophages in the environment (Zhu et al., 2022). Some of these bacteriophages (*Delepquintavirus, Agricanvirus,* and *Derbicusvirus*) are found in bacteria that live in soil and plants such as *Erwinia sp.* and *Stenotrophomonas maltophilia* was one of the top 15 bacteria. *Pahexavirus* bacteriophages are found in commensal human bacteria, mostly from *Propionibacterium sp.*

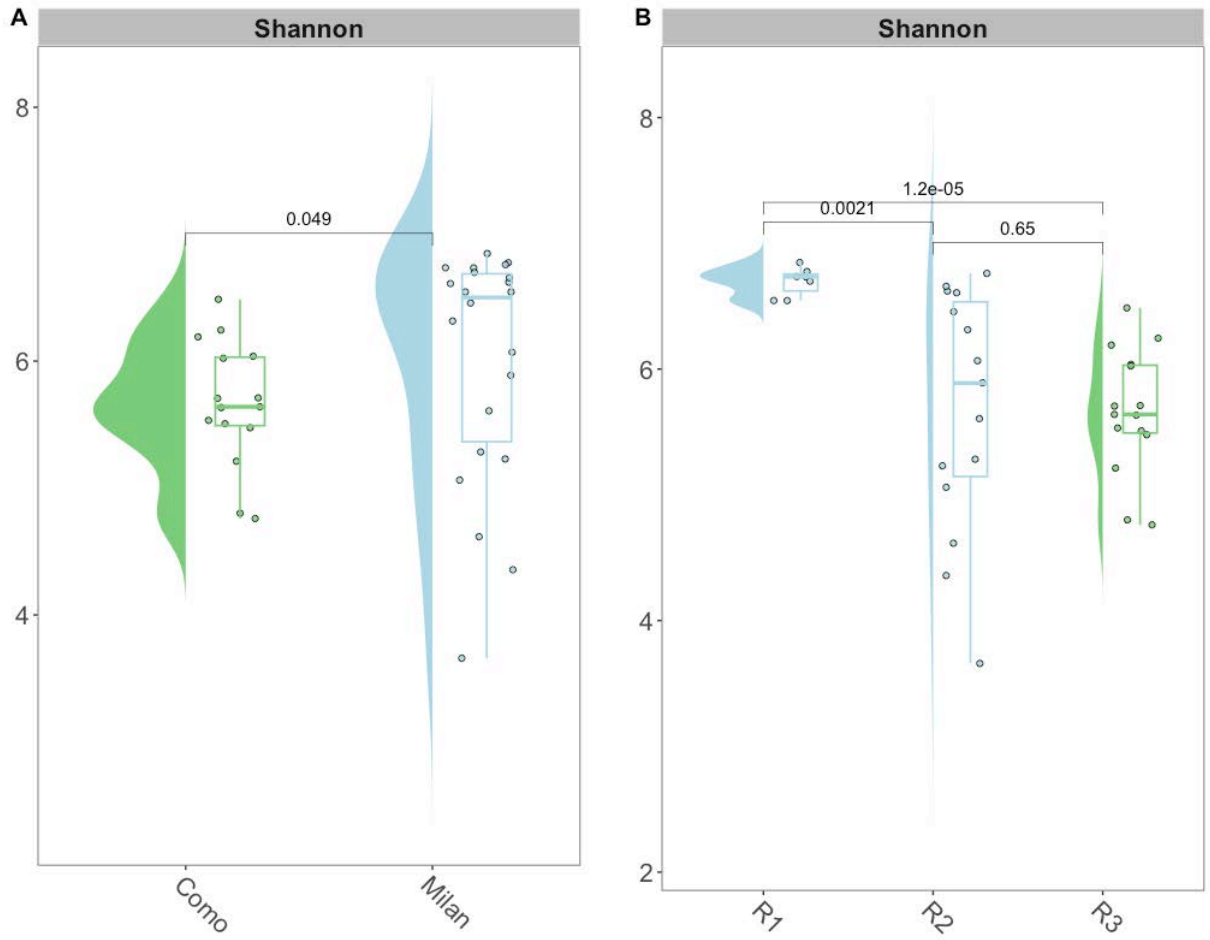

Figure 15. Boxplots showing the alpha diversity in indoor TSP samples. The dots represent the alpha diversity of each sample, the y axis indicates the alpha diversity estimated using the Shannon Index. (**A**) Comparison of the alpha diversity of samples from Milan and Como. (**B)** Comparison of alpha diversity among the three different groups (R1, R2, R3). In both plots, Milan samples are in light blue color and Como samples in green. These images were generated using *MicrobiotaProcess* (v 1.10).

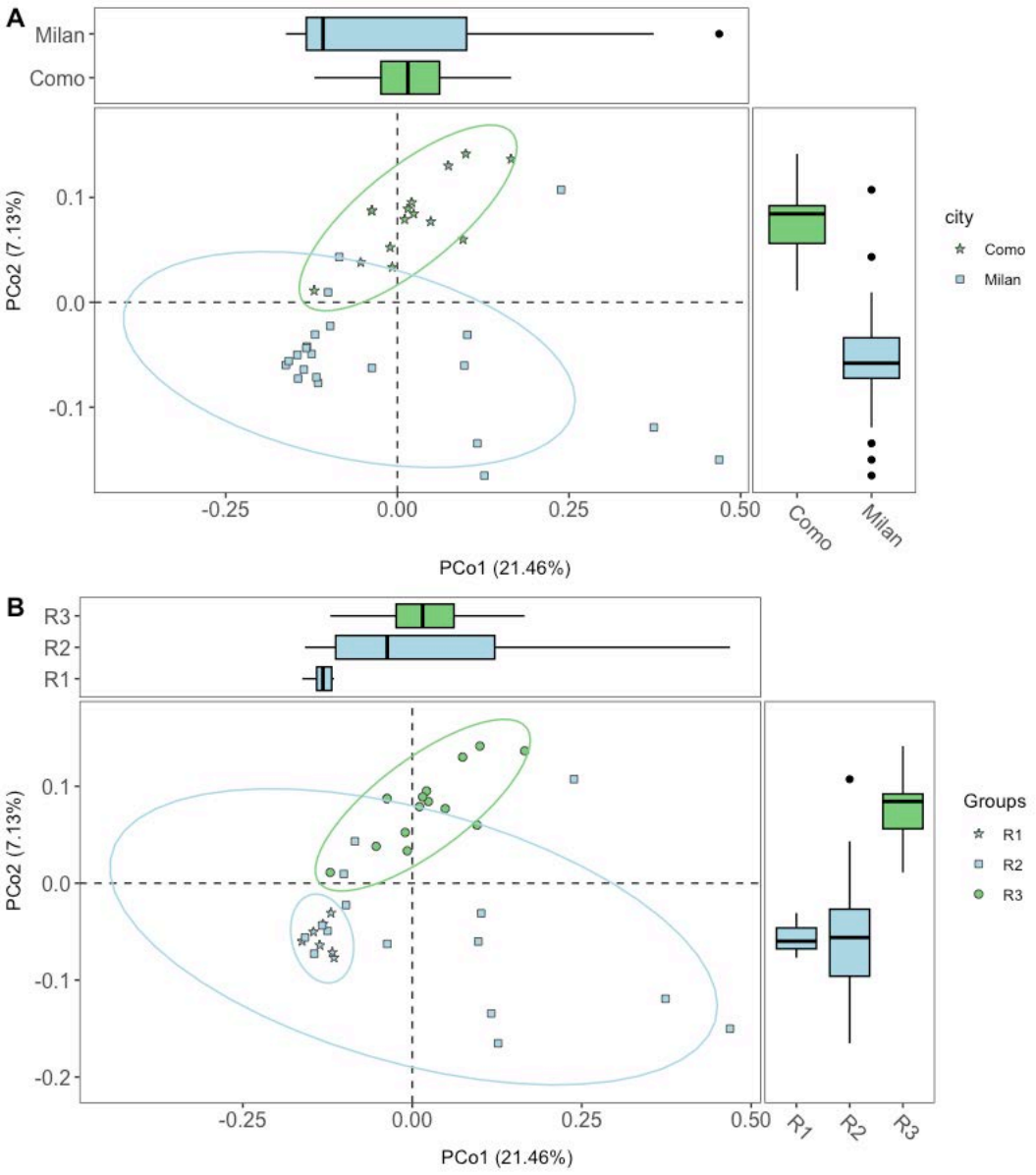

Figure 16. Principal coordinate analysis (PCoA) was conducted using the Bray-Curtis distance matrix to analyze the microbiota of indoor TSP samples. The y-axis and x-axis represent the two main coordinate axes. The **A** plot shows the samples clustered by city, while in the **B** plot the samples are clustered R1, R2, R3. In both plots, the light blue color indicates the TSP samples collected in Milan, the green indicates the indoor TSP samples collected in Como. These images were generated using *MicrobiotaProcess* (v 1.10).

A.

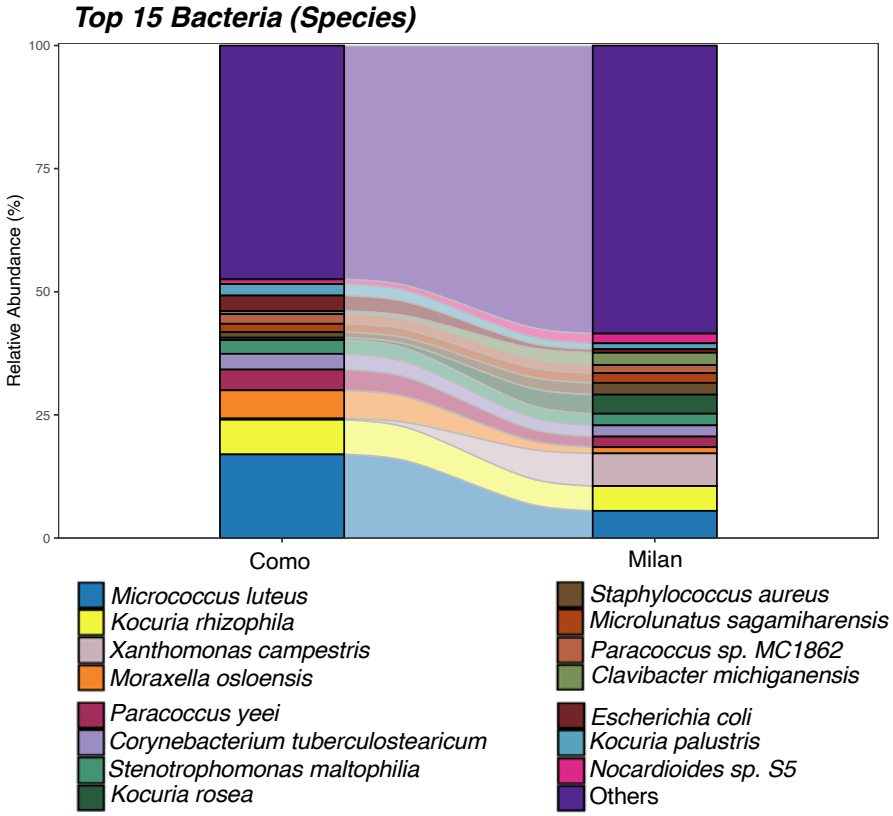

B.

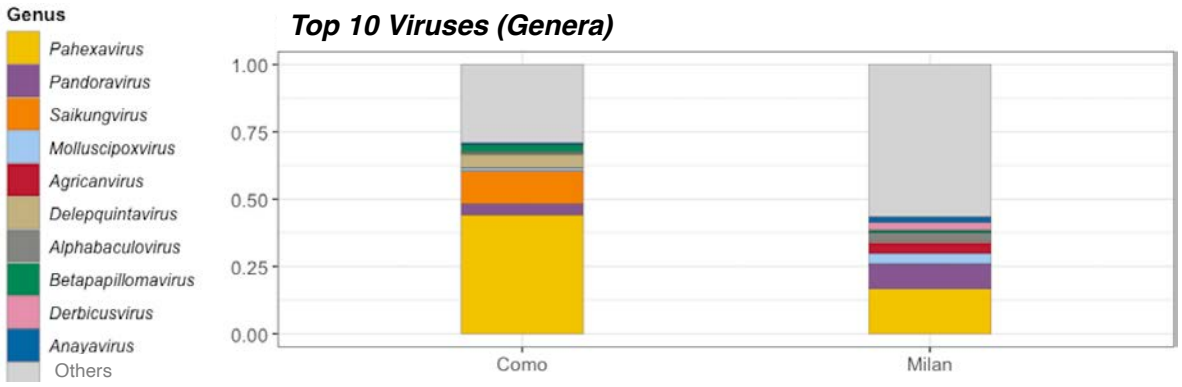

Figure 17. The barplots describe the most abundant taxa found across all the indoor TSP samples collected from Como (left) and from Milan (right). In Panel A: the top 15 bacteria species. Panel B: top 10 virus genera, the y axis indicates the relative abundance of each genus. In both plots, "*Others*" indicates the species out of the top taxa. These images were generated using *MicrobiotaProcess* (v 1.10) and *microViz* (v 0.10).

1.3.3 Comparison of outdoor and indoor TSP microbiome

The mean concentration of DNA extracted from outdoor filters was 26.2 ng/µL (sd = 12.3). After sequencing, we excluded from the analysis samples with sequencing depth less than 100,000 reads. We analyzed 14 outdoor TSP samples (median sequencing depth = 299,543, range = 128,280 – 2,198,650), **Supplemental Table 3**. The top 15 bacterial species identified across all the outdoor samples are described in **Figure 18A**. Some of these bacteria were seen in the indoor samples, such as *Micrococcus luteus*, *Kocuria rhizophila*, *Staphylococcus aureus*, *Kocuria rosea*, and *Nocardiodes sp S5*. The top 10 viruses (genus level) across the two cities are described in Figure **18B.** As seen for the indoor samples, most of the viruses identified in the outdoor samples are from the *Caudoviricetes* class: *Pahexavirus*, *Anayavirus, Andhravirus, Fromanvirus, Pamexvirus, Dexdertvirus,* and *Mosigvirus*. Besides the bacteriophages described in the indoor TSP (*Pahexavirus* and *Anayavirus*), we identified the following top 10 genera: *Staphylococcus* phages (*Andhravirus*) associated with *Staphylococcus aureus*, a common member of the upper-respiratory microbiota; *Pseudomonas* phages (*Pamexvirus*) found in *Pseudomonas aeruginosa,* a bacterium that can cause disease in plants and humans; and *Gordonia* phages (*Dexdertvirus*) found in *Gordonia terrae*, a bacterium isolated from soil.

When we compared the 37 TSP indoor samples collected in the office with the 14 TSP outdoor samples, we did not observe a significant difference in alpha diversity (Wilcoxon test, p-value = 0.2). However, the beta diversity was significantly different between the two groups (ANOSIM, R = 0.25, p-value = 0.01), and it explains about the 4% of the diversity (PERMANOVA, p-value = 0.01), **Figure 19**. In addition, we also observed differences in microbiota composition (**Table 4)**. The abundance of several *Micrococcus* and *Paracoccus* species (e.g., *Micrococcus luteus*, *Micrococcus yunnanensis*, *Micrococcus sp. KBS0714*, *Paracoccus contaminans*, *Paracoccus yeei*, *Paracoccus sanguinis*, *Paracoccus sp. MC1862*) was higher in the indoor TSP samples compared to the outdoor, also the relative abundance of *Moraxella osloensis* and *Corynebacterium diphtheriae* were higher in the indoor samples. The only species more abundant in the outdoor samples was *Pantoea agglomerans* a bacterium commonly found in plants. We did not observe a difference in virus abundance at the genus level because the *Pahexavirus* was the dominant genus in both sample types. When we analyzed all the pathways (N of pathways = 432, range of reads assigned = 372,214 – 3,276) through ANCOM-BC analysis, the differences between the two types of exposures were plant and yeast pathways that enriched in the outdoor samples compared to the

indoor. These include Flavone and flavonol biosynthesis (lfc = 0.9, p-value < 0.001, FDR < 0.001), cell cycle – yeast (lfc = 0.6, p-value = 0.02, FDR = 0.07), and mitophagy – yeast (lfc = 0.6, p-value = 0.02, FDR = 0.08). Finally, when we analyzed the antimicrobial resistance profile in both indoor and outdoor TSP samples, we did not find significant differences. Both indoor and outdoor TSP samples contained broad spectrum antibiotic resistance genes (i.e., tetracyclines). The top 20 antimicrobial chemical classes identified in our samples are shown in **Figure 20**. The Lead resistance, quaternary ammonium compounds [QACs] resistance, Trimethoprim, Zinc resistance were only in indoor TSP samples and the Nucleosides, Pactamycin, and Sodium resistance were found only in outdoor TSP samples. All these results suggested that the TSP microbiome reflects the complexity of the environment.

Table 4. ANCOM-BC analysis on bacterial abundance in outdoor and indoor TSP samples

Species	**Log-fold change (TSP outdoor)**	**FDR**
Moraxella osloensis	-1.53	0.01
Micrococcus luteus	-0.56	0.10
Paracoccus contaminans	-1.41	0.02
Paracoccus yeei	-1.72	0.01
Paracoccus sanguinis	-1.71	0.01
Micrococcus yunnanensis	-1.27	0.07
Paracoccus sp. MC1862	-1.73	0.01
Micrococcus sp. KBS0714	-1.46	0.01
Corynebacterium diphtheriae	-1.77	0.01
Pantoea agglomerans	0.88	0.02

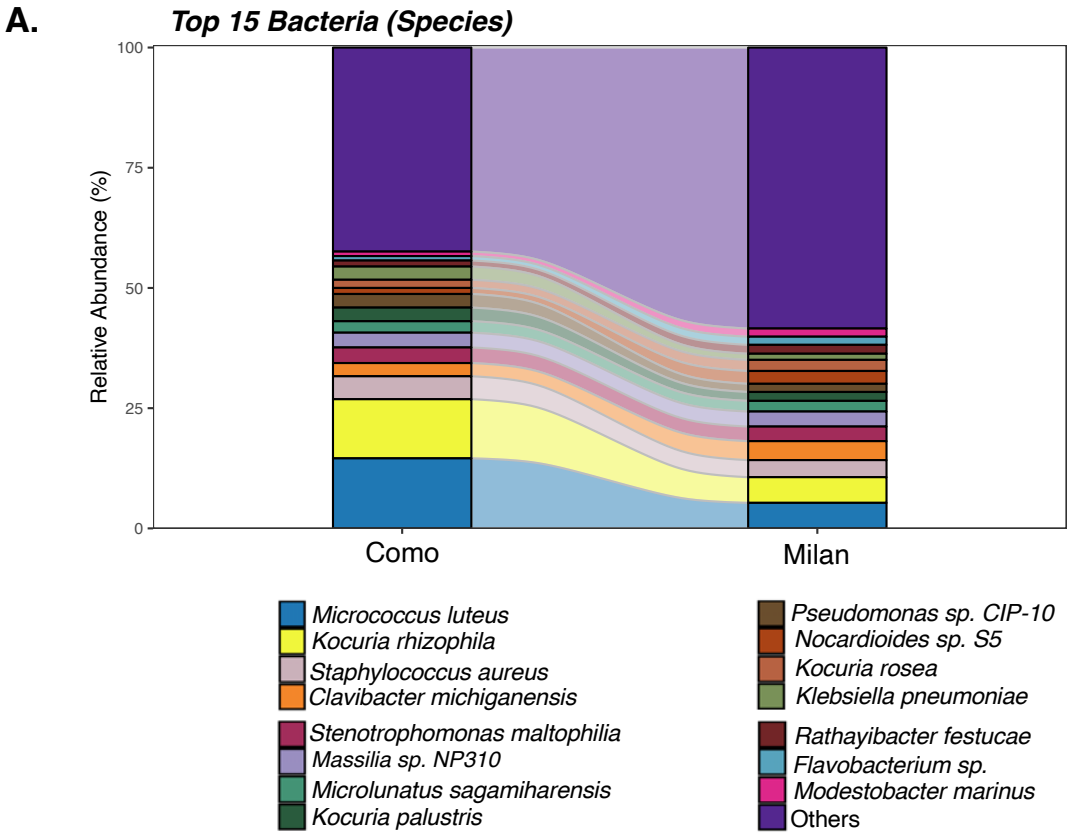

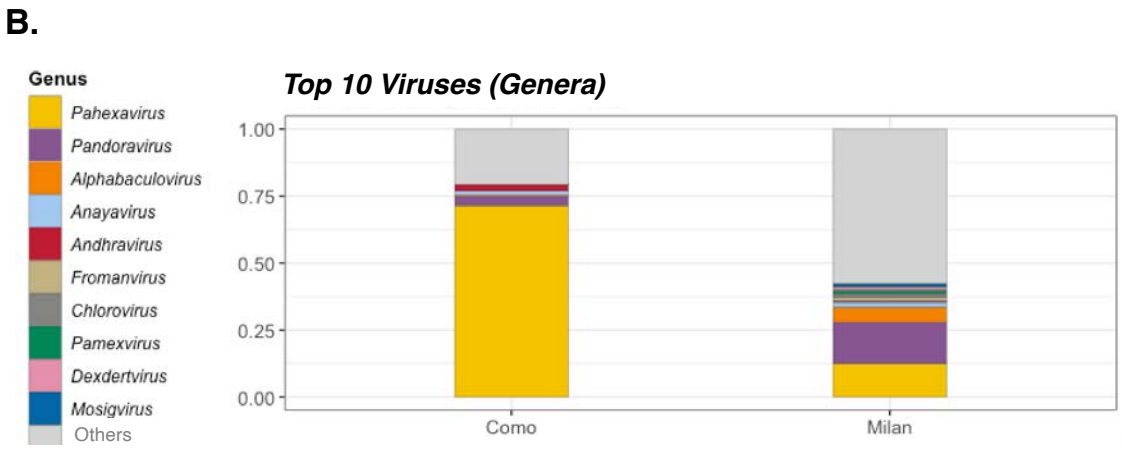

Figure 18. The barplots describe the most abundant taxa found across all outdoor TSP samples from Como (left) and from Milan (right). In panel A: the top 15 bacterial species. In panel B: the top 10 virus genera, the y axis indicates the relative abundance of each genus. In both plots, "*Others*" indicates the species out of the top taxa. These images were generated using *MicrobiotaProcess* (v 1.10) and *microViz* (v 0.10).

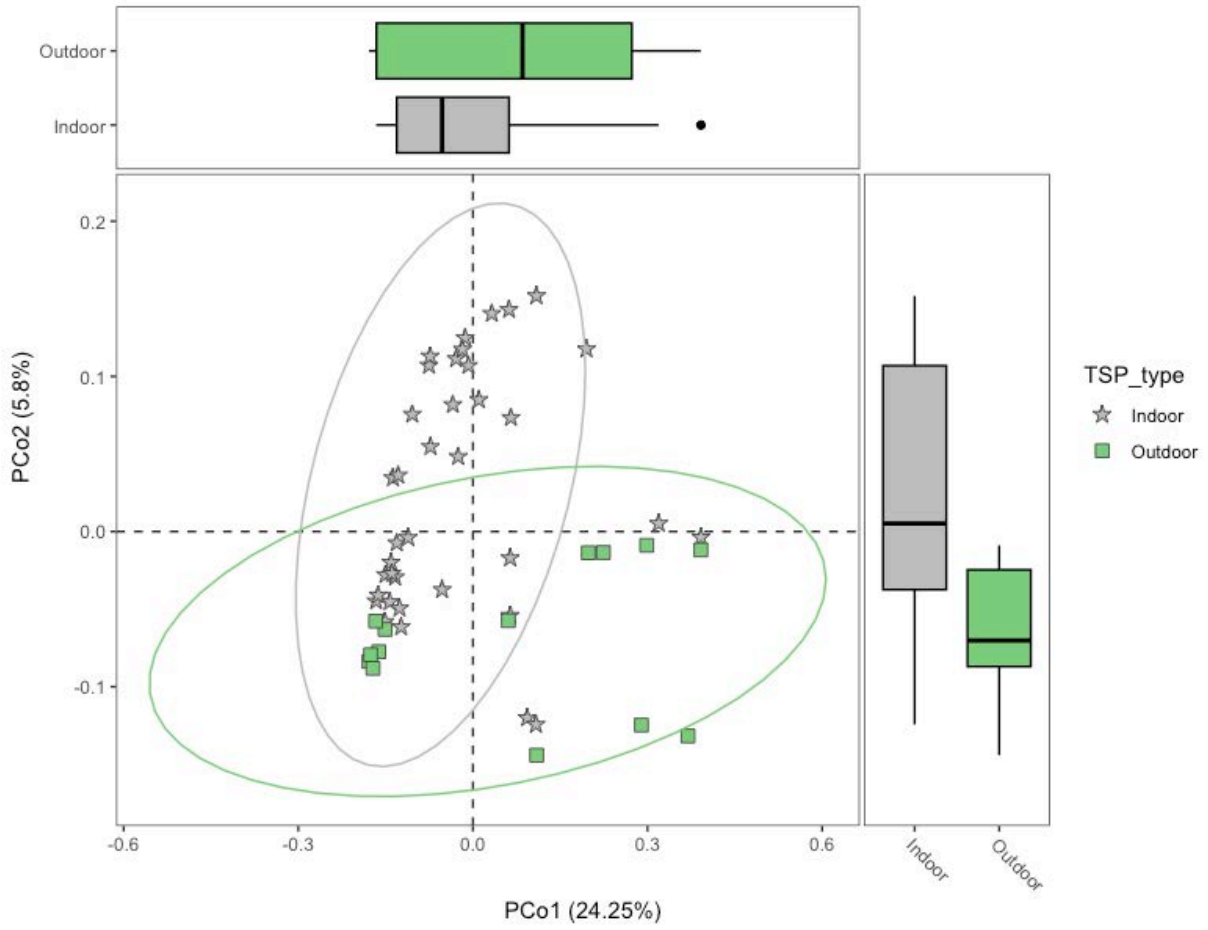

Figure 19. The plot shows the difference in beta diversity (Bray-Curtis) between the TSP indoor samples (grey stars) and the TSP outdoor samples (green squares). This plot was generated using *MicrobiotaProcess* (v 1.10).

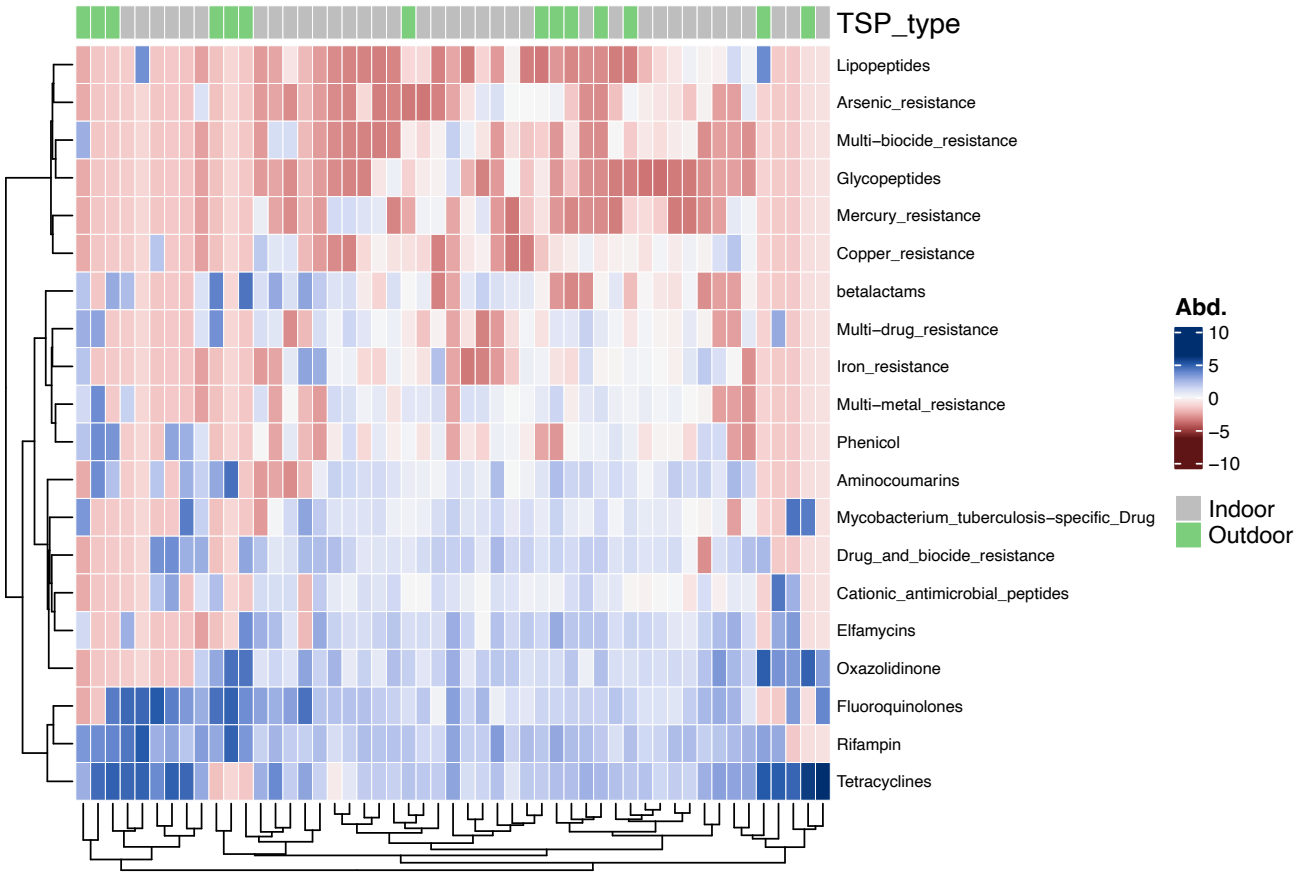

Figure 20. The top 20 antimicrobial chemical classes identified in both outdoor and indoor TSP samples using shotgun sequencing data and the MEGARes (v3.0) database. Each row represents a distinct class, and the color indicates the abundance in each sample. The abundance was centered log-ratio (CLR) transformed. This plot was generated using *microViz* (v 0.10).

1.4 DISCUSSION

Air particulate matter is widely studied for its adverse effects on human health, but few studies have analyzed the microbiome associated with these particles. The particulate matter microbiota was characterized only in a few cities located in China (Beijing and Urumqi) and Italy (Milan), and these studies focused on outdoor exposure of PM_{10} or $PM_{2.5}$ (Bertolini et al., 2013; Cao et al., 2014; Gou et al., 2016; Qin et al., 2020). In this section, we analyzed both the concentration and the microbiome of indoor and outdoor TSP samples collected weekly over 3 weeks in Milan and Como.

When we analyzed the concentration of TSP between the two seasons, we obtained different results based on the type of exposure. The indoor TSP concentrations did not differ between the two seasons, while the outdoor TSP concentrations were higher in winter compared to summer. Only the first group (R1) did not report a significant difference, probably due to the occurrence of intense rainy events that caused a sharp decrease in the measured TSP levels. Our analysis also suggested that the outdoor TSP variations only partially influenced indoor exposure, as indicated by the absence of correlations between the indoor and outdoor levels. As it is well documented, the PM concentration levels in an indoor environment are influenced by multiple variables (Li et al., 2017). In addition, the measured indoor TSP concentrations were lower than the corresponding outdoor ones, with indoor/outdoor (I/O) ratios <1. The lowest I/O ratios (on average ~ 0.2 and 0.4 during winter and summer, respectively) were observed for the basement offices in Como (R3) which were characterized by very low indoor TSP levels, probably because of the general building characteristics (building of recent construction, without operable windows and served by a mechanical HVAC system equipped with filters) and geographical setting (a low-density suburban area of a medium-sized city).

In the indoor TSP samples, we observed differences in alpha and beta diversity among the cities. It seems that the city with a higher concentration of TSP has also higher diversity; this could be a consequence of the higher number of particles that are available to transport microorganisms. The bacteria identified in these samples seem to include mostly soil, plants, and human skin bacteria. The *Micrococcus luteus* was found in almost every sample. This bacterium, *Micrococcus luteus,* is found in human skin, soil, dust and air (Ahle et al., 2023; Cao et al., 2014; Madsen et al., 2023.).

Other bacteria already found in airborne samples and abundant in our samples were *Paracoccus yeei, Kocuria rosea, Kocuria rhizophila,* and *Moraxella osloensis* (Cao et al., 2014; Kooken et al., 2012; Madsen et al., 2023). We also found opportunistic pathogens of the upper respiratory tract such as *Staphylococcus aureus.* Interestingly, in a few samples of offices located close to green areas and with operable windows, we found a high relative abundance of *Xanthomonas campestris* and *Clavibacter michiganensis*, two common plant pathogens. This might suggest that the outdoor environment affected the indoor TSP microbiome. The viruses identified in the indoor samples were mostly bacteriophages and they reflected the bacterial composition found in our samples. They were mostly bacteriophages of bacteria found in soil and human skin, such as *Agricanvirus* and *Pahexavirus.* Overall, it seems that the concentration of indoor TSP correlates with the diversity of its microbiota. Additionally, the bacteria and viruses found in the samples are closely related to the environment and are probably influenced by the presence of plants, animals, and people, as suggested by the opportunistic pathogens identified in the samples.

Finally, we compared the indoor TSP microbiome with the outdoor. The outdoor TSP microbiome included in its top taxa some of the bacteria identified in the indoor samples, such as *Kocuria rhizophila* and *Micrococcus luteus* which are bacteria found in soil and on human skin. There was also the presence of opportunistic pathogens of the respiratory tract like *Staphylococcus aureus, Pseudomonas sp.*, and *Klebsiella pneumoniae.* However, the antimicrobial resistance profile was very similar between the two sample types. Besides these similarities, several species of *Corynebacterium* and *Paracoccus* were enriched in the indoor samples, and we also found differences in the microbial pathways. This highlights how the indoor TSP can be influenced by multiple variables other than the outdoor environment, as already suggested by the differences in TSP levels between the indoor and the outdoor samples. However, we did not observe a difference in virus relative abundance at the genus level because the *Pahexavirus* was the dominant genus in both samples. This could be a consequence of the limited number of sequences due to the low DNA concentration in the environmental samples. Overall, we noticed differences in both concentrations and microbiome composition between the different types of TSP samples.

SECTION 2

The association of TSP with the upper respiratory microbiome

2.1 SUMMARY

The upper respiratory tract is an important interface with the external environment, and its microbiome is a key factor in the host defense mechanisms. However, the microbial community of the upper respiratory tract in healthy adults remains less well characterized compared to other microbiomes (e.g. gut, and vaginal microbiomes). In addition, current studies on the effects of particulate matter exposure on the respiratory microbiome are limited to PM_{10} and $PM_{2.5}$. TSP exposure has never yet been studied in association with the upper respiratory tract microbiota. In this section, we describe the upper respiratory tract microbiome in healthy subjects and analyze the effects of indoor TSP exposure on the microbial community using the data and the biological samples described in **Section 1.2**. First, we characterized the microbiome of the anterior nares and compared microbial profiles between winter and summer using both 16S rRNA gene targeting sequencing and whole genome shotgun (WGS) sequencing data. We also provide a comparative analysis of the microbiome between the anterior nares microbiome and the nasopharynx microbiome using WGS sequencing data. Finally, we investigated how indoor TSP exposure affects both the anterior nares and the nasopharynx microbiome taking into account hours spent and use of face masks in the office.

2.2 MATERIAL AND METHODS

2.2.1 Respiratory Samples: collection and DNA extraction

Anterior nares and nasopharynx swabs were collected from each subject using FLOQSwab (Copan, Italy). To sample the anterior nares, the swab was inserted in the subject's nostril and was slowly rotated 4-5 times, pressing against the inside of the nostril. The same swab was also used to sample the other nostril. To sample the nasopharynx area, a swab was gently inserted in one nostril and stopped when resistance was met. It was then rotated for a few seconds. During the sample collection, clean swabs were opened and swirled in the room as negative controls. Right after the collection, all samples were stored at -80ºC. The DNA was extracted from all biological samples using the QIAmp UCP Pathogen Mini kit spin column protocol (Qiagen, Hilde, Germany); we included negative controls during the extraction process. After DNA extraction the DNA was quantified using the Qubit dsDNA High Sensitivity Assay kit (Invitrogen).

2.2.2 Respiratory Samples: 16S rRNA and shotgun sequencing

An aliquot of the DNA extracted from the anterior nares was shipped to the sequencing service facility Personal Genomics Srl (Verona, Italy) for target gene (amplicon) sequencing of the 16S rRNA gene. The Labchip DNA High Sensitivity kit (Perkin Elmer, Waltham, MA, USA) and the Qubit dsDNA BR assay kit (Thermofisher Scientific, Waltham, MA, USA) were used to evaluate and quantify the library. The V3-V4 region of this gene was amplified using the Pro314F and Pro805R. The Illumina MiSeq platform (Illumina, San Diego, CA, USA) was used to sequence the samples and produce a paired-end library of 300 bp. The remaining DNA extracted from anterior nares swabs and the DNA extracted from nasopharynx swabs were used to sequence the whole genome by shotgun sequencing as described in **Section 1.2.2.** Briefly, the paired-end libraries were prepared using the NexteraXT DNA library preparation kit (Illumina). Three negative controls were included: sampling negative control (clean swabs swirled in the room); one negative control from DNA extraction and one negative control for library preparation. Finally, an equimolar pool was created, and it was quantified and sequenced on the Illumina Novaseq 6000 S2 in one single run.

2.2.3 Bioinformatics and Statistical analysis (16S rRNA sequencing data)

The sequences generated from the 16S rRNA sequencing were imported and denoised using QIIME 2 v. 2022 DADA2 pipeline (Bolyen et al., 2019). Taxonomy was assigned using a pre-trained Naïve Bayes classifier (Silva database, release 138, 99%). The QIIME outputs were imported in R using the *qiime2R* package to perform the diversity and taxonomic analyses. Both alpha and beta diversities were analyzed using *phyloseq* (v 1.42) and *MicrobiotaProcess* (v 1.12) packages. The alpha (α) diversity was estimated using the Shannon Index, Chao1, and Observe species metrics. The difference in alpha between the two seasons was tested using a paired t-test. The beta (ß) diversity was estimated with a Bray-Curtis distance matrix. We analyzed the beta diversity in the two seasons using the Analysis of Similarities (ANOSIM) and the permutational multivariate analysis of variance (PERMANOVA) with 999 permutations. Among the most abundant 200 taxa found across all samples in each season, we selected the ones that were shared across season to analyze their association with seasons. We used the Analysis of Compositions of Microbiomes with Bias Correction (ANCOM-BC) package (v. 1.6.4) to analyze observed relative

abundance corrected for the three independent cohorts. In the model, we included season, age, and gender. The ANCOM-BC was performed using the default settings, and the mean difference (W) was considered significant when a p-value < 0.05 and FDR < 0.10 were reached. All 16S rRNA sequence analyses are summarized in **Figure 21**. All statistical analyses were performed in R, v 4.2.1.

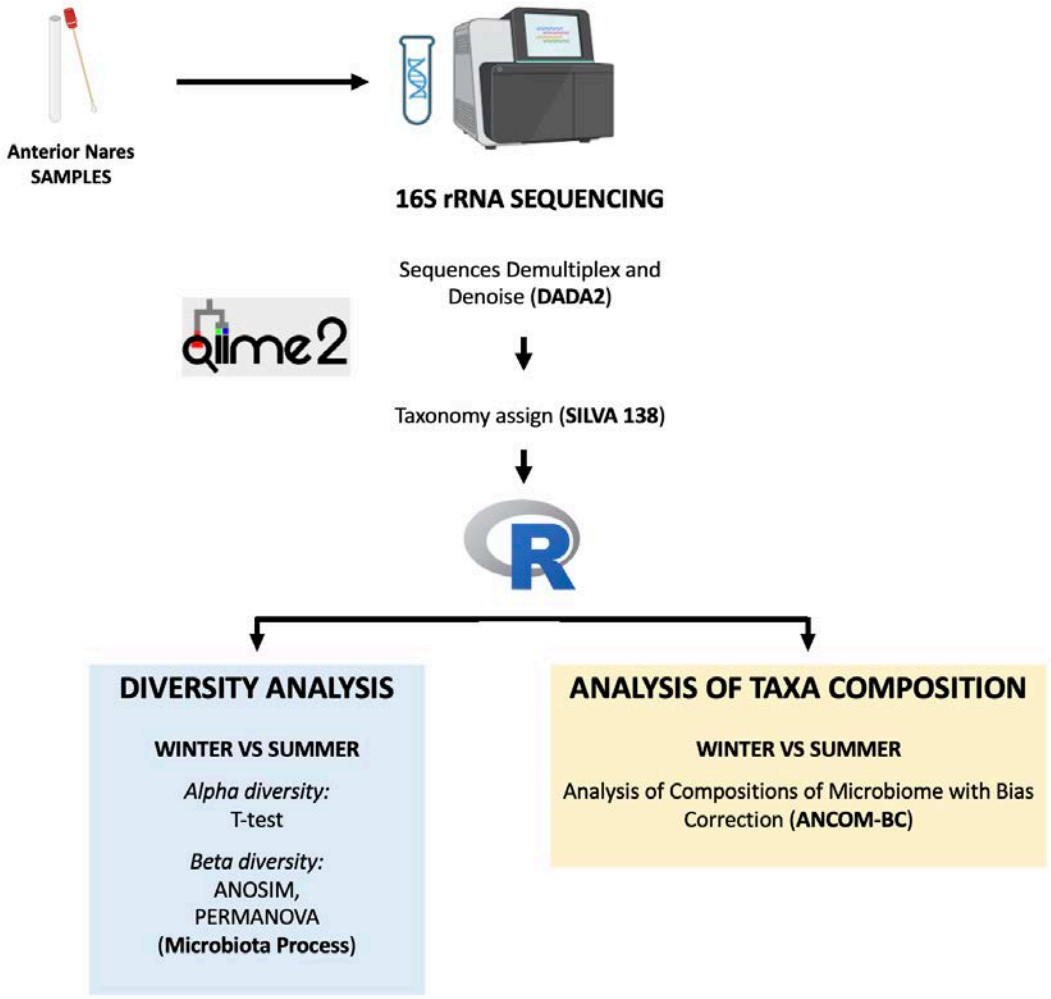

Figure 21. The bioinformatic pipeline used to analyze the anterior nares (AN) 16S rRNA data. First, the sequencing data were cleaned, demultiplexed and denoised using DADA2 on QIIME 2. Then, taxonomy was assigned using the SILVA 138 database. All QIIME outputs were imported in R for downstream analysis. Alpha diversity (blue box) was estimated using the Shannon Index and then compared between the two seasons using a paired t-test. Beta diversity (blue box) was calculated using the Bray-Curtis matrix. ANOSIM and PERMANOVA were performed to assess differences between the seasons. Finally, the top 200 bacteria were selected (yellow box) to analyze differences in bacterial abundance among the two seasons.

2.2.4 Bioinformatics and Statistical analysis (metagenomics)

The reads obtained from the WGS sequencing were analyzed following the same steps described in **Section 1.2.3** for the TSP samples. We used Bcl2fastq (v 2.20) and fastp (v 0.20.1) to demultiplex and trim our sequences, and Kraken (v 2.1.2) and Bracken (v 2.5) to assign the taxonomy. The contaminants in the OTU tables were identified using the R package *Decontam*, and the *phyloseq* (v 1.42) and *MicrobiotaProcess* (v 1.10) were used to analyze the microbiome diversity. The alpha and the beta diversities were analyzed using the same methods described in **Section 2.2.4**. The co-occurrence between the bacterial taxa was analyzed using the Spearman correlation test (Spearman test, rho > 0.50, p-value < 0.05) and the networks were generated using *phylosmith* (v. 1.0.6). The most abundant 200 taxa across all samples were selected to analyze their difference between the two seasons using the Analysis of Compositions of Microbiomes with Bias Correction (ANCOM-BC) package (v. 1.6.4). The model also included age and gender, and corrected for the three independent cohorts (G1, G2, and G3). The ANCOM-BC was performed using the default settings, and the mean difference (W) was considered significant when a p-value < 0.05 and FDR < 0.10 were reached. The same model was also used to analyze the difference in taxa compositions between the anterior nares and the nasopharynx microbiome. The association between indoor TSP exposure and the microbiome was analyzed through multivariable association using the *nlme* package (v. 3.1). Before, we transformed the bacterial abundance using the centered log-ratio (CLR) transformation. The model was adjusted for age, gender, days spent in the office, and habitual use of a face mask. The sample observations were grouped by "*subject id"*. We also check if the respiratory microbiome correlates with the microbiome of TSP indoor using the R package *ggstatsplot* (v. 0.12.2). Finally, we analyzed the correlation (Spearman test) between the indoor TSP exposure and the KEGG pathways of both anterior nares and nasopharynx microbiome using the R package *phylosmith*. All statistical analyses were performed with R software, v 4.2.1.

2.3 RESULTS

2.3.1 Description and characteristics of the enrolled subjects

This study involved 34 healthy subjects: 22 workers employed at the University of Milan and 12 at the University of Insubria in Como. These 34 subjects were separated into 3 sub-groups (G1, G2 and G3) and were first recruited in the winter season; 26 of these subjects remained in the study for the summer season (G1: November/May; G2: January-February/June; G3: March/July). The main characteristics of these volunteers are described in **Table 5.** Most of the subjects lived in the city or small towns in residential areas with moderate traffic. In both seasons, we observed that the subjects spent on average 4 days per week in the office, but in the summer the number of people wearing masks in the office was lower compared to the winter. Most of the people recruited (about 70%) were not smokers and they did not share indoor space with smokers (apartment and/or office). At the end of the recruitment, we collected 173 nasal swabs (anterior nares): 99 during the winter and 74 during the summer. In the summer, we also collected 74 nasopharynx swabs.

Table 5. Subject Characteristics

Characteristics	Winter season (N= 34)	Summer season (N= 26)	p-value*
Gender, **n (%)**			
Female	19 (55.9%)	17 (65.4%)	0.7
Male	15 (44.1%)	9 (34.6%)	
Age**, mean (SD)**	38.3 (9.9)	38.8 (8.7)	0.8
BMI**, mean (SD)**	23.9 (3.2)	24.3 (3.2)	0.6
Smoking**, n (%)**			
No	26 (76.5%)	19 (73.1%)	1.0
Yes	8 (23.5%)	7 (26.9%)	
Indoor space shared with Smokers, **n (%)**			
No	32 (94%)	26 (100%)	0.5
Yes	2 (0.06%)	0 (0)	

***Days in office per week,* mean (SD)**	4.3 (0.9)	4.4 (0.8)	0.9
***Wearing face mask in the office*, n (%)**			
No	11 (32%)	21 (81%)	0.0003*
Yes	23 (68%)	5 (19%)	
***Residential area*, n (%)**			
City	17 (50%)	12 (46.2%)	0.7
Small town	15 (44.1%)	13 (50%)	
Rural area	2 (5.9%)	1 (3.8%)	
***Traffic level in residential area*, n (%)**			
High	11 (32%)	7 (27%)	0.6
Medium	18 (53%)	16 (62%)	
Low	5 (15%)	3 (12%)	
***Pets*, n (%)**			
Yes	12 (35%)	10 (38%)	0.7
No	22 (65%)	16 (62%)	

*The Wilcoxon rank-sum test was performed for the continuous variables and the Fisher test for the categorical variables

2.3.2 The microbiota of anterior nares and seasonal variations

We determined whether season could affect the microbiota in healthy subjects using both 16S rRNA and shotgun sequencing data. All the samples with sequencing depth less than 4,000 reads were excluded from the analysis. After filtering, we had 16S rRNA data available for 156 samples: 95 samples collected during the winter and 61 anterior nares swabs collected during the summer (median sampling depth = 13,241 reads, range: 4,106 – 57,834 reads). From the metagenomics data, we were able to analyze 162 samples: 89 samples from the winter, and 74 samples from the summer (median sampling depth = 3,506,075 reads, range: 2,180,154 – 94,975,134). Before the analysis, we checked if alpha and beta diversity were comparable among sub-groups (G1, G2, and G3), and we did not find any difference in alpha diversity (t-test, p-value > 0.05) neither in beta diversity in both sequencing data: 16S rRNA and metagenomics data (**Supplemental Figure 3**).

First, we analyzed the difference in microbiota diversity between the two seasons using the 16S rRNA data. The alpha diversity, estimated with the Shannon Index, was significantly higher (t-test, p-value = 0.01) in the summer compared to the winter season (**Figure 22A**). The same significant lower diversity in the summer was observed with Chao1 and Observe metrics (**Supplemental Figure 4**). The beta diversity was significantly different between the two seasons (PERMANOVA, Bray-Curtis: $R^2 = 0.04$, p-value = 0.001; **Figure 22B**). Therefore, we analyzed how the microbial composition was impacted by season using both the 16S rRNA and the metagenomics data. The top 10 genera in the 16S rRNA data found in both seasons are described in **Figure 23A**, and the top 15 in species metagenomics data are described in **Figure 23B**. At the genus level (16S rRNA data), we found significantly higher relative abundance of *Moraxella* (W = 3.0, p-value = 0.002, FDR = 0.03) in the winter and a significant lower abundance of *Staphylococcus* (W = -4.3, p-value < 0.0001, FDR = 0.0004), *Cutibacterium* (W = -4.4, p-value < 0.0001, FDR = 0.0004) and *Alloprevotella* (W = -2.9, p-value = 0.004, FDR = 0.04). In line with these results, at the species level (metagenomics data) we found a significant increase in *Moraxella nonliquefaciens* relative abundance (W = 4.4, p-value < 0.0001, FDR = 0.002) and *Moraxella catarrhalis* (W = 3.6, p-value = 0.0004, FDR = 0.03) in the winter (**Figure 24**). In the summer, we found an increase in the relative abundance of many *Staphylococcus* and *Cutibacterium* species. Specifically, *Staphylococcus hominis* (W = -3.0, p-value = 0.003); *Staphylococcus epidermidis* (W = -2.5, p-value = 0.01); *Cutibacterium acnes* (W = -2.5, p-value = 0.01); *Cutibacterium avidum* (W = -2.5, p-value = 0.01); *Cutibacterium granulosum* (W = -2.3, p-value = 0.02). Although these analyses showed an FDR higher than 0.10. From the co-occurrence analysis, we found a positive correlation between the relative abundance of *Moraxella catarrhalis* and *Moraxella nonliquefaciens* (rho = 0.4, p-value < 0.001). The *Staphylococcus* and *Cutibacterium* species with lower relative abundance in the winter were correlated with each other, (**Figure 25**). These results suggested a higher relative abundance of gram-negative bacteria in the anterior nares during the cold season.

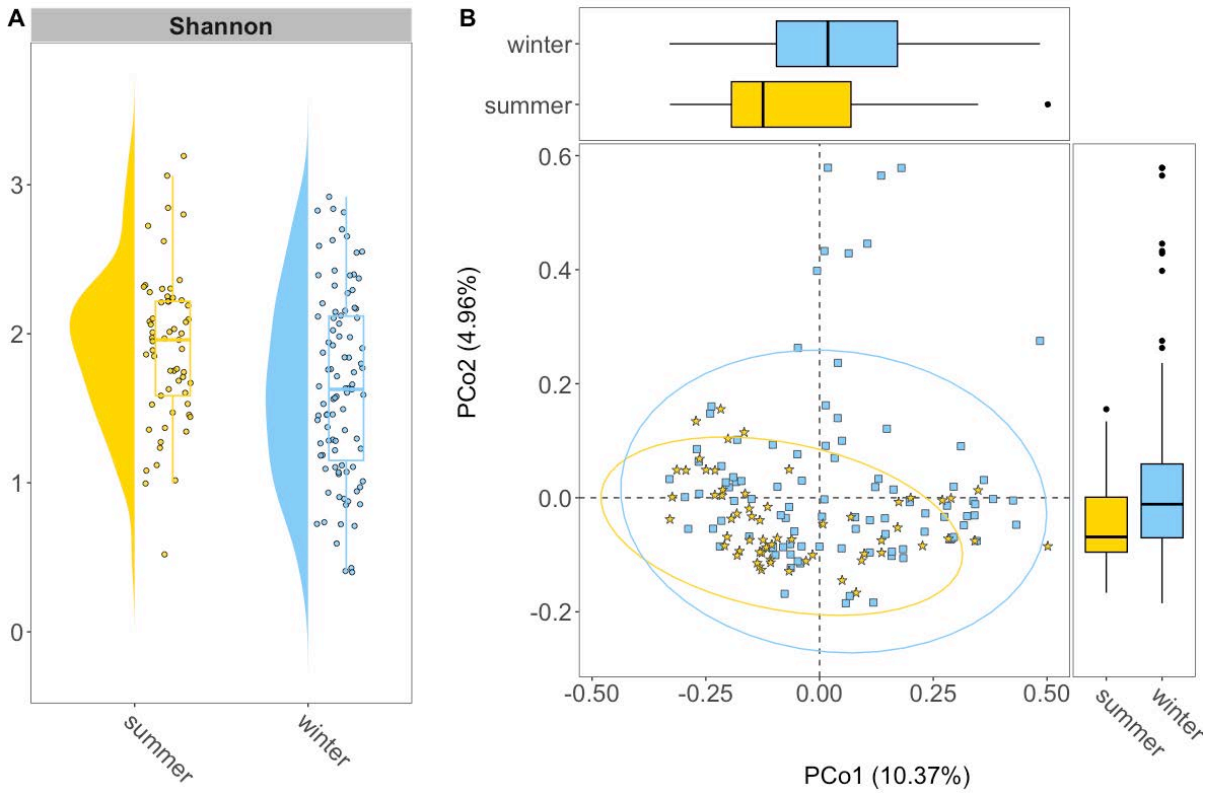

Figure 22. (**A)** The boxplot shows the alpha diversity (Shannon index) in samples from summer (yellow) and winter (blue). Dots indicate the alpha diversity of each sample. (**B)** Principal coordinate analysis (PCoA) calculated from the Bray-Curtis distance matrix in anterior nares microbiota samples from healthy subjects during summer (yellow) and winter (blue). These images were generated using *MicrobiotaProcess* (v 1.10).

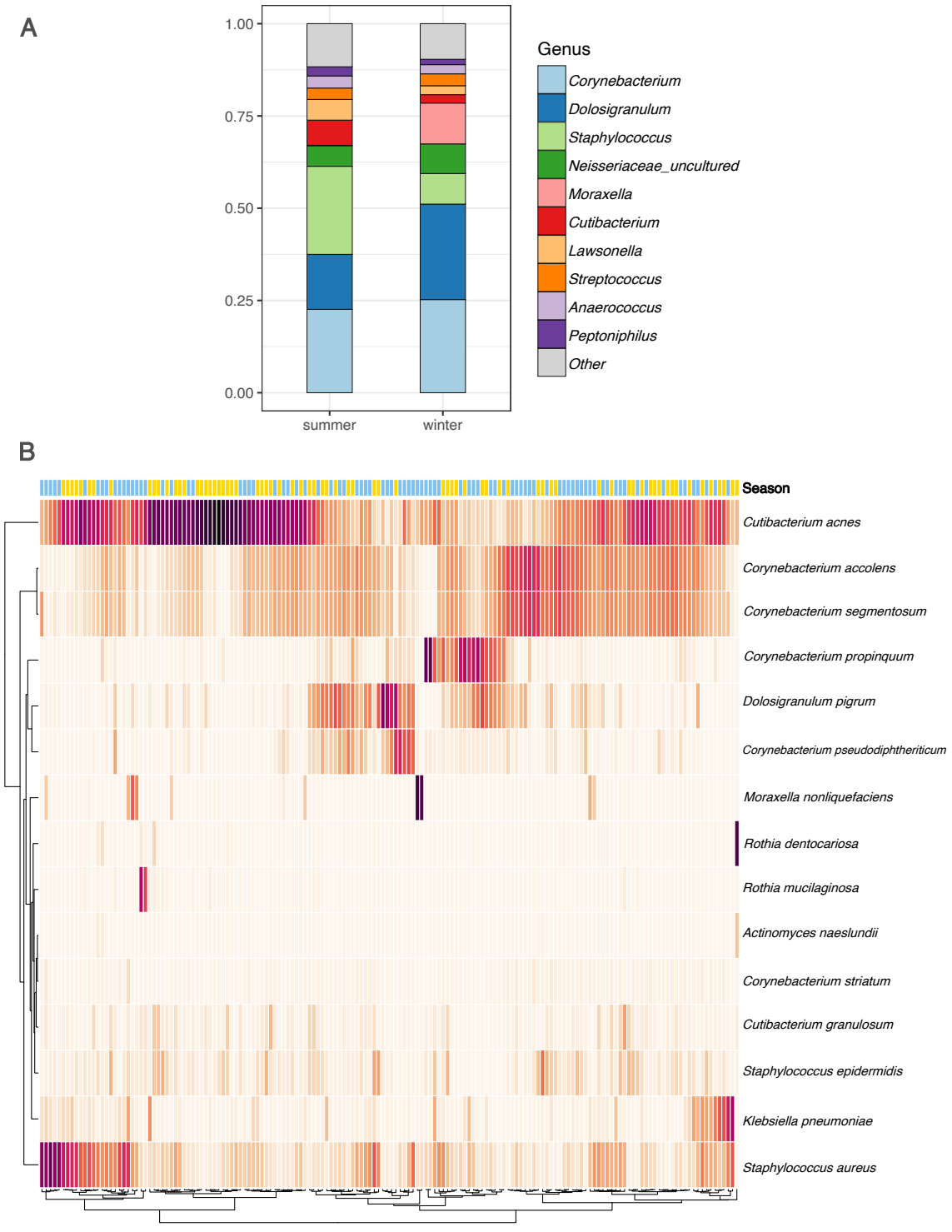

Figure 23. (A) Displays the relative abundance of the top 10 bacterial genera identified in both seasons using the 16S rRNA sequencing data. (B) Features a heatmap of the top 15 species found in the two seasons: winter (blue rectangles) and summer (yellow rectangles). In each row, color intensity indicates the relative abundance of that bacterial species in the samples, the darker the color, the higher the relative abundance. These images were generated using *microViz* (v 1.10).

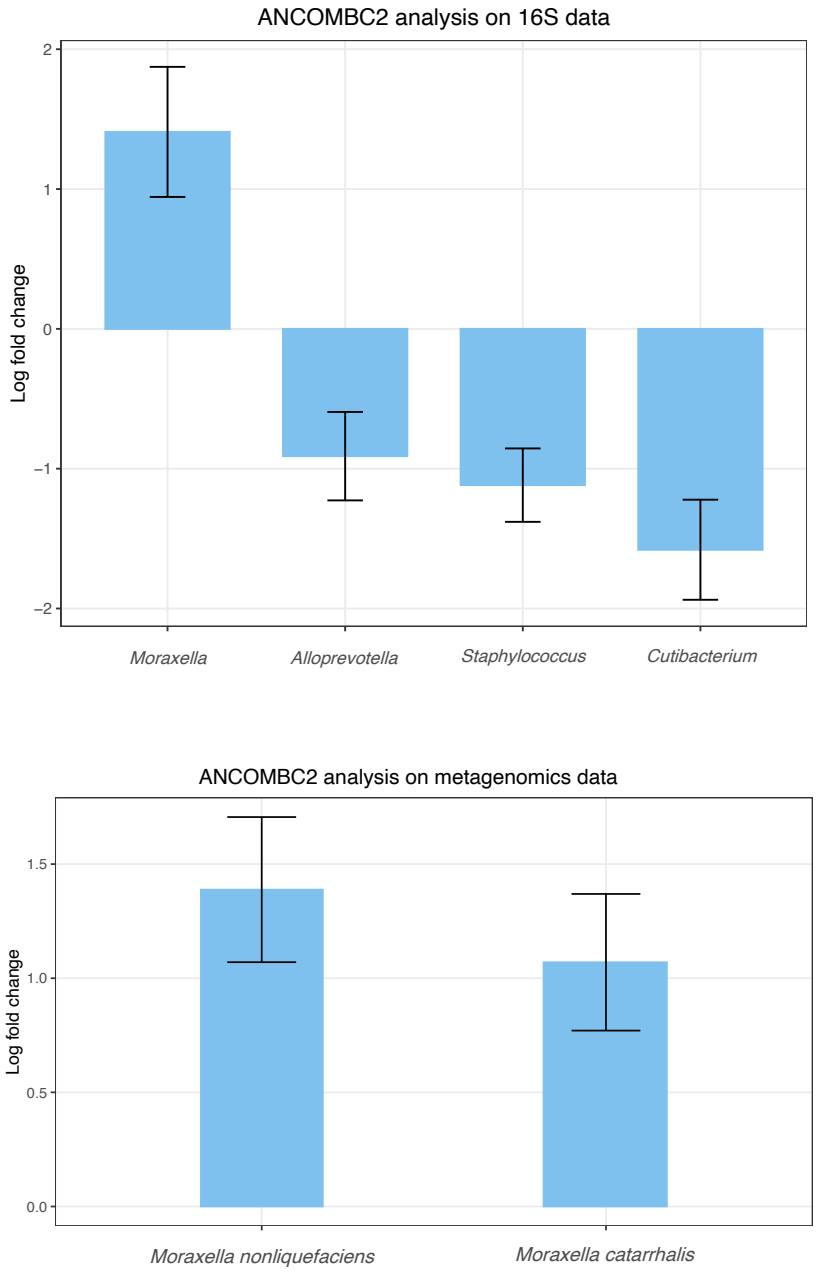

Figure 24. The bar plot shows the log fold changes in the winter season for taxa identified using ANCOM-BC analysis (p-value < 0.05, FDR < 0.10) using both 16S rRNA data (upper panel) and metagenomics data (lower panel).

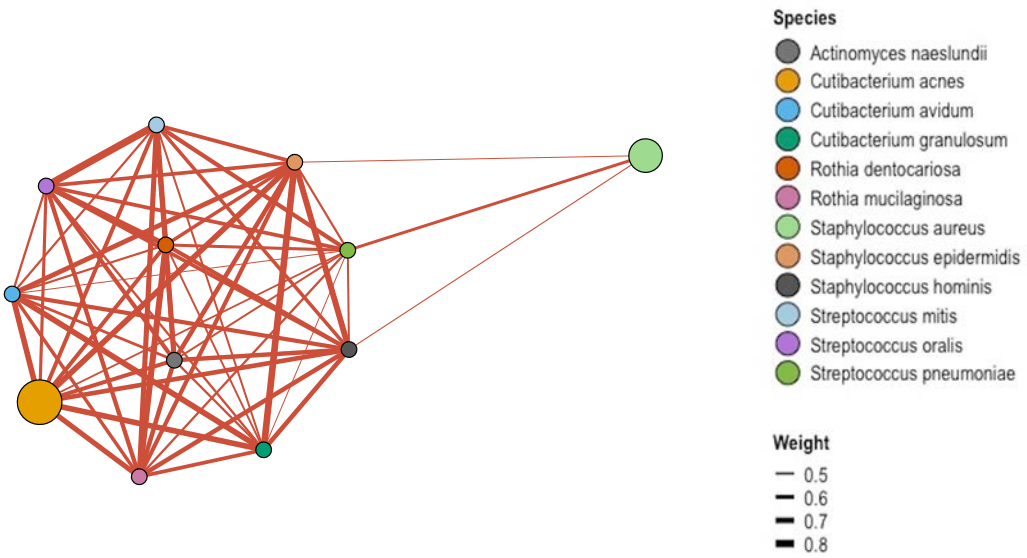

Figure 25. A co-occurrence network was created to examine the correlation between bacterial relative abundances, calculated using the Spearman test (rho > 0.50, p-value < 0.05). The size of the points indicates the mean relative abundance of each bacterium across the samples. This image was generated using *phylosmith* (v 1.0.6).

2.3.3 Comparison of anterior nares and nasopharynx microbiome

In the summer, we collected 74 nasopharynx (NP) swabs (median sampling depth = 26,430,743, range = 4,302,478 – 41,851,762). We compared these samples with the 74 anterior nares (AN) samples collected in the summer and described in **Section 2.3.2**. The alpha diversity was higher (t-test, p-value < 0.01) in the NP samples (Shannon Index, mean = 3.5, sd = 0.5), compared to the AN (Shannon Index, mean = 2.8, sd = 0.6) (**Supplemental Figure 5)**. We observed that 85% of our samples collected from the same subject at the same time point had higher alpha diversity in the NP compared to the AN, 4% had about the same value of alpha diversity, and only 11% had higher alpha diversity in the AN samples compared to the NP **(Figure 26A).** The beta diversity was also different between the two types of microbiomes (PERMANOVA, Bray-Curtis: R2 = 0.12, p-value < 0.001) (**Figure 26B)**. The top 10 taxa identified in both AN and NP samples are represented in **Figure 27**. When we compared the relative abundance of these species, we found several species that were differentially abundant (**Supplemental Figure 6)**. Among the top 10 shared species (**Figure 27**), the AN microbiome showed a higher relative abundance of several *Corynebacterium*, *Cutibacterium* and *Staphylococcus epidermidis*. Specifically, the AN samples

had higher relative abundance of *Cutibacterium acnes* (W = 4.2, p-value < 0.0001, FDR = 0.0001), *Corynebacterium accolens* (W = 2.7, p-value = 0.01, FDR = 0.01), *Corynebacterium segmentosum* (W = 2.8, p-value = 0.01, FDR = 0.01), *Corynebacterium macginleyi* (W = 2.8, p-value = 0.01, FDR = 0.01), *Staphylococcus epidermidis* (W = 4.5, p-value < 0.0001, FDR < 0.0001), and *Corynebacterium kefirresidentii* (W = 3.8, p-value = 0.0001, FDR = 0.001). The NP samples had a higher relative abundance of *Staphylococcus aureus* (W = 6.4, p-value < 0.0001, FDR < 0.0001).

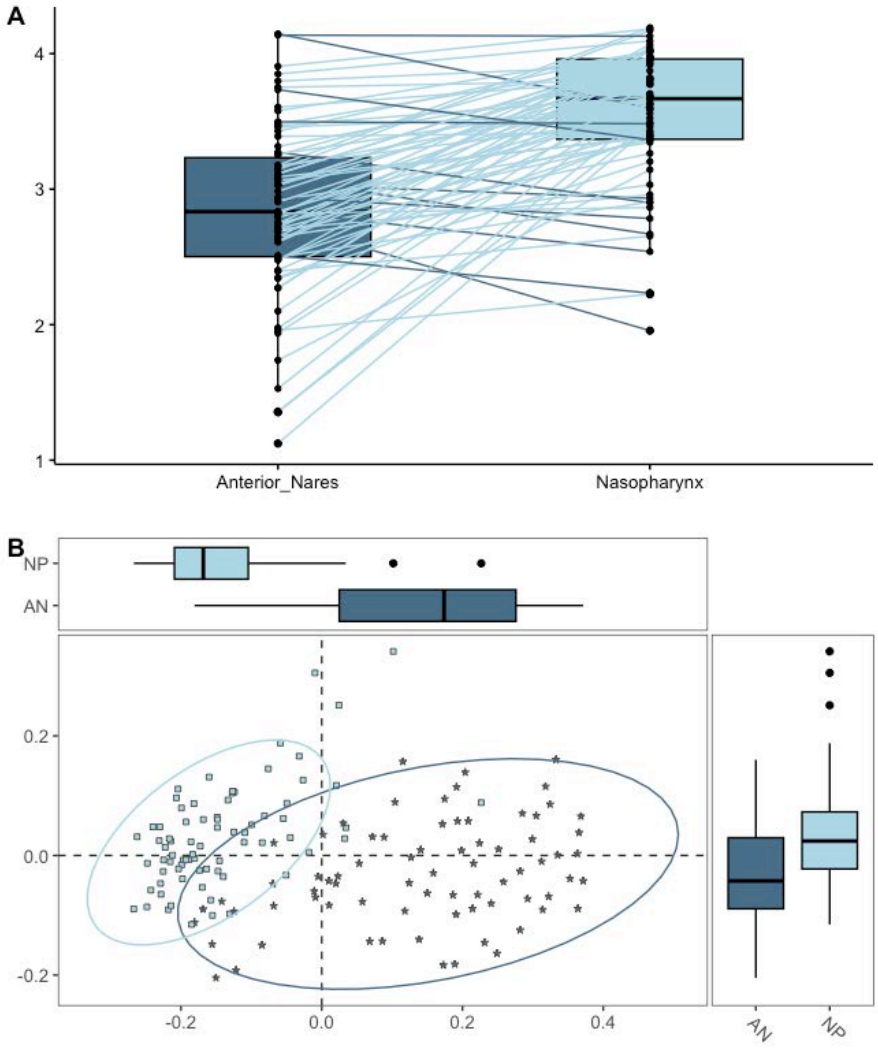

Figure 26. (A) Alpha diversity in the anterior nares microbiome (dark blue) and the nasopharynx microbiome (light blue). The y axis shows the alpha diversity values calculated using the Shannon Index. Each line connects two samples from the same subject, with dark lines indicating samples with higher alpha diversity in anterior nares. (B) Principal coordinate analysis (PCoA) calculated from the Bray-Curtis distance matrix in nasal microbiota samples from healthy subjects in anterior nares (dark blue) and the nasopharynx (light blue).

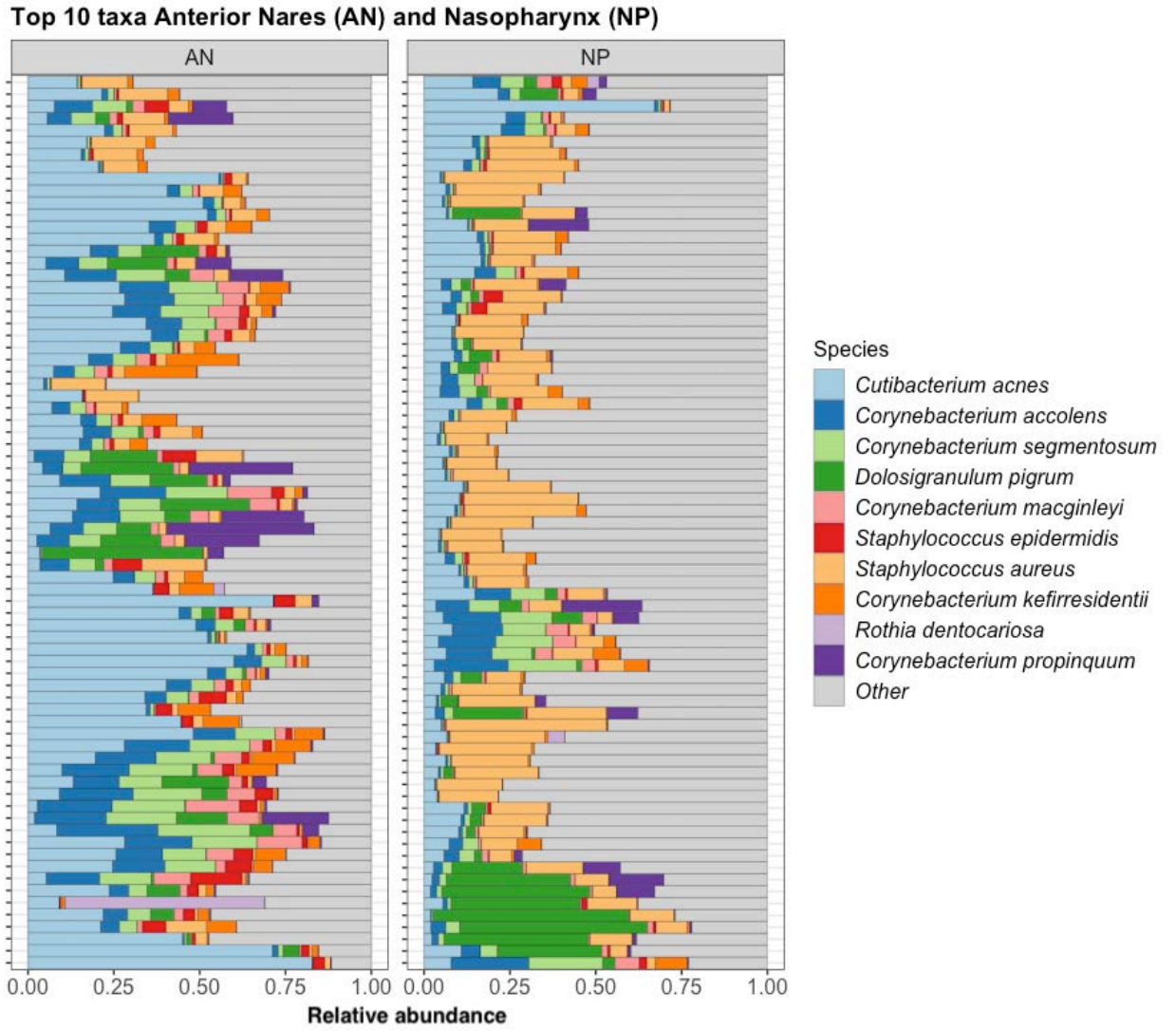

Figure 27. The top 10 bacterial taxa identified in the upper respiratory samples of healthy subjects: on the left the anterior nares microbiome (AN) and on the right the nasopharynx microbiome (NP). The relative abundance of each species is calculated from the OTU table created from the shotgun sequencing data (metagenomics data). This image was generated using *microViz* (v 1.10).

2.3.4 Upper respiratory microbiome and its association with indoor TSP

We analyzed the associations between indoor TSP exposure and respiratory microbiome at the level of species. We analyzed both the AN microbiome and the NP microbiome collected in the summer season. The top bacterial species in the AN microbiome are described in **Figure 23B** and **Figure 25**. The indoor TSP exposure was negatively associated with the relative abundance of *Streptococcus pneumoniae* (beta = -0.015, 95% CI = 0.7 – 0.9, p-value = 0.01), while we found a positive association between the indoor TSP exposure and relative abundance of *Klebsiella aerogenes* (beta = 0.041, 95% CI = 1.7 – 2.2, p-value = 0.004) and *Prevotella buccalis* (beta = 0.045, 95% CI = 1.7 – 2.2, p-value = 0.02). The top bacterial species in the NP microbiome are described in **Figure 27**. Three species of *Corynebacterium* were negatively associated with indoor TSP exposure: *Corynebacterium accolens* (beta = -0.036, 95% CI = 0.9 – 1.3, p-value = 0.03), *Corynebacterium macginleyi* (beta = -0.033, 95% CI = 0.7 – 1.1, p-value = 0.05), and *Corynebacterium segmentosum* (beta = -0.033, 95% CI = 0.8 – 1.2, p-value = 0.05). *Staphylococcus aureus* was positively associated with the indoor TSP (beta = 0.012, 95% CI = 0.4 – 0.5, p-value = 0.03). The abundance of some respiratory bacteria found in indoor TSP samples correlates with the abundance found in the respiratory samples, **Supplemental Figure 7**.

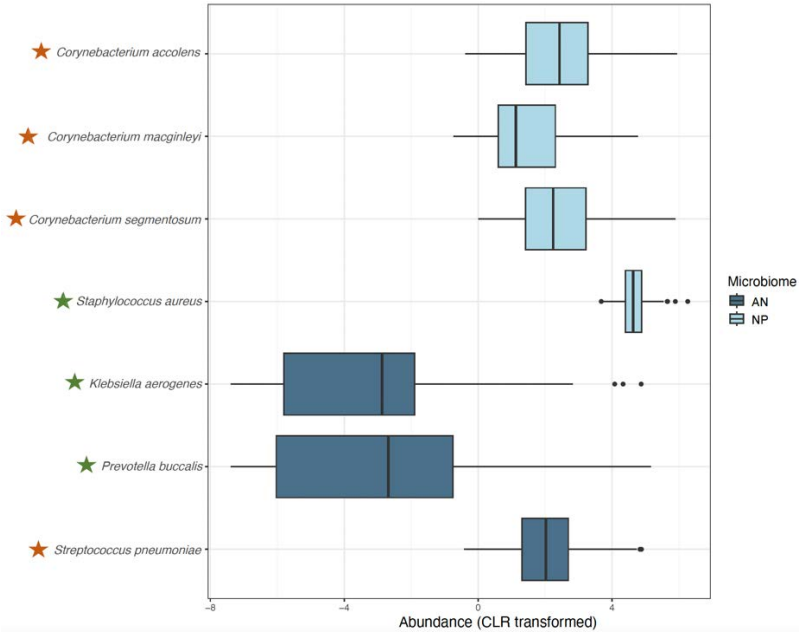

Figure 28. The abundance of bacterial species associated with indoor TSP exposure in anterior nares microbiome (AN) and nasopharynx microbiome (NP). The bacteria abundance was centered log-ratio (CLR) transformed. Positive associations are indicated with the green stars, while negative associated are indicated with orange stars.

Finally, we analyzed the correlation between the top 50 pathways (range of reads assigned = 2,703,286 – 1,042) and indoor TSP exposure (**Figure 29)**. In the anterior nares samples, we did not find any correlations. In the nasopharynx samples, we found negative correlations with amino acid biosynthesis (valine, leucine, isoleucine, phenylalanine, tyrosine, and tryptophan) and metabolism (glycerophospholipid, porphyrin and chlorophyll, 2-Oxocarboxylic acid).

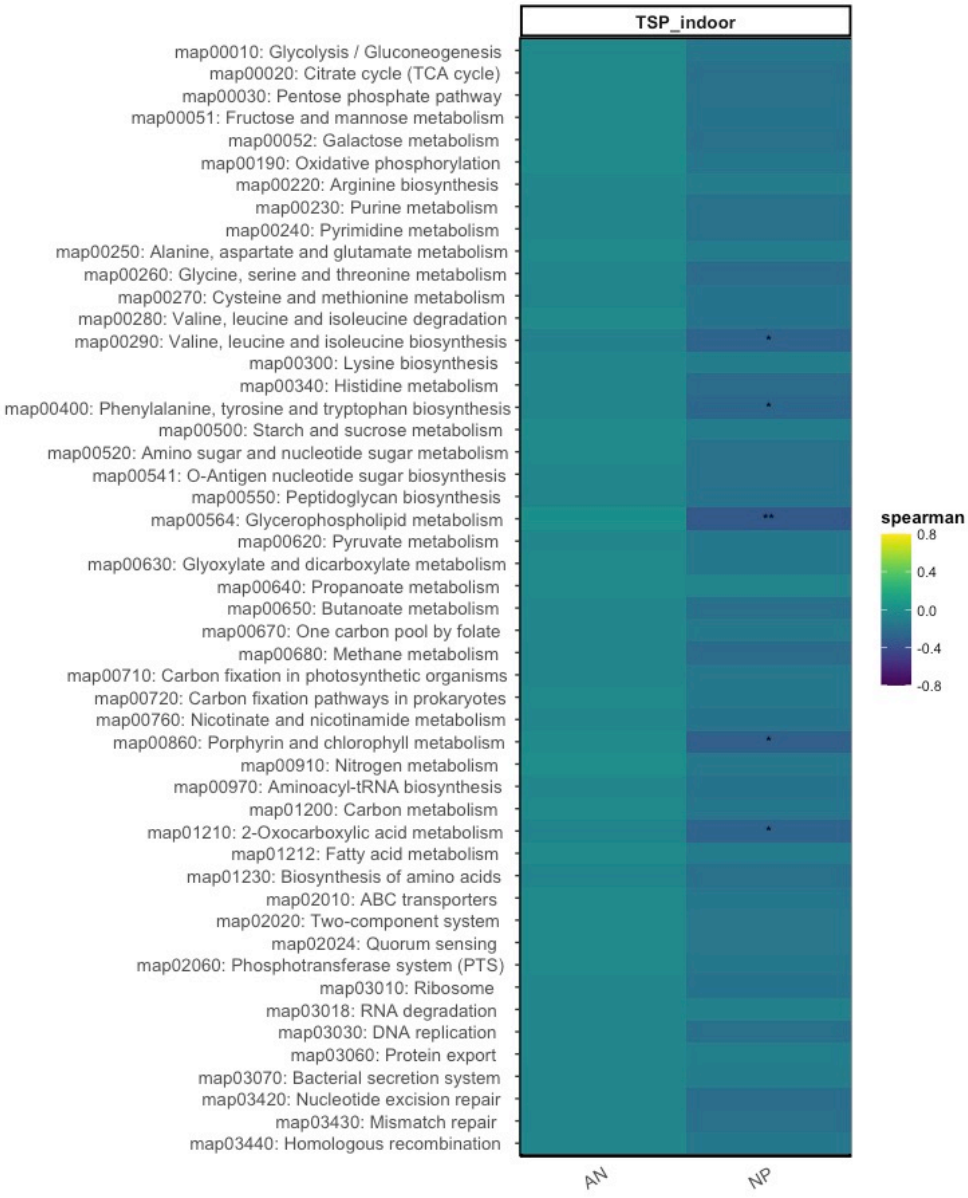

Figure 29. The heatmap shows the correlations between KEGG pathways and indoor TSP concentrations. The AN column displays correlations found in anterior nares and the NP column shows correlations found in nasopharynx. Significant correlations are marked with black asterisks. This image was generated using *phylosmith* (v 1.0.6).

2.4 DISCUSSION

The upper respiratory microbiome plays an important role in host homeostasis and human health. However, the microbiome of this environment is still understudied and the healthy respiratory microbiome is not fully characterized (Kumpitsch et al., 2019; Paulo et al., 2023). Additionally, even though the upper respiratory microbiome is an important interface to the external environment, only a few studies have investigated the relationship between the microbiome of the upper respiratory tract and air pollution (Mariani et al., 2018; Vieceli et al., 2023). In this section, we analyzed the upper respiratory microbiome in 34 healthy subjects, recruited for 6 weeks in the cities of Milan and Como. We collected weekly anterior nares swabs and nasopharynx swabs from the subjects. We then evaluated the association of the upper respiratory microbiome with the indoor TSP exposure measured in their workplaces.

We analyzed the differences in the microbiota of the anterior nares across two seasons, winter and summer, using 16S rRNA target gene sequencing and whole genome shotgun sequencing. From the 16S rRNA data, we observed that seasonal variation seemed to affect both the alpha and beta diversities in the anterior nares of healthy subjects. Specifically, we found that the diversity is higher in the summer season compared to the winter. There are only a few studies that have previously investigated seasonal variation in the human microbiota, including a study of the gut microbiota reporting significant differences in diversity between the winter and summer seasons (Davenport et al., 2014). These variations could be the result of changes in weather conditions and human habits between seasons. Overall, from both 16S rRNA and metagenomics data, we observed that the anterior nares microbiome is mostly colonized by gram-positive bacteria from *Corynebacterium*, *Staphylococcus*, and *Dolosigranulum* species. This is in line with previous studies that have characterized the respiratory microbiome in healthy adults (de Steenhuijsen Piters et al., 2015). From the 16S rRNA data, we also noticed a change in bacterial relative abundance between the two seasons. In the winter, the relative abundance of species of the *Moraxella* genus was higher, while in the summer there was a higher relative abundance of *Alloprevotella*, *Staphylococcus*, and *Cutibacterium*. The metagenomics data also reported a significantly higher relative abundance of *Moraxella* in the winter, specifically *Moraxella catarrhalis* and *Moraxella nonliquefaciens*. The *Staphylococcus* and *Cutibacterium* species that we observed (*Staphylococcus hominis, Staphylococcus epidermidis*, *Cutibacterium acnes*, *Cutibacterium avidum, Cutibacterium*

granulosum) were more prevalent in the summer. These are bacterial species that are usually described in respiratory samples. It was not surprising that we did not observe drastic changes between the two seasons because all the samples came from healthy subjects. However, it is interesting that the season with lower taxonomic diversity, winter, had a higher relative abundance of *Moraxella*. We found this genus to be less "dominant" in the microbiome of healthy adults compared to other genera. A study suggested that *Moraxella* appeared to be the least tolerant to other bacteria, compared to the other taxa that are usually very abundant in the anterior nares, such as *Cutibacterium* and *Corynebacterium*. This could explain the decrease in diversity observed in a season where the relative abundance of *Moraxella* was higher (de Steenhuijsen Piters et al., 2015). In addition, *Moraxella* is an opportunistic pathogen commonly found to be associated with viral infections, with incidences that are higher during the cold season (McCauley et al., 2021; Welp and Bomberger, 2020).

After characterizing the seasonal variations in the microbiota of the anterior nares, we also analyzed the difference between the anterior nares and the nasopharynx microbiome. We noticed a difference in taxonomic diversity. When compared to samples from the same subjects, the nasopharynx samples showed higher diversity than the anterior nares samples. However, the taxonomic composition was very similar, as already reported in a previous study (De Boeck et al., 2017). Even if the taxonomic composition did not differ significantly between the two microbiomes, in the ANCOM-BC analysis we observed a difference in bacterial abundance between the two types of samples. We found that the dominant species in the nasopharynx was *Staphylococcus aureus*, while in the anterior nares, we found a higher relative abundance of *Cutibacterium acnes, Staphylococcus epidermidis,* and several *Corynebacterium*. These bacteria that are more abundant in the anterior nares are taxa commonly found in the skin microbiome. Considering that the anterior nares are the most external part of the upper respiratory tract, it is not surprising that some taxa are shared with the skin microbiome (Smythe and Wilkinson, 2023). Besides these differences, the anterior nares and nasopharynx microbiota appeared to be similar and mostly dominated by gram-positive taxa. Finally, we investigated how the TSP indoor exposure affected the taxonomic composition of both microbiota. In the anterior nares, we observed that an increase of indoor TSP exposure was associated with a decrease of *Streptococcus pneumoniae*, and an increase of *Klebsiella aerogenes* and *Prevotella buccalis*. While not

specifically on the microbial composition of anterior nares and its relationship with air pollution as done here, previous studies of the upper airways observed a decrease of gram-positive bacteria in response to air pollution and an increase of gram-negative bacteria (Mariani et al., 2018; Xue et al., 2020). In the nasopharynx, the increase of indoor TSP concentrations was associated with a decrease of *Corynebacterium accolens, Corynebacterium macginleyi,* and *Corynebacterium segmentosum*. *Corynebacterium*, a gram-positive bacteria, is a common commensal in the upper airways that is usually dominant in healthy adults (De Boeck et al., 2017). A decrease of *Corynebacterium* species was previously observed in a study of the nasopharynx in response to cigarette smoke and particulate matter exposure (e.g., $PM_{2.5}$ and PM_{10}), (Elgamal et al., 2021; Mariani et al., 2018). On the other hand, we observed that an increase of indoor TSP exposure was positively associated with an increase of *Staphylococcus aureus*, also a gram-positive bacterium. Previous in vitro studies have reported that both particulate matter and cigarette smoke increased the presence of *Staphylococcus aureus* in the nasopharynx, leading to potentially pathogenic levels (Lacoma et al., 2019; Purves et al., 2022). Additionally, we found that the abundance of respiratory bacteria identified in indoor TSP (i.e, *Staphylococcus aureus*, *Klebsiella pneumoniae*, *Cutibacterium granulosum*) correlates with the abundance of these bacteria in the upper respiratory microbiome. Finally, we evaluated if the indoor TSP exposure affects not only the taxonomic composition but also the microbial pathways. In the correlation analysis, we found that an increase of indoor TSP exposure is associated with a decrease in amino acid biosynthesis and metabolism in the nasopharynx. This might be a consequence of the decrease of bacterial commensal in response to indoor TSP, as described above, and also reported in previous studies, (Elgamal et al., 2021; Mariani et al., 2018).

Taken together, these findings suggest that the upper respiratory microbiome of healthy subjects can be affected by indoor TSP exposure.

SECTION 3

Indoor TSP exposure, respiratory microbiome and HERV methylation

3.1 SUMMARY

Human endogenous retroviruses (HERVs) are viral elements integrated into the human genome that are involved in immune response (Rangel et al., 2022). The methylation of these genes regulates their activation, usually, the promoter region of these sequences is methylated, and these genes are inactivated. However, external stimuli can lead to loss of methylation and activation of these genes which are associated with inflammation and immune response (Rangel et al., 2022). Because air pollution is often associated with global hypomethylation some studies suggest that these pollutants can activate the HERV genes (Byun et al., 2013; Reddam et al., 2023). In this section, we analyze if the indoor TSP exposure can affect the DNA methylation of HERV genes. In addition, we investigate if the upper respiratory microbiome, which contributes to the homeostasis of the host immune system, can be involved. First, we evaluated the DNA methylation of four HERV genes (e.g., HERV-K, HERV-W, HERV-P, and HERV-H) in the healthy subjects described in **Section 2.3**. Then, we analyzed the association between the methylation levels of these genes and the indoor TSP exposure. Finally, we performed an interaction analysis to see if the microbiome might influence the effects of TSP on HERV methylation.

3.2 MATERIAL AND METHODS

3.2.1 Buccal brush: collection, DNA extraction and pyrosequencing

A buccal brush was collected from each subject for 2 weeks during the winter campaign as described in **Section 1**. The sponge was gently rotated for a few seconds on both sides of the mouth. After the sample collection, each sponge was centrifuged at 3000g for 10 minutes. Then the sample was stored at -80ºC. The DNA was extracted using NucleoSpin cfDNA XS kit (Macherey-Nagel), and then each DNA sample at a concentration of 25 ng/µL was treated with sodium bisulfite using the EZ-96 DNA Methylation-Gold™ Kit (Zymo Research; Irvine, CA, USA). Therefore, 10 µL of bisulfite-treated DNA of each sample was used for PCR amplification and then pyrosequencing. The pyrosequencing was used to evaluate the methylation levels of four HERV genes: HERV-K, HERV-W, HERVP, and HERV-H, and it was performed using the PyroMark MD System (QIAGEN). We used the Pyro Q-CpG software (Biotage, Uppsala, Sweden) to quantify the methylation level at individual CpG positions in each gene's promoter region of interest. The protocol followed for the PCR amplification and the pyrosequencing are

described by Monti (Monti et al., 2021). Each sample was measured twice to test the reproducibility of the experimental setting.

3.2.2 Statistical analysis

We used a linear mixed-effects model to evaluate the effects of indoor TSP exposure on HERV gene methylation. We also evaluated the association of HERV gene methylation with alpha diversity and the top 15 bacteria species identified in the anterior nares (**Figure 23**) and described in **Section 2.3.2**. All these models were adjusted for outdoor TSP, run, and sub-group (R1, R2, R3). The time was used as a random effect. Finally, we tested the interaction between indoor TSP exposure and respiratory microbiome on HERV methylation. We tested both the interaction between indoor TSP exposure and alpha diversity and the interaction between indoor TSP exposure and the abundance of the top 15 bacteria. Each HERV gene was analyzed in a separate model. We considered an association significant when a p-value < 0.05 was reached. All statistical analyses were performed in SAS 9.4 statistical software (SAS Institute Inc., Cary, NC, USA).

3.3 RESULTS

3.3.1 Description and characteristics of the enrolled subjects

During the winter season (G1: November; G2: January-February; G3: March), we collected for 2 weeks buccal brush from 23 subjects (**Table 6**) among the 34 subjects described in **Section 2.3**. In the end, we were able to collect 46 buccal brushes and evaluate the methylation of four HERV genes: HERV-K, HERV-W, HERV-P and HERV-H. The methylation levels of these genes are described in **Table 7**.

Table 6. Description of the subjects randomly selected for the evaluation of HERV methylation	
Characteristics	**Winter season (N= 23)**
***Gender,* n (%)**	
Female	14 (61%)
Male	9 (39%)
***Age*, mean (SD)**	41.3 (10)
***BMI*, mean (SD)**	23.6 (3.1)
***Smoking*, n (%)**	
No	19 (83%)
Yes	4 (17%)

Table 7. DNA methylation level identified in each HERV gene analyzed			
HERV gene	**Position**	**Median**	**Q1 - Q3**
HERV-H	1	81.1	75.9 – 86.3
HERV-K	1	46.2	44.2 - 48.2
HERV-P	1	36.4	25.1 - 45.6
HERV-W	1	96.2	95.5 – 96.9
	2	98.2	97.5 – 99.9
	3	77.4	74.2 – 80.2

3.3.2 DNA methylation of HERV genes, TSP exposure and microbiome

When we evaluated the association between indoor TSP exposure and HERV methylation, we did not observe any significant association between indoor TSP exposure and the methylation of the four HERV genes analyzed. On the contrary, the microbiome of the anterior nares seems associated with the methylation of HERV-K in different ways. First, we found a negative association between

HERV-K and the alpha diversity (beta = -1.7, p-value = 0.006). Then, we observed that the methylation of HERV-K was negatively associated with the relative abundance of *Staphylococcus aureus* (beta = -0.9, p-value = 0.004), *Staphylococcus epidermidis* (beta = -0.89, p-value = 0.03) and *Klebsiella pneumoniae* (beta = -0.66, p-value = 0.02). The relative abundance of *Corynebacterium pseudodiphtheriticum* (beta = 0.44, p-value = 0.04). We also found one negative association between the methylation of HERV-H and *Cutibacterium acnes* (beta = -2.7, p-value = 0.01), and one positive association between the methylation of HERV-W and *Cutibacterium granulosum* (beta = 0.7, p-value = 0.01). In the interaction models (**Figure 30**), when the relative abundance of *Cutibacterium acnes* and *Actinomyces neaslundii* is low, the indoor TSP exposure is positively associated with the methylation of HERV-W. However, we found this association significant only in one out of the three promoter regions analyzed for HERV-W, **Supplemental Table 4**.

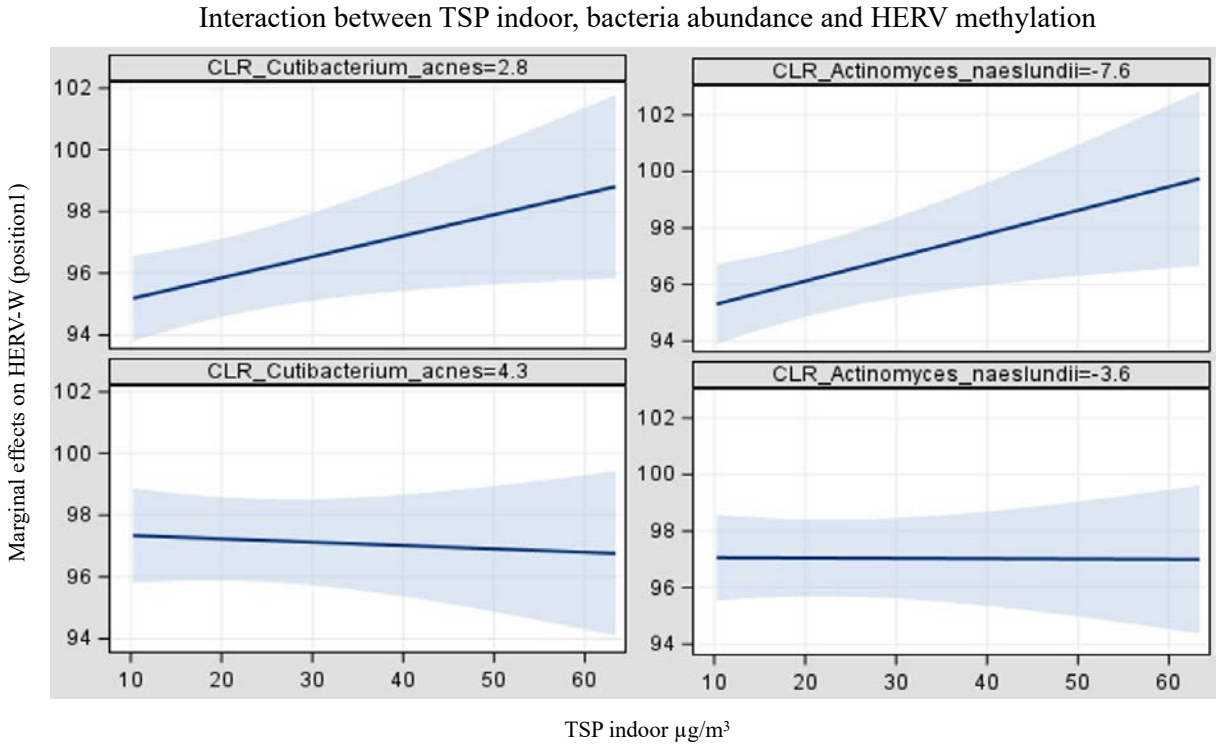

Figure 30. The effect modifier of *Cutibacterium acnes* and *Actinomyces naeslundii* relative abundance (CLR transformed) on the association between indoor TSP exposure and DNA methylation of HERV-W (position 1). Estimates were obtained using a multiple linear regression model for repeated measures, with adjustments for outdoor TSP, sequencing run, and sample subgroup (R1, R2, R3).

3.4 DISCUSSION

The DNA methylation of promoter regions consents to inactivate the expression of HERV genes which are viral genes integrated in our genome. However, these genes can be demethylated, then activated, and involved in immune system response (Rangel et al., 2022; Reddam et al., 2023). A recent study suggested that because air pollution is associated with global hypomethylation, exposure to these pollutants could affect HERV methylation (Reddam et al., 2023). In addition, because the microbiome plays an important role in host immunity, other evidence suggested that HERV can communicate with the microbiome to control inflammation (Jichang Wang et al., 2023). In this part of the project, we analyzed if the indoor TSP exposure and/or the respiratory can affect the methylation of HERV genes. Finally, we analyzed the interaction of microbiome and indoor TSP exposure on the HERV methylation.

In this section, we analyzed the data collected from 23 healthy subjects out of the 34 described in **Section 2**. In this part of the project, we consider for the analysis: 46 buccal brushes to evaluate the methylation, 46 anterior nares swab to characterize the anterior nares microbiome, and the weekly indoor TSP measurements of their offices. Four HERV genes (e.g., HERV-K, HERV-H, HERV-W, HERV-P) were selected to evaluate their methylation through pyrosequencing. All these HERV genes selected have been associated with human diseases like cancer and neurodegenerative disease (Christensen, 2010; Garcia-Montojo et al., 2018; Rangel et al., 2022; Qianqian Wang et al., 2023). When we evaluate the association between the indoor TSP exposure and the methylation of each HERV, we did not find any significant results. However, the microbiome was associated in multiple ways with HERV-K. First, we observed a negative association with alpha diversity. Then we found that among the most abundant bacteria in the anterior nares, three were negatively associated with the methylation of HERV-K: *Staphylococcus aureus*, *Staphylococcus epidermidis*, and *Klebsiella pneumoniae*. While the relative abundance of *Corynebacterium pseudodiphtheriticum* was positively associated. All these results suggest that microbiome and HERV-K can affect each other, but further investigation is necessary to understand the possible mechanism. However, a previous study on HERVs and skin microbiota, has already found associations between commensal bacteria and HERVs. From their experiments in mice, these researchers found that *Staphylococcus epidermidis* and *Staphylococcus aureus* promoted the expression of several families of HERVs (Lima-Junior et al., 2021). Finally, from

our interaction analyses, we did not find significant association, except for two associations at one specific position for HERV-W. We observed that at low abundance of *Cutibacterium acnes* and *Actinomyces naeslundii*, the indoor TSP exposure is positively associated with the methylation of HERV-W at the first position, among the three investigated. A previous study has already described hypermethylation of HERV-W in response to coarse PM (Reddam et al., 2023). These authors suggested that the hypermethylation of HERV-W can have adverse health outcomes because HERV-W has a protective role against exogenous infections and excessive immune activation (Grandi and Tramontano, 2017). Overall, from these analyses, we found that the respiratory microbiome is correlated with the methylation of HERV genes, and it also seems to influence the association between indoor TSP and the methylation of HERV-W.

CONCLUSION

In this project, we analyzed the effect of indoor TSP exposure on healthy subjects. We analyzed the bacteria that inhabit our upper airways (upper respiratory microbiome) and the viral genes integrated in our genome (HERVs). When we analyzed the environmental data we collected, we noticed that in addition to their concentrations, the outdoor and indoor TSP differed also in their microbiome composition. We found that these particles carry several bacteria and viruses that reflect the characteristics of the environment. Indoor TSP exposure was mostly associated with gram-positive bacteria in the respiratory microbiome. We found negative associations with common commensals such as *Corynebacterium* and *Streptococcus*. We also noticed a positive association with *Staphylococcus aureus*, a bacterium that was already found to be positively associated with other types of exposure such as smoke and PM. In vitro studies suggest that exposure to these pollutants induce virulence in this bacterium. Finally, our analysis showed some association between the upper respiratory microbiome and the methylation of HERV-K, while indoor TSP did not report any association with HERV methylation. However, when we considered the influence of the microbiome in the association between indoor TSP and HERV methylation, we found that a low abundance of *Cutibacterium acnes* and *Actinomyces naeslundii*, the indoor TSP is associated with hypermethylation of HERV-W. A hypermethylation of this HERV gene was previously found in association with coarse PM, and the inactivation of this gene might be adverse because HERV-W has a protective role against infections. Taken together these observations suggest that indoor TSP exposure can directly affect the respiratory microbiome, and also, through its effect on microbiome, indirectly affect the methylation of HERV genes. Further study is necessary to support this hypothesis.

REFERENCES

Ahle, C.M., Feidenhansl, C., Brüggemann, H., 2023. Cutibacterium acnes. Trends in Microbiology 31, 419–420. https://doi.org/10.1016/j.tim.2022.10.006

Baumgartner, J., Schauer, J.J., Ezzati, M., Lu, L., Cheng, C., Patz, J., Bautista, L.E., 2011. Patterns and predictors of personal exposure to indoor air pollution from biomass combustion among women and children in rural China. Indoor Air 21, 479–488. https://doi.org/10.1111/j.1600-0668.2011.00730.x

Belshaw, R., Katzourakis, A., Paces, J., Burt, A., Tristem, M., 2005. High copy number in human endogenous retrovirus families is associated with copying mechanisms in addition to reinfection. Mol Biol Evol 22, 814–817. https://doi.org/10.1093/molbev/msi088

Bennitt, F.B., Wozniak, S.S., Causey, K., Burkart, K., Brauer, M., 2021. Estimating disease burden attributable to household air pollution: new methods within the Global Burden of Disease Study. The Lancet Global Health 9, S18. https://doi.org/10.1016/S2214-109X(21)00126-1

Bertolini, V., Gandolfi, I., Ambrosini, R., Bestetti, G., Innocente, E., Rampazzo, G., Franzetti, A., 2013. Temporal variability and effect of environmental variables on airborne bacterial communities in an urban area of Northern Italy. Appl Microbiol Biotechnol 97, 6561–6570. https://doi.org/10.1007/s00253-012-4450-0

Bezirtzoglou, C., Dekas, K., Charvalos, E., 2011. Climate changes, environment and infection: Facts, scenarios and growing awareness from the public health community within Europe. Anaerobe, Cruising in the Amazing World of Microbial Ecosystems 17, 337–340. https://doi.org/10.1016/j.anaerobe.2011.05.016

Biesbroek, G., Tsivtsivadze, E., Sanders, E.A.M., Montijn, R., Veenhoven, R.H., Keijser, B.J.F., Bogaert, D., 2014. Early Respiratory Microbiota Composition Determines Bacterial Succession Patterns and Respiratory Health in Children. Am J Respir Crit Care Med 190, 1283–1292. https://doi.org/10.1164/rccm.201407-1240OC

Bolyen, E., Rideout, J.R., Dillon, M.R., Bokulich, N.A., Abnet, C.C., Al-Ghalith, G.A., Alexander, H., Alm, E.J., Arumugam, M., Asnicar, F., Bai, Y., Bisanz, J.E., Bittinger, K., Brejnrod, A., Brislawn, C.J., Brown, C.T., Callahan, B.J., Caraballo-Rodríguez, A.M., Chase, J., Cope, E.K., Da Silva, R., Diener, C., Dorrestein, P.C., Douglas, G.M., Durall, D.M., Duvallet, C., Edwardson, C.F., Ernst, M., Estaki, M., Fouquier, J., Gauglitz, J.M., Gibbons, S.M., Gibson, D.L., Gonzalez, A., Gorlick, K., Guo, J., Hillmann, B., Holmes, S., Holste, H., Huttenhower, C., Huttley, G.A., Janssen, S., Jarmusch, A.K., Jiang, L., Kaehler, B.D., Kang, K.B., Keefe, C.R., Keim, P., Kelley, S.T., Knights, D., Koester, I., Kosciolek, T., Kreps, J., Langille, M.G.I., Lee, J., Ley, R., Liu, Y.-X., Loftfield, E., Lozupone, C., Maher, M., Marotz, C., Martin, B.D., McDonald, D., McIver, L.J., Melnik, A.V., Metcalf, J.L., Morgan, S.C., Morton, J.T., Naimey, A.T., Navas-Molina, J.A., Nothias, L.F., Orchanian, S.B., Pearson, T., Peoples, S.L., Petras, D., Preuss, M.L., Pruesse, E., Rasmussen, L.B., Rivers, A., Robeson, M.S., Rosenthal, P., Segata, N., Shaffer, M., Shiffer, A., Sinha, R., Song, S.J., Spear, J.R., Swafford, A.D., Thompson, L.R., Torres, P.J., Trinh, P., Tripathi, A., Turnbaugh, P.J., Ul-Hasan, S., van der Hooft, J.J.J., Vargas, F., Vázquez-Baeza, Y., Vogtmann, E., von Hippel, M., Walters, W., Wan, Y., Wang, M., Warren, J., Weber, K.C., Williamson, C.H.D., Willis, A.D., Xu, Z.Z., Zaneveld, J.R., Zhang, Y., Zhu, Q., Knight, R., Caporaso, J.G., 2019. Reproducible, interactive, scalable and extensible microbiome data science using QIIME 2. Nat Biotechnol 37, 852–857. https://doi.org/10.1038/s41587-019-0209-9

Byun, H.-M., Motta, V., Panni, T., Bertazzi, P.A., Apostoli, P., Hou, L., Baccarelli, A.A., 2013. Evolutionary age of repetitive element subfamilies and sensitivity of DNA methylation to airborne pollutants. Particle and Fibre Toxicology 10, 28. https://doi.org/10.1186/1743-8977-10-28

Cao, C., Jiang, W., Wang, B., Fang, J., Lang, J., Tian, G., Jiang, J., Zhu, T.F., 2014. Inhalable Microorganisms in Beijing's PM2.5 and PM10 Pollutants during a Severe Smog Event. Environ Sci Technol 48, 1499–1507. https://doi.org/10.1021/es4048472

Charlson, E.S., Chen, J., Custers-Allen, R., Bittinger, K., Li, H., Sinha, R., Hwang, J., Bushman, F.D., Collman, R.G., 2010. Disordered Microbial Communities in the Upper Respiratory Tract of Cigarette Smokers. PLOS ONE 5, e15216. https://doi.org/10.1371/journal.pone.0015216

Chen, S., Zhou, Y., Chen, Y., Gu, J., 2018. fastp: an ultra-fast all-in-one FASTQ preprocessor. Bioinformatics 34, i884–i890. https://doi.org/10.1093/bioinformatics/bty560

Christensen, T., 2010. HERVs in Neuropathogenesis. J Neuroimmune Pharmacol 5, 326–335. https://doi.org/10.1007/s11481-010-9214-y

Clark, M.L., Bachand, A.M., Heiderscheidt, J.M., Yoder, S.A., Luna, B., Volckens, J., Koehler, K.A., Conway, S., Reynolds, S.J., Peel, J.L., 2013. Impact of a cleaner-burning cookstove intervention on blood pressure in Nicaraguan women. Indoor Air 23, 105–114. https://doi.org/10.1111/ina.12003

Davenport, E.R., Mizrahi-Man, O., Michelini, K., Barreiro, L.B., Ober, C., Gilad, Y., 2014. Seasonal Variation in Human Gut Microbiome Composition. PLoS One 9, e90731. https://doi.org/10.1371/journal.pone.0090731

Davis, N.M., Proctor, D.M., Holmes, S.P., Relman, D.A., Callahan, B.J., 2018. Simple statistical identification and removal of contaminant sequences in marker-gene and metagenomics data. https://doi.org/10.1101/221499

De Boeck, I., Wittouck, S., Wuyts, S., Oerlemans, E.F.M., van den Broek, M.F.L., Vandenheuvel, D., Vanderveken, O., Lebeer, S., 2017. Comparing the Healthy Nose and Nasopharynx Microbiota Reveals Continuity As Well As Niche-Specificity. Front Microbiol 8, 2372. https://doi.org/10.3389/fmicb.2017.02372

de Steenhuijsen Piters, W.A.A., Sanders, E.A.M., Bogaert, D., 2015. The role of the local microbial ecosystem in respiratory health and disease. Philosophical Transactions of the Royal Society B: Biological Sciences 370, 20140294. https://doi.org/10.1098/rstb.2014.0294

Dickson, R.P., Huffnagle, G.B., 2015. The Lung Microbiome: New Principles for Respiratory Bacteriology in Health and Disease. PLOS Pathogens 11, e1004923. https://doi.org/10.1371/journal.ppat.1004923

Dopkins, N., Nixon, D.F., 2023. Activation of human endogenous retroviruses and its physiological consequences. Nat Rev Mol Cell Biol 1–11. https://doi.org/10.1038/s41580-023-00674-z

Elgamal, Z., Singh, P., Geraghty, P., 2021. The Upper Airway Microbiota, Environmental Exposures, Inflammation, and Disease. Medicina 57, 823. https://doi.org/10.3390/medicina57080823

Garcia-Montojo, M., Doucet-O'Hare, T., Henderson, L., Nath, A., 2018. Human endogenous retrovirus-K (HML-2): a comprehensive review. Critical Reviews in Microbiology 44, 715–738. https://doi.org/10.1080/1040841X.2018.1501345

Gou, H., Lu, J., Li, S., Tong, Y., Xie, C., Zheng, X., 2016. Assessment of microbial communities in PM1 and PM10 of Urumqi during winter. Environmental Pollution 214, 202–210. https://doi.org/10.1016/j.envpol.2016.03.073

Grandi, N., Tramontano, E., 2017. Type W Human Endogenous Retrovirus (HERV-W) Integrations and Their Mobilization by L1 Machinery: Contribution to the Human Transcriptome and Impact on the Host Physiopathology. Viruses 9, 162. https://doi.org/10.3390/v9070162

Hamidou Soumana, I., Carlsten, C., 2021. Air pollution and the respiratory microbiome. Journal of Allergy and Clinical Immunology 148, 67–69. https://doi.org/10.1016/j.jaci.2021.05.013

Hassoun, A., Huff, M.D., Weisman, D., Chahal, K., Asis, E., Stalons, D., Grigorenko, E., Green, J., Malone, L.L., Clemmons, S., Lu, S., 2015. Seasonal variation of respiratory pathogen colonization in asymptomatic health care professionals: A single-center, cross-sectional, 2-season observational study. American Journal of Infection Control 43, 865–870. https://doi.org/10.1016/j.ajic.2015.04.195

Hou, K., Wu, Z.-X., Chen, X.-Y., Wang, J.-Q., Zhang, D., Xiao, C., Zhu, D., Koya, J.B., Wei, L., Li, J., Chen, Z.-S., 2022. Microbiota in health and diseases. Sig Transduct Target Ther 7, 1–28. https://doi.org/10.1038/s41392-022-00974-4

Kalisa, E., Clark, M.L., Ntakirutimana, T., Amani, M., Volckens, J., 2023. Exposure to indoor and outdoor air pollution in schools in Africa: Current status, knowledge gaps, and a call to action. Heliyon 9, e18450. https://doi.org/10.1016/j.heliyon.2023.e18450

Kooken, J.M., Fox, K.F., Fox, A., 2012. Characterization of Micrococcus strains isolated from indoor air. Molecular and Cellular Probes 26, 1–5. https://doi.org/10.1016/j.mcp.2011.09.003

Kumpitsch, C., Koskinen, K., Schöpf, V., Moissl-Eichinger, C., 2019. The microbiome of the upper respiratory tract in health and disease. BMC Biol 17, 87. https://doi.org/10.1186/s12915-019-0703-z

Lacoma, A., Edwards, A.M., Young, B.C., Domínguez, J., Prat, C., Laabei, M., 2019. Cigarette smoke exposure redirects Staphylococcus aureus to a virulence profile associated with persistent infection. Sci Rep 9, 10798. https://doi.org/10.1038/s41598-019-47258-6

Langmead, B., Trapnell, C., Pop, M., Salzberg, S.L., 2009. Ultrafast and memory-efficient alignment of short DNA sequences to the human genome. Genome Biology 10, R25. https://doi.org/10.1186/gb-2009-10-3-r25

Li, P., Koziel, J.A., Paris, R.V., Macedo, N., Zimmerman, J.J., Wrzesinski, D., Sobotka, E., Balderas, M., Walz, W.B., Liu, D., Yedilbayev, B., Ramirez, B.C., Jenks, W.S., 2023. Indoor air quality improvement with filtration and UV-C on mitigation of particulate matter and airborne bacteria: Monitoring and modeling. J Environ Manage 351, 119764. https://doi.org/10.1016/j.jenvman.2023.119764

Li, Z., Wen, Q., Zhang, R., 2017. Sources, health effects and control strategies of indoor fine particulate matter (PM2.5): A review. Science of The Total Environment 586, 610–622. https://doi.org/10.1016/j.scitotenv.2017.02.029

Lima-Junior, D.S., Krishnamurthy, S.R., Bouladoux, N., Collins, N., Han, S.-J., Chen, E.Y., Constantinides, M.G., Link, V.M., Lim, A.I., Enamorado, M., Cataisson, C., Gil, L., Rao, I., Farley, T.K., Koroleva, G., Attig, J., Yuspa, S.H., Fischbach, M.A., Kassiotis, G., Belkaid, Y., 2021. Endogenous retroviruses promote homeostatic and inflammatory responses to the microbiota. Cell 184, 3794-3811.e19. https://doi.org/10.1016/j.cell.2021.05.020

Lin, H., Peddada, S.D., 2020. Analysis of compositions of microbiomes with bias correction. Nat Commun 11, 3514. https://doi.org/10.1038/s41467-020-17041-7

Liu, X., Liu, Z., Wu, Z., Ren, J., Fan, Y., Sun, L., Cao, G., Niu, Y., Zhang, B., Ji, Q., Jiang, X., Wang, C., Wang, Q., Ji, Z., Li, L., Esteban, C.R., Yan, K., Li, W., Cai, Yusheng, Wang, S., Zheng, A., Zhang, Y.E., Tan, S., Cai, Yingao, Song, M., Lu, F., Tang, F., Ji, W., Zhou, Q., Belmonte, J.C.I., Zhang, W., Qu, J., Liu, G.-H., 2023. Resurrection of endogenous retroviruses during aging reinforces senescence. Cell 186, 287-304.e26. https://doi.org/10.1016/j.cell.2022.12.017

Lloyd-Price, J., Mahurkar, A., Rahnavard, G., Crabtree, J., Orvis, J., Hall, A.B., Brady, A., Creasy, H.H., McCracken, C., Giglio, M.G., McDonald, D., Franzosa, E.A., Knight, R., White, O., Huttenhower, C., 2017. Strains, functions and dynamics in the expanded Human Microbiome Project. Nature 550, 61–66. https://doi.org/10.1038/nature23889

Lu, J., Breitwieser, F.P., Thielen, P., Salzberg, S.L., 2017. Bracken: estimating species abundance in metagenomics data. PeerJ Comput. Sci. 3, e104. https://doi.org/10.7717/peerj-cs.104

Madsen, A.M., Moslehi-Jenabian, S., Frankel, M., White, J.K., Frederiksen, M.W., n.d. Airborne bacterial species in indoor air and association with physical factors. UCL Open Environ 5, e056. https://doi.org/10.14324/111.444/ucloe.000056

Man, W.H., de Steenhuijsen Piters, W.A.A., Bogaert, D., 2017. The microbiota of the respiratory tract: gatekeeper to respiratory health. Nat Rev Microbiol 15, 259–270. https://doi.org/10.1038/nrmicro.2017.14

Manisalidis, I., Stavropoulou, E., Stavropoulos, A., Bezirtzoglou, E., 2020. Environmental and Health Impacts of Air Pollution: A Review. Front Public Health 8, 14. https://doi.org/10.3389/fpubh.2020.00014

Mariani, J., Favero, C., Spinazzè, A., Cavallo, D.M., Carugno, M., Motta, V., Bonzini, M., Cattaneo, A., Pesatori, A.C., Bollati, V., 2018. Short-term particulate matter exposure influences nasal microbiota in a population of healthy subjects. Environmental Research 162, 119–126. https://doi.org/10.1016/j.envres.2017.12.016

Mariani, J., Iodice, S., Cantone, L., Solazzo, G., Marraccini, P., Conforti, E., Bulsara, P.A., Lombardi, M.S., Howlin, R.P., Bollati, V., Ferrari, L., 2021. Particulate Matter Exposure and Allergic Rhinitis: The Role of Plasmatic Extracellular Vesicles and Bacterial Nasal Microbiome. Int J Environ Res Public Health 18, 10689. https://doi.org/10.3390/ijerph182010689

Mazúrová, M., Kabát, P., 2023. The role of endogenous retroviruses in the human body. Epidemiol Mikrobiol Imunol 72, 140–150.

McCauley, K.E., DeMuri, G., Lynch, K., Fadrosh, D.W., Santee, C., Nagalingam, N.N., Wald, E.R., Lynch, S.V., 2021. Moraxella-dominated pediatric nasopharyngeal microbiota associate with upper respiratory infection and sinusitis. PLoS One 16, e0261179. https://doi.org/10.1371/journal.pone.0261179

McMurdie, P.J., Holmes, S., 2013. phyloseq: An R Package for Reproducible Interactive Analysis and Graphics of Microbiome Census Data. PLOS ONE 8, e61217. https://doi.org/10.1371/journal.pone.0061217

Monti, P., Iodice, S., Tarantini, L., Sacchi, F., Ferrari, L., Ruscica, M., Buoli, M., Vigna, L., Pesatori, A.C., Bollati, V., 2021. Effects of PM Exposure on the Methylation of Clock Genes in A Population of Subjects with Overweight or Obesity. International Journal of Environmental Research and Public Health 18, 1122. https://doi.org/10.3390/ijerph18031122

Padhye, L.V., Kish, J.L., Batra, P.S., Miller, G.E., Mahdavinia, M., 2021. The impact of levels of particulate matter with an aerodynamic diameter smaller than 2.5 μm on the nasal microbiota in chronic rhinosinusitis and healthy individuals. Annals of Allergy, Asthma & Immunology 126, 195–197. https://doi.org/10.1016/j.anai.2020.10.006

Palacio, L.C., Pachajoa, D.C., Echeverri-Londoño, C.A., Saiz, J., Tobón, C., 2023. Air Pollution and Cardiac Diseases: A Review of Experimental Studies. Dose-Response 21, 15593258231212793. https://doi.org/10.1177/15593258231212793

Panumasvivat, J., Pratchayasakul, W., Sapbamrer, R., Chattipakorn, N., Chattipakorn, S.C., 2023. The possible role of particulate matter on the respiratory microbiome: evidence from in vivo to clinical studies. Arch Toxicol 97, 913–930. https://doi.org/10.1007/s00204-023-03452-0

Paulo, A.C., Lança, J., Almeida, S.T., Hilty, M., Sá-Leão, R., 2023. The upper respiratory tract microbiota of healthy adults is affected by Streptococcus pneumoniae carriage, smoking habits, and contact with children. Microbiome 11, 199. https://doi.org/10.1186/s40168-023-01640-9

Peden, D.B., 2024. Respiratory Health Effects of Air Pollutants. Immunology and Allergy Clinics of North America, Climate Change And Allergy 44, 15–33. https://doi.org/10.1016/j.iac.2023.07.004

Peixoto, C., Pereira, M. do C., Morais, S., Slezakova, K., 2023. Assessment of indoor air quality in health clubs: insights into (ultra)fine and coarse particles and gaseous pollutants. Frontiers in Public Health 11.

Phipps, J.C., Aronoff, D.M., Curtis, J.L., Goel, D., O'Brien, E., Mancuso, P., 2010. Cigarette Smoke Exposure Impairs Pulmonary Bacterial Clearance and Alveolar Macrophage Complement-Mediated Phagocytosis of Streptococcus pneumoniae. Infect Immun 78, 1214–1220. https://doi.org/10.1128/IAI.00963-09

Purves, J., Hussey, S.J.K., Corscadden, L., Purser, L., Hall, A., Misra, R., Selley, L., Monks, P.S., Ketley, J.M., Andrew, P.W., Morrissey, J.A., 2022. Air pollution induces Staphylococcus aureus USA300 respiratory tract colonization mediated by specific bacterial genetic responses involving the global virulence gene regulators Agr and Sae. Environ Microbiol 24, 4449–4465. https://doi.org/10.1111/1462-2920.16076

Qin, N., Liang, P., Wu, C., Wang, G., Xu, Q., Xiong, X., Wang, T., Zolfo, M., Segata, N., Qin, H., Knight, R., Gilbert, J.A., Zhu, T.F., 2020. Longitudinal survey of microbiome associated with particulate matter in a megacity. Genome Biol 21, 55. https://doi.org/10.1186/s13059-020-01964-x

Qin, T., Zhang, F., Zhou, H., Ren, H., Du, Y., Liang, S., Wang, F., Cheng, L., Xie, X., Jin, A., Wu, Y., Zhao, J., Xu, J., 2019. High-Level PM2.5/PM10 Exposure Is Associated With Alterations in the Human Pharyngeal Microbiota Composition. Frontiers in Microbiology 10.

Rangel, S.C., da Silva, M.D., da Silva, A.L., dos Santos, J. de M.B., Neves, L.M., Pedrosa, A., Rodrigues, F.M., Trettel, C. dos S., Furtado, G.E., de Barros, M.P., Bachi, A.L.L., Romano, C.M., Nali, L.H.D.S., 2022. Human endogenous retroviruses and the inflammatory response: A vicious circle associated with health and illness. Frontiers in Immunology 13.

Reddam, A., Bollati, V., Wu, H., Favero, C., Tarantini, L., Hoxha, M., Comfort, N., Gold, D.R., Phipatanakul, W., Baccarelli, A.A., 2023. Air pollution and human endogenous retrovirus methylation in the school inner-city asthma intervention study. Toxicological Sciences 193, 166–174. https://doi.org/10.1093/toxsci/kfad035

Rylance, J., Kankwatira, A., Nelson, D.E., Toh, E., Day, R.B., Lin, H., Gao, X., Dong, Q., Sodergren, E., Weinstock, G.M., Heyderman, R.S., Twigg, H.L., Gordon, S.B., 2016. Household air pollution and the lung microbiome of healthy adults in Malawi: a cross-sectional study. BMC Microbiol 16, 182. https://doi.org/10.1186/s12866-016-0803-7

Sahin-Yilmaz, A., Naclerio, R.M., 2011. Anatomy and physiology of the upper airway. Proc Am Thorac Soc 8, 31–39. https://doi.org/10.1513/pats.201007-050RN

Smythe, P., Wilkinson, H.N., 2023. The Skin Microbiome: Current Landscape and Future Opportunities. Int J Mol Sci 24, 3950. https://doi.org/10.3390/ijms24043950

Vargiu, L., Rodriguez-Tomé, P., Sperber, G.O., Cadeddu, M., Grandi, N., Blikstad, V., Tramontano, E., Blomberg, J., 2016. Classification and characterization of human endogenous retroviruses; mosaic forms are common. Retrovirology 13, 7. https://doi.org/10.1186/s12977-015-0232-y

Vieceli, T., Tejada, S., Martinez-Reviejo, R., Pumarola, T., Schrenzel, J., Waterer, G.W., Rello, J., 2023. Impact of air pollution on respiratory microbiome: A narrative review. Intensive and Critical Care Nursing 74, 103336. https://doi.org/10.1016/j.iccn.2022.103336

Wang, Jinze, Du, W., Lei, Y., Chen, Y., Wang, Z., Mao, K., Tao, S., Pan, B., 2023. Quantifying the dynamic characteristics of indoor air pollution using real-time sensors: Current status and future implication. Environment International 175, 107934. https://doi.org/10.1016/j.envint.2023.107934

Wang, Jichang, Lu, X., Zhang, W., Liu, G.-H., 2023. Endogenous retroviruses in development and health. Trends Microbiol S0966-842X(23)00267–6. https://doi.org/10.1016/j.tim.2023.09.006

Wang, Qianqian, Shi, Y., Bian, Q., Zhang, N., Wang, M., Wang, J., Li, X., Lai, L., Zhao, Z., Yu, H., 2023. Molecular mechanisms of syncytin-1 in tumors and placental development related diseases. Discov Oncol 14, 104. https://doi.org/10.1007/s12672-023-00702-6

Welp, A.L., Bomberger, J.M., 2020. Bacterial Community Interactions During Chronic Respiratory Disease. Front Cell Infect Microbiol 10, 213. https://doi.org/10.3389/fcimb.2020.00213

Wood, D.E., Salzberg, S.L., 2014. Kraken: ultrafast metagenomic sequence classification using exact alignments. Genome Biology 15, R46. https://doi.org/10.1186/gb-2014-15-3-r46

Xu, S., Zhan, L., Tang, W., Wang, Q., Dai, Z., Zhou, L., Feng, T., Chen, M., Wu, T., Hu, E., Yu, G., 2023. MicrobiotaProcess: A comprehensive R package for deep mining microbiome. Innovation (Camb) 4, 100388. https://doi.org/10.1016/j.xinn.2023.100388

Xue, Y., Chu, J., Li, Y., Kong, X., 2020. The influence of air pollution on respiratory microbiome: A link to respiratory disease. Toxicol Lett 334, 14–20. https://doi.org/10.1016/j.toxlet.2020.09.007

Young, B.N., Clark, M.L., Rajkumar, S., Benka-Coker, M.L., Bachand, A., Brook, R.D., Nelson, T.L., Volckens, J., Reynolds, S.J., L'Orange, C., Good, N., Koehler, K., Africano, S., Osorto Pinel, A.B., Peel, J.L., 2019. Exposure to household air pollution from biomass cookstoves and blood pressure among women in rural Honduras: A cross-sectional study. Indoor Air 29, 130–142. https://doi.org/10.1111/ina.12507

Zhang, Y., Li, X.-Y., Jiang, L.-J., Wei, J.-R., Sheng, X., Liu, Y., Guo, X., 2005. [Primary research on indoor air concentration of particulate matter in residential house and its relationship with ambient pollution level]. Wei Sheng Yan Jiu 34, 407–409.

Zhao, H., Chen, S., Yang, F., Wu, H., Ba, Y., Cui, L., Chen, R., Zhu, J., 2022. Alternation of nasopharyngeal microbiota in healthy youth is associated with environmental factors: implication for respiratory diseases. International Journal of Environmental Health Research 32, 952–962. https://doi.org/10.1080/09603123.2020.1810209

Zhao, H., Liu, J., Zhu, J., Yang, F., Wu, H., Ba, Y., Cui, L., Chen, R., Chen, S., 2020. Bacterial composition and community structure of the oropharynx of adults with asthma are associated with environmental factors. Microbial Pathogenesis 149, 104505. https://doi.org/10.1016/j.micpath.2020.104505

Zhou, Z.-C., Liu, Y., Lin, Z.-J., Shuai, X.-Y., Zhu, L., Xu, L., Meng, L.-X., Sun, Y.-J., Chen, H., 2021. Spread of antibiotic resistance genes and microbiota in airborne particulate matter, dust, and human airways in the urban hospital. Environ Int 153, 106501. https://doi.org/10.1016/j.envint.2021.106501

Zhu, Y., Shang, J., Peng, C., Sun, Y., 2022. Phage family classification under Caudoviricetes: A review of current tools using the latest ICTV classification framework. Frontiers in Microbiology 13.

SUPPLEMENTAL MATERIALS

Supplemental Table 1. Indoor/Outdoor (I/O) ratios, calculated by dividing each TSP indoor concentration with the average of the corresponding outdoor ones. Ratios > 1 are highlight in red.

I/O ratios (µg/m^3) – Winter								
OFFICE	**Sub-group**	**T1**	**T2**	**T3**	**average of the three weeks**	**ST. DEV.**	**MIN.**	**MAX.**
Office 1	R1	1,3	1,4	0,8	1,2	0,3	0,8	1,4
Office 2	R1	1,1	1,3	0,7	1,0	0,3	0,7	1,3
Office 3	R1	1,1	1,8	0,7	1,2	0,5	0,7	1,8
Office 4	R1	0,5	1,1	0,7	0,8	0,3	0,5	1,1
Office 5	R1	0,5	1,0	0,6	0,7	0,3	0,5	1,0
Office 6	R1	0,6	0,9	0,8	0,8	0,1	0,6	0,9
Office 7	R2	0,5	0,5	0,5	0,5	0,02	0,5	0,5
Office 8	R2	0,4	0,5	0,5	0,5	0,1	0,4	0,5
Office 9	R2	0,4	0,5	0,5	0,5	0,05	0,4	0,5
Office 10	R2	0,4	0,5	0,6	0,5	0,1	0,4	0,6
Office 11	R2	0,5	0,4	0,5	0,5	0,05	0,4	0,5
Office 12	R2	0,5	0,3	0,5	0,5	0,1	0,3	0,5
Office 13	R3	0,5	0,5	0,7	0,6	0,1	0,5	0,7
Office 14	R3	0,6	0,5	0,7	0,6	0,1	0,5	0,7
Office 15	R3	0,3	0,2	0,4	0,3	0,1	0,2	0,4
Office 16	R3	0,2	0,1	0,2	0,1	0,1	0,1	0,2
Office 17	R3	0,2	0,1	0,3	0,2	0,1	0,2	0,3
I/O ratios (µg/m^3) – Summer								
Office 1	R1	0,9	0,7	0,8	0,8	0,1	0,7	0,9
Office 4	R1	0,8	0,8	0,8	0,8	0,03	0,8	0,8
Office 5	R1	1,1	1,2	1,0	1,1	0,1	1,0	1,2
Office 7	R2	0,8	0,6	0,6	0,7	0,1	0,6	0,8
Office 8	R2	0,9	0,6	0,5	0,6	0,2	0,5	0,9
Office 9	R2	1,1	0,8	0,8	0,9	0,1	0,8	1,1
Office 10	R2	0,9	0,6	0,5	0,7	0,2	0,5	0,9
Office 11	R2	0,7	0,6	0,5	0,6	0,1	0,5	0,7
Office 13	R3	0,6	0,6	0,5	0,6	0,04	0,5	0,6
Office 14	R3	0,7	0,6	0,5	0,6	0,1	0,5	0,7
Office 15	R3	0,4	0,3	0,4	0,4	0,1	0,3	0,4
Office 16	R3	0,3	0,4	0,4	0,4	0,04	0,3	0,4
Office 17	R3	0,4	0,4	0,4	0,4	0,01	0,4	0,4

Supplemental Table 2. The number of indoor TSP DNA samples per office and time collected during the summer season.					
City	Office	Time			Total
		T4	T5	T6	
Milan	office 2	1	1	0	2
	office 4	1	1	1	3
	office 6	1	1	0	2
	office 7	1	1	1	3
	office 8	1	1	1	3
	office 9	1	1	1	3
	office 10	1	1	1	3
	office 11	1	1	1	3
	ALL	8	8	6	22
Como	office 13	1	1	1	3
	office 14	1	1	1	3
	office 15	1	1	1	3
	office 16	1	1	1	3
	office 17	1	1	1	3
	ALL	5	5	5	15

Supplemental Table 3. The number of outdoor TSP DNA samples per office and time collected during the summer season.					
City	Outdoor	Time			Total
		T4	T5	T6	
Milan	Building 1 (R1)	1	1	1	3
	Building 2 (R1)	0	1	0	1
	Building 1 (R2)	1	1	1	3
	Building 2 (R2)	1	0	0	1
	ALL	3	3	2	8
Como	Building 1 (R3)	1	1	1	3
	Building 2 (R3)	1	1	1	3
	ALL	2	2	2	6

Supplemental Table 4. Significant results of the interaction analysis: indoor TSP, top bacteria species, and HERV methylation					
Outcome	**Effect modifier**	**Selected value of the effect modifier**	**Beta**	**p-value**	**p-value interaction (TSP indoor*Species)**
HERVW assay1 pos1	*Cutibacterium acnes*	p25=2.8	0.07	0.036	0.025
		q50=3.8	0.02	0.546	
		p75=4.3	-0.01	0.713	
HERVW assay1 pos1	*Actinomyces naeslundii*	p25=-7.6	0.08	0.017	0.021
		q50=-4.7	0.02	0.382	
		p75=-3.6	0.00	0.965	

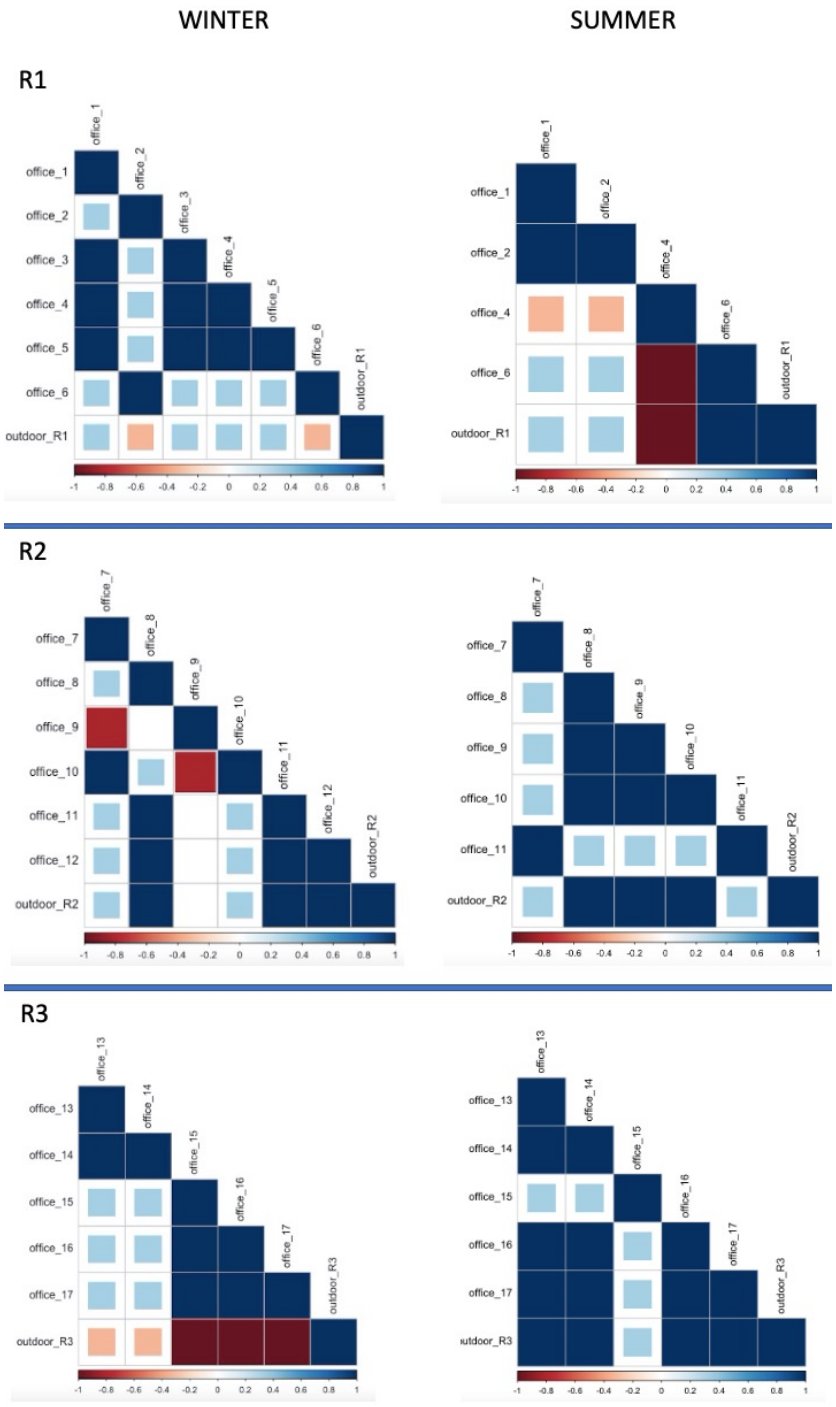

Supplemental Figure 1. The heatmaps indicate the correlation between indoor and outdoor TSP exposure. Red squares represent negative correlations, while the blue squares represent positive correlations.

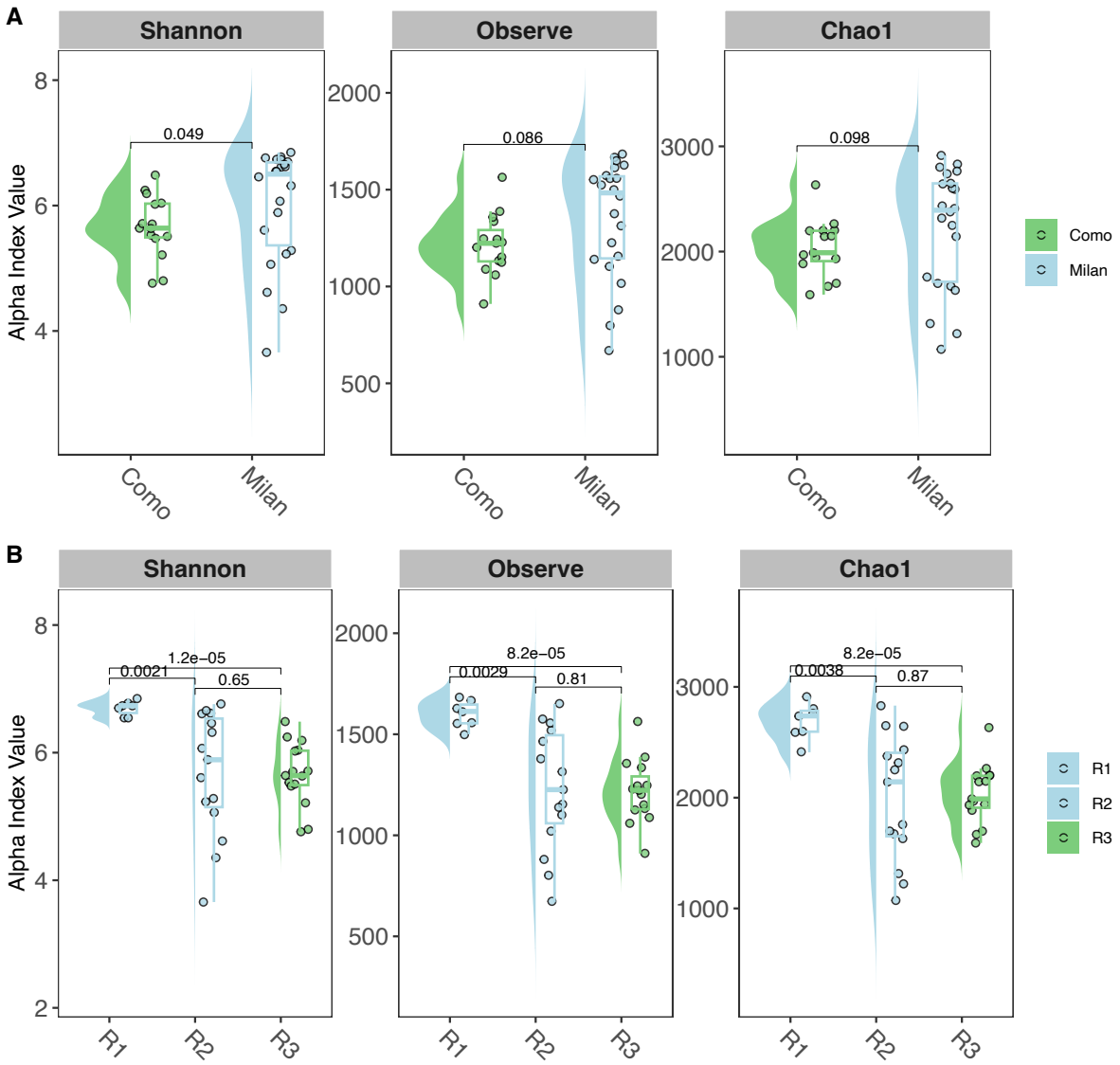

Supplemental Figure 2. Boxplots showing the alpha diversity in indoor TSP samples. The dots represent the alpha diversity of each sample. (**A**) Comparison of the alpha diversity of samples from Milan and Como. (**B**) Comparison of alpha diversity among the three different groups (R1, R2, R3). In both plots, Milan samples are in light blue color and Como samples in green. These images were generated using *MicrobiotaProcess* (v 1.10).

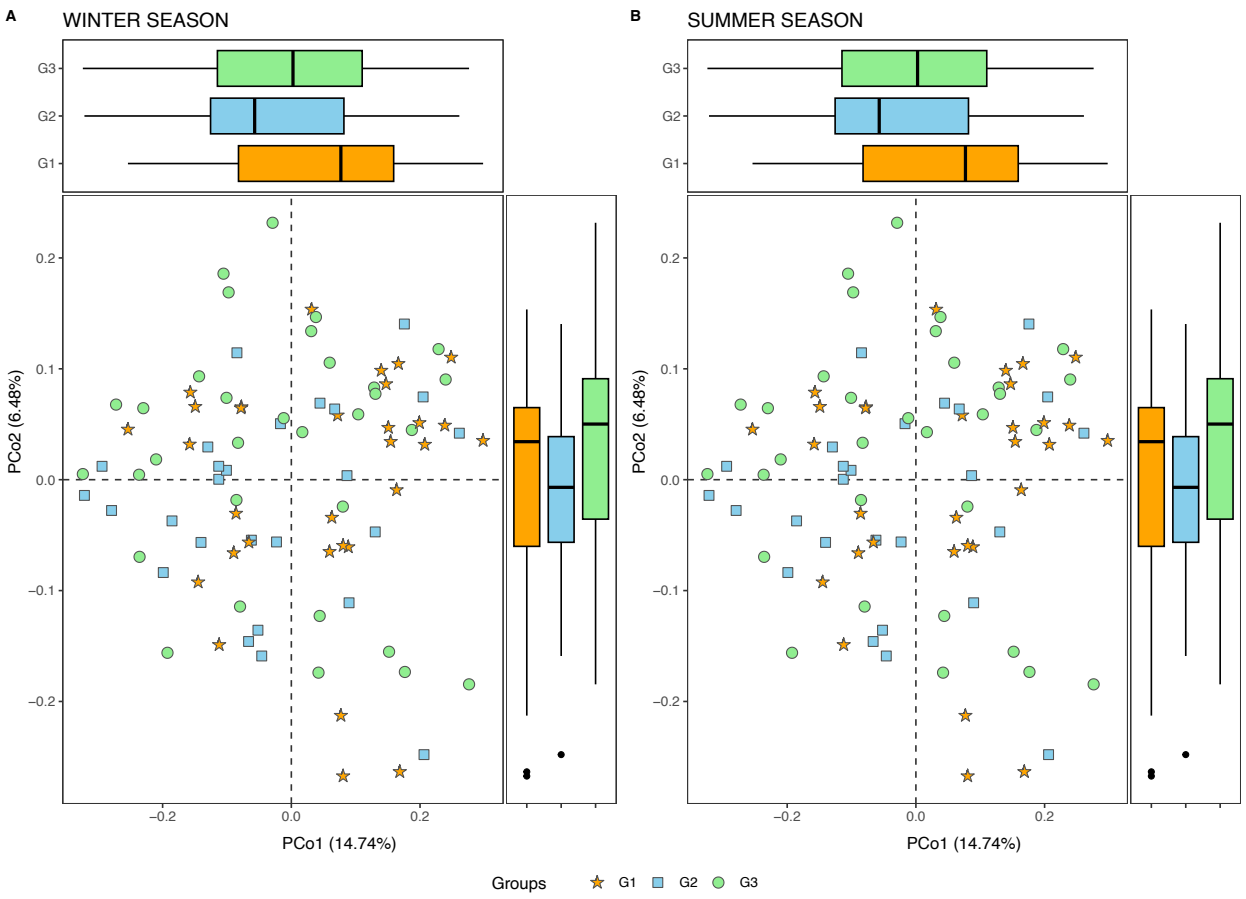

Supplemental Figure 3. Principal coordinate analysis (PCoA) calculated from the Bray-Curtis distance matrix in Anterior Nares (AN) samples from healthy subjects. (**A**) Comparison of beta diversity among the three sub-groups of healthy people during the winter season (**B)** Comparison of beta diversity among the three sub-groups of healthy people during the summer season. These images were generated using *MicrobiotaProcess* (v 1.10).

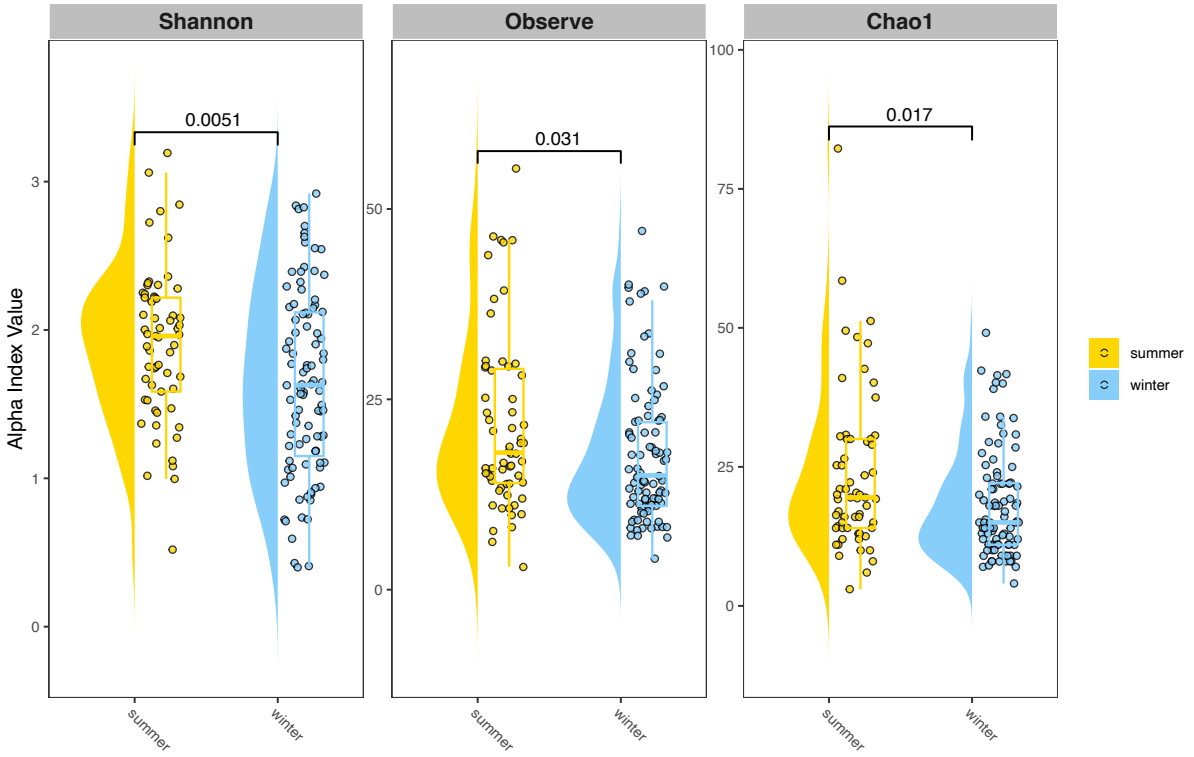

Supplemental Figure 4. Boxplots showing the alpha diversity in Anterior Nares (AN) samples between the two seasons: summer (yellow boxplots) and winter (blue boxplots). These images were generated using *MicrobiotaProcess* (v 1.10).

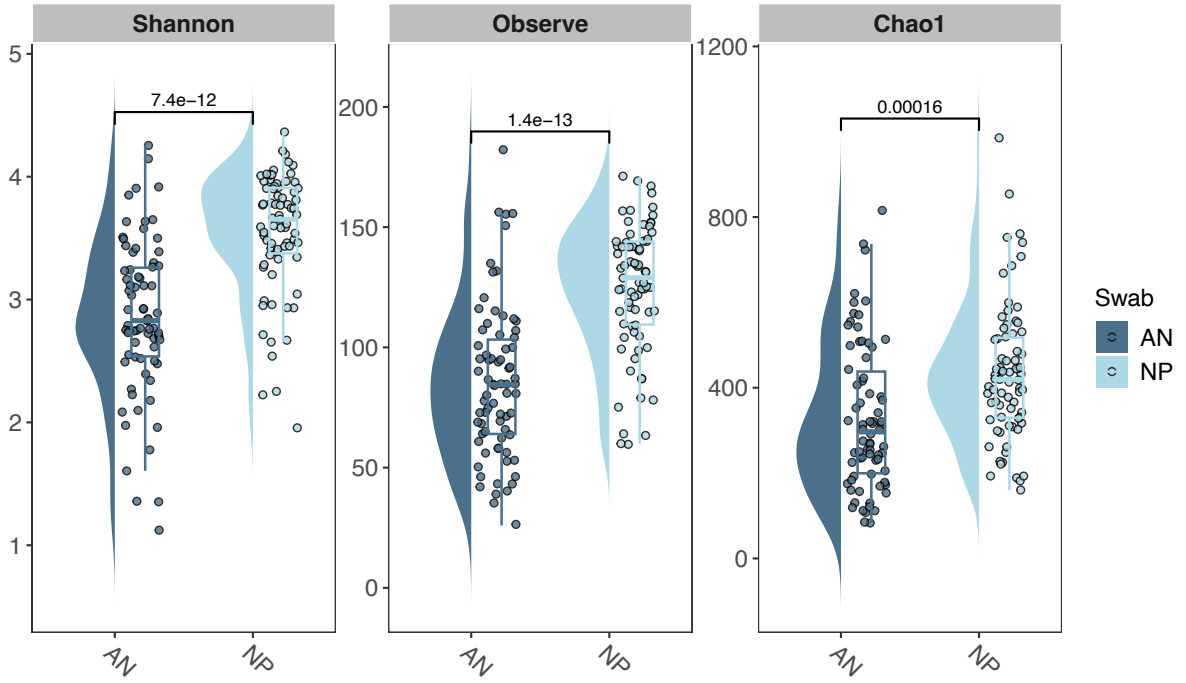

Supplemental Figure 5. Boxplots showing the alpha diversity between Anterior Nares (AN) samples (dark blue boxplots) and Nasopharynx (NP) samples (light blue boxplots). These images were generated using *MicrobiotaProcess* (v 1.10).

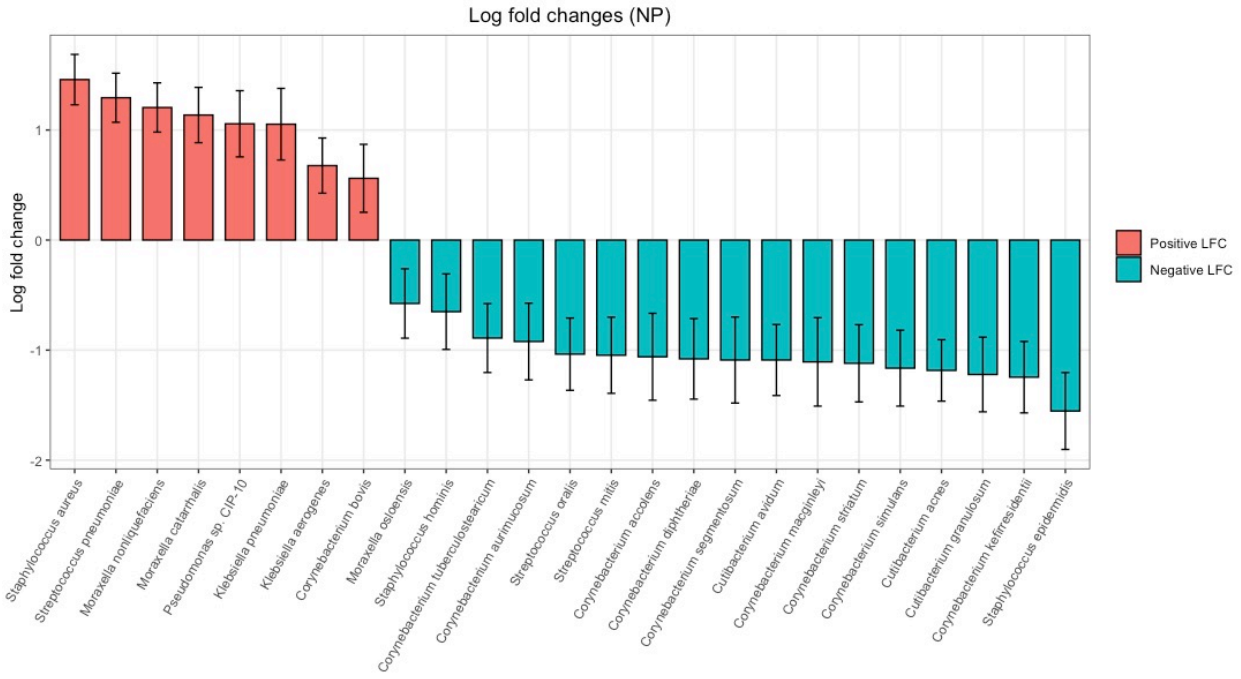

Supplemental Figure 6. The bar plot shows the difference (log fold changes) in bacterial abundance between the nasopharynx microbiome and the anterior nares microbiome. This difference was identified using ANCOM-BC analysis (p-value < 0.05, FDR < 0.10). The red bars indicate bacteria with higher relative abundance in the nasopharynx microbiome, while the blue bars indicate the one with higher abundance in anterior nares microbiome.

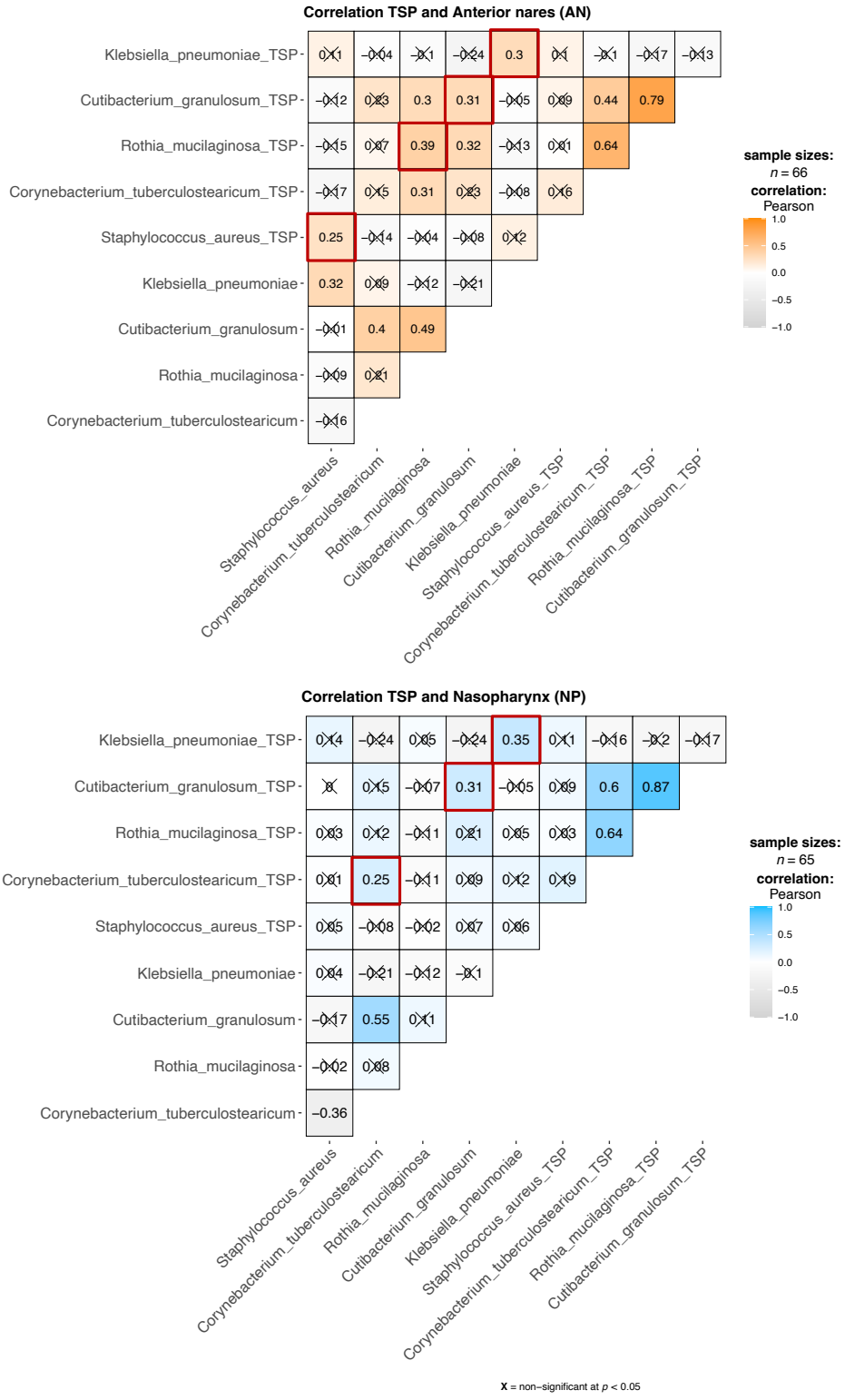

Supplemental Figure 7. Correlations in bacteria abundance between indoor TSP and respiratory samples: anterior nares (AN) and nasopharynx (NP). The correlation was estimated using the Pearson correlation test (p-value < 0.05), the plots were created using the R package *ggstatsplot* (v. 0.12.2).

LIST OF PUBLICATIONS

Published during the Ph.D.

Respiratory Microbiota, viral infections, and Human Health

"Pyroptosis: A Promising Mechanism Linking SARS-CoV-2 Infection to Adverse Pregnancy Outcomes".

Monti P, **Solazzo G**, Accurti V, Gambitta B, Iodice S, Boito S, Cantone L, Manenti A, Dioni L, Montomoli E, Persico N, Bollati V. Int J Mol Sci. 2023 May 25;24(11):9278. doi: 10.3390/ijms24119278. PMID: 37298229; PMCID: PMC10252646

"Upper Respiratory Microbiome in Pregnant Women: Characterization and Influence of Parity".

Solazzo G, Iodice S, Mariani J, Persico N, Bollati V, Ferrari L; INSIDE Consortium Investigators. Microorganisms. 2022 Nov 4;10(11):2189. doi: 10.3390/microorganisms10112189. PMID: 36363781; PMCID: PMC9699484.

"Nasopharyngeal Bacterial Microbiota Composition and SARS-CoV-2 IgG Antibody Maintenance in Asymptomatic/Paucisymptomatic Subjects".

Ferrari L, Favero C, **Solazzo G**, Mariani J, Luganini A, Ferraroni M, Montomoli E, Milani GP, Bollati V. Front Cell Infect Microbiol. 2022 Jul 6;12:882302. doi: 10.3389/fcimb.2022.882302. PMID: 35873175; PMCID: PMC9297915.

"Digital RT-PCR Chip method for detection of SARS-CoV-2 virus".

Dioni L, Orlandi A, Uceda Renteria S, Favero C, **Solazzo G**, Oggioni M, Bollati V. J Immunol Methods. 2022 Oct;509:113339. doi: 10.1016/j.jim.2022.113339. Epub 2022 Aug 17. PMID: 35985558; PMCID: PMC9383957.

"Particulate Matter Exposure and Allergic Rhinitis: The Role of Plasmatic Extracellular Vesicles and Bacterial Nasal Microbiome".

Mariani J, Iodice S, Cantone L, **Solazzo G**, Marraccini P, Conforti E, Bulsara PA, Lombardi MS, Howlin RP, Bollati V, Ferrari L. Int J Environ Res Public Health. 2021 Oct 12;18(20):10689. doi: 10.3390/ijerph182010689. PMID: 34682436; PMCID: PMC8535327.

Other papers

"Effect of environmental exposures on cancer risk: Emerging role of non-coding RNA shuttled by extracellular vesicles".

Monti P, **Solazzo G**, Bollati V. Environ Int. 2023 Nov;181:108255. doi: 10.1016/j.envint.2023.108255. Epub 2023 Oct 10. PMID: 37839267.

"PCSK9 Confers Inflammatory Properties to Extracellular Vesicles Released by Vascular Smooth Muscle Cells".

Greco MF, Rizzuto AS, Zarà M, Cafora M, Favero C, **Solazzo G**, Giusti I, Adorni MP, Zimetti F, Dolo V, Banfi C, Ferri N, Sirtori CR, Corsini A, Barbieri SS, Pistocchi A, Bollati V, Macchi C, Ruscica M. Int J Mol Sci. 2022 Oct 28;23(21):13065. doi: 10.3390/ijms232113065. PMID: 36361853; PMCID: PMC9655172.

"Extracellular vesicles and their miRNA contents counterbalance the pro-inflammatory effect of air pollution during physiological pregnancy: A focus on Syncytin-1 positive vesicles".

Ferrari L, Iodice S, Cantone L, **Solazzo G**, Dioni L, Hoxha M, Vicenzi M, Mozzoni P, Bergamaschi E, Persico N, Bollati V. Environ Int. 2022 Nov;169:107502. doi: 10.1016/j.envint.2022.107502. Epub 2022 Sep 6. PMID: 36095930

"Brain-Derived Neurotrophic Factor and Extracellular Vesicle-Derived miRNAs in an Italian Cohort of Individuals With Obesity: A Key to Explain the Link Between Depression and Atherothrombosis".

Amadio P, Macchi C, Favero C, Zarà M, **Solazzo G**, Dioni L, Sandrini L, Vigna L, Greco MF, Buoli M, Sirtori CR, Pesatori AC, Ieraci A, Ruscica M, Barbieri SS, Bollati V. Front Cardiovasc Med. 2022 Jul 13;9:906483. doi: 10.3389/fcvm.2022.906483. PMID: 35911513; PMCID: PMC9326054

"Associations Among PCSK9 Levels, Atherosclerosis-Derived Extracellular Vesicles, and Their miRNA Content in Adults With Obesity".

Macchi C, Greco MF, Favero C, Dioni L, Cantone L, Hoxha M, Vigna L, **Solazzo G**, Corsini A, Banach M, Pesatori AC, Bollati V, Ruscica M. Front Cardiovasc Med. 2022 Jan 7;8:785250. doi: 10.3389/fcvm.2021.785250. PMID: 35071356; PMCID: PMC8782054.

"Extracellular Vesicles: Footprints of environmental exposures in the aging process?".
Monti P, **Solazzo G**, Ferrari L, Bollati V. Curr Environ Health Rep. 2021 Dec;8(4):309-322. doi: 10.1007/s40572-021-00327-3. Epub 2021 Nov 6. PMID: 34743313.

In preparation for submission:

"Characterization of the Total Suspended Particles (TSP) microbiome and its correlation with the upper respiratory microbiome of healthy office workers"
Solazzo G., Rovelli S., Iodice S., Bollati V., Ferrari L., Ghedin E.